Alma Mater Studiorum – Università di Bologna

DOTTORATO DI RICERCA IN

Scienze e Tecnologie Agrarie, Ambientali e Alimentari

Ciclo XXX

Settore Concorsuale di afferenza: 07/E1

Settore Scientifico disciplinare:AGR/07

High-throughput phenotyping for the genetic dissection of drought tolerance related traits in *Zea mays* and *Triticum durum* Desf.

Tesi presentata da: Dott. Giuseppe Sciara

Coordinatore Dottorato: Chiar.mo Prof. Giovanni Dinelli

Relatore: Chiar.mo Prof Silvio Salvi

Correlatori: Chiar.mo Prof. Roberto Tuberosa

Dott. Marco Maccaferri

Table of Contents

1. Introduction

1.1. Cereals in the world

Cereals are the main staple food in human diet and livestock feeding. Indeed, out of 1.4 billion of hectares of cultivated land, almost a half (0.72 Mha) are used for cereal production (FAOSTAT, 2014). Almost 89% of world cereal production is from three main crops: maize (*Zea mays*), wheat (*Triticum spp.*) and rice (*Oryza spp.*). In the last 57 years, global wheat and rice production increased of more than 300% while maize production increased of almost five folds. This astounding result are not the consequence of higher land investments but rather of constant yield increase. This has been possible thank to a parallel development of agronomical practices and genetic improvement. At the same time, the proportion of peoples living under the hungry threshold moved from 30% to 10%. This none withstanding, malnutrition is still the main cause of death in the world with more than 668 million of people still living without an adequate nutrients intake, especially in Africa and Asia (Alderman et al., 2006; Mayer et al., 2008; Müller and Krawinkel, 2005). As consequence of that, United Nations declared sustainable food safety as one of the major goals of the humanity in the next future (https://sustainabledevelopment.un.org). Various factors hinder the reaching of such an ambitious goal. First, the global population will keep increasing at least until the 2050 until it will reach nine or ten billion individuals. Secondly, the parallel growth of *per-capita* income will cause a corresponding increase in *per-capita* food consumption (Tester and Langridge, 2010b). Last but not least, anthropic activity will severely impact the climatic equilibrium of the planet, with consequences which might be catastrophic. The global agro-system will have to respond to a more and more intense food demand in climatic conditions totally different from those of the last century. Droughts, floods and extremely high temperature will hit the planet with a frequency and strength never observed before (Mickelbart et al., 2015). Is therefore crucial that research focuses on those mechanisms which might guarantee a better resilience of the plants to such extreme conditions. Furthermore, this must be reached by reducing at the same time the agricultural environmental footprint. Given their role in human nutrition, this is particularly urgent for cereals. In this dissertation we will focus on the genetic and phenotypical dissection of those traits that are involved in drought tolerance mechanisms in durum wheat and maize. In particular, we will expose the results of two research conducted using high-throughput phenotyping techniques with the aim of discovery the genetic bases underling drought adaptive traits.

1.2. Gene, genotype, genome - phene, phenotype, phenome

When referred to cultivated species, genetic improvement refers to all those voluntary or involuntary, conscious or unconscious strategies that humans have used to adapt plants to different growing environments and/or uses. In agriculture, genetic improvement has two goals: or to increase the amount of good produced per resource unit (yield, productivity, stability, sustainability…) or to ameliorate the suitability of the goods to the consumption chain (qualities) (Poehlman, 1987).

From domestication to our days, genetic improvement has been essentially a two-step procedure: in the first step, we observe or measure one or more properties of individuals belonging to a certain population; in the second step, we destine to reproduction those individuals that, because of their superior ranking in the properties we are interested in, have more chances to produce a progeny superior to the population they come from. In order to be inheritable and therefore subjectable to genetic improvements, traits should have a genetic determinism; such traits are referred as **phenes**; the global set of phenes is usually referred as **phenome**. The set of phenes that functionally and or morphologically allow to distinguish between individuals of the same population is referred as **phenotype** (Fiorani and Schurr, 2013; Mahner and Kary, 1997). Phenotypes which are considered optimal for a certain scope are defined as **ideotypes**. Parallelly to phene, phenome and phenotype we could define **gene**, **genome** and **genotype**. Genes are parts of nucleic acids able to produce functional molecules. The genome is the set of genes plus non-coding and regulatory regions of the DNA. Genotypes are sets of molecular features of the DNA which allow to distinguish between individuals of the same population (Mahner and Kary, 1997). Having this said, we can summarize that genetic improvement is the process that, by manipulating the genotype, makes the phenotype more similar to the ideotype.

1.3. A brief overview on crop genetic improvement

Since there is a bi-univocal correspondence between genotype and phenotype, genetic improvement might be achieved both selecting phenotypes, selecting genotypes or both. Since domestication up to the second half of the XX century, genetic improvement was solely guided by phenotypic selection (Tester and Langridge, 2010b). Despite breeding history underwent dramatic changes in the way populations were constituted and the ideotypes inspiring the selection, the criteria used by humans to select the best individuals was exclusively the direct observation or measurement of phenes; since the modification of phenotypes is the goal of any genetic improvement effort, this strategy is theoretically the most solid; indeed, as long as the progeny is cultivated in the same environment and under the same management conditions of

their parentals, select the parentals with best phenotypes will guarantee a progeny with the best possible phenotypes. The limits of phenotypic selection came to the surface in the XIX century, when genetic improvement of crops started to be scientifically executed. Indeed, selection began to be performed in experimental stations where many individuals were evaluated in experimental conditions. Progeny of selected individuals, after multiplication, was cultivated in areas other than those where the selection was performed. This caused the phenotypic selection for target traits, chiefly yield and quality, to lack predictivity. The reason of that is basically that yield and, to a certain extent, qualities, are complex traits resulting from the complex interaction of simpler phenes. Phenes expression could either be beneficial, neutral or detrimental for a complex trait depending on environment and management conditions. E.g. resistance to a certain disease has no impact on yield in those environments where the disease is absent while it is advantageous under strong disease pressure. Another example is deep rooting: it might be advantageous in drought scenarios (if soils are deep and a deep water-plane is available) while, in well-watered conditions, it might just be a waste of carbon.

The lack of predictivity of direct phenotypic selection for yield and qualities, caused ideotypes and phenotypes to include more and more phenes, each of which functionally involved in the resulting complex trait. One of the direct consequences of this approach was the more and more frequent – and successful – adoption of intraspecific hybridization for the constitution of breeding population (Borojevic and Borojevic, 2005b; Salvi et al., 2013; Scarascia Mugnozza, 2005). Indeed, to introduce a desired phene into the cultivated elite material, breeders begun to cross it with exotic germplasm which, despite it was not valuable from an agronomical standpoint, was carrier of few useful phenes. The impact of such approach has been tremendous. The pioneering work of Nazareno Strampelli in the early XX century is a glaring example of the successes obtained by phene manipulation (Salvi et al., 2013; Scarascia Mugnozza, 2005). Italian wheat breeding at the Strampelli's time was facing three major challenges:

1. adapt wheat to new farming conditions established after the introduction of ammonium fertilization in agriculture;
2. reduce the dramatic yield reduction due to terminal drought;
3. improve leaf rust resistance;

Strampelli is the first scientist who obtained to adapt wheat to the fertility boost due to the introduction of ammonium fertilization in agriculture. One of the major constrain to ammonium fertilization was indeed the lodging phenomenon, overcame by Strampelli introducing in the elite "Rieti originario" derived material, dwarfing alleles of the *Rht8* gene from Japanese local variety "Akakomugi" (Borojevic and Borojevic, 2005a, 2005b). The same cross allowed Strampelli to

introgress the early variant of the *ppd*-D1 gene producing a sensible reduction in flowering time (Salvi et al., 2013). This allowed, by reducing the length of the wheat cycle, to plummet the risk of droughts during flowering/grain filling, especially in Mediterranean climates. Finally the introduction of the resistant variant of the *Lr34* (Kolmer et al., 2008; Lagudah et al., 2009) gene, conferred good levels of resistance to leaf rust. Three decades later, the Nobel laureate Norman Borlaug used the Strampelli's lines and strategy to constitute the lines of the green revolution. The progressive introgression of favorable alleles in the elite germplasm is one of the crucial factors that permitted the crops productivity to increase of more than 300%. Introgression of favorable alleles into the elite germplasm has several limitations that pushed breeders, physiologists and geneticists to develop strategies more and more sophisticated. One of the major constrain for phenes manipulation is for sure the limited, if not null, variability in terms of alleles affecting phenes in the desired direction. Different approaches have been used to enrich germplasm of potentially beneficial alleles. The first attempts in this direction have been through physical and chemical mutagenesis (D'Amato et al., 1962; Neuffer and Ficsor, 1963; Oladosu et al., 2016; Shama Rao and Sears, 1964). These techniques cause random changes in the DNA both at sequence or structure level. Most of the mutations occur in neither genic or regulatory regions of the DNA thus having no phenotypic consequences. In the case mutations occur in functional genomic regions, they might cause aminoacidic change and, therefore, changes in the protein which might in turn cause phenotypic variation. The International Atomic Energy Agency (IAEA), reports in its databases (https://mvd.iaea.org/) over 3200 cultivars of 232 species developed using one of the following mutagenesis-based breeding techniques:

1. direct use of a mutant line obtained after physical or chemical mutagenesis
2. use of a mutant as parent in crosses
3. use of a mutant allele
4. irradiation-facilitated translocation of genes from wild ancestors to elite germplasm.

Rice is by far the specie with more mutagenesis-breeding derived cultivar (821), followed by barley (304), chrysanthemum (281), wheat (255) and soybean (173). The same database reports a total of 31 durum wheat cultivar released after the use of one of the above-mentioned strategies. Being mutations randomly distributed in the genome, many individuals are needed to have good chances that at least one of them carry an ameliorative mutation. Furthermore, both physical and chemical mutagenesis cause mutations in numerous loci in the genome with possible negative effects on other phenes. These two aspects represent strong limitations to the effective employment of mutagenesis in breeding. Another major limiting factor is the fact that through mutagenesis it is not possible to tune gene expression levels.

Parallelly to mutagenesis, the development of genomics and biotechnologies marked the beginning of a new era in breeding. The use of biotechnologies in genetic improvement has had two major finalities: i) to enrich natural genetic variation, ii) to enhance selection efficiency by integration of phenotypic and genotypic information. Biotechnologies started to impact plant breeding as soon as genetic transformation through *Agrobacterium* was developed (Bevan et al., 1983; Herrera-Estrella et al., 1983; Parmar et al., 2017). This strategy permits the stable integration of genetic material from any species into the genome of a recipient species. Individuals which genome was enriched by mean of this technology are commonly referred as Genetically Modified (GM). Classic examples of GM uses are the incorporation in vegetal genomes of bacterial toxins from *Bacillus thuringiensis* to obtain insect resistant crops or the artificial enhancement or introgression of biosynthetic pathways to produce bio-fortified food i.e. "Golden rice" (Mayer et al., 2008; Sanahuja et al., 2011). Other biotechnological tools that allow the direct modification of the genetic pool of plants are referred as genome editing (GE) techniques. The most important family of these techniques is that of site direct nucleases (SDNs). SDNs permit the precise cut of a specific genomic region; they can either be DNA-binding restriction proteins able to recognize, bind and cut in a certain position of the genome (meganuclease) or heterodimers of two proteins having one the function to recognize the genomic region and the other to cause the actual cut. Zinc finger nucleases (ZFNs) and transcription activator-like effector nucleases (TALENs) are two representative examples of this technology. These proteins are usually coupled with *Fok1*, which cause the actual cut of the DNA. In order to permit the editing to occur, is therefore needed that two genes encoding for the above-mentioned proteins are expressed in the cells. SDNs could be used for single point mutation, insertions or deletions of entire gene or genomic regions (D'Halluin et al., 2013; Osakabe et al., 2010; Petolino et al., 2010; Shukla et al., 2009; Townsend et al., 2009). In the last few years, an innovative technology is emerged which, because of its precision and ease of use, promises to revolutionize the impact of GE in plant breeding. This technology is named CRISPR/Cas9 and is a SDN where the Cas9 nuclease is directed to the target genomic region by an ad hoc designed RNA guide (Barrangou et al., 2007; Cai et al., 2018; Jinek et al., 2012; Wang et al., 2017; Zhou et al., 2016).

Despite the above-mentioned biotechnological tools permit a much more accurate control of genetic modification as compared to mutagenesis, their application in breeding has faced several constrains which have strongly limited their wide diffusion. First of all, they need long and costly development for the discovery, modification and patenting of the genes to insert or modify; secondly, in several developed countries, especially in Europe, they found an harsh opposition by large part of the public opinion because of often unfounded safety concerns which translates;

finally, because they permit the modification of a relatively low number of *loci* thus being unsuitable for the improvement of very complex traits such yield or most of stresses tolerances (Hartung and Schiemann, 2014; Tester and Langridge, 2010a).

As above mentioned, biotechnologies have not only allowed for the enrichment of genetic variability of germplasms but also they have been used to increase selection predictivity accuracy in breeding. The main use of biotechnologies in this direction is commonly referred as marker assisted selection (MAS). MAS fundamentally take advantage of detectable variation (molecular markers) present in the DNA sequence to track and monitor specific regions of the genomes during crossing and selection (Moose and Mumm, 2008). Because of linkage disequilibrium, markers might be predictive of the allelic status of the genetically linked *loci*. Those *loci* where one or more genes are involved in the control of a quantitative trait are referred as quantitative trait *loci* (QTLs). The allelic status at a certain marker linked to a QTL might therefore be predictive of a certain phenotype. MAS consists in the integration of phenotype-based selection with genotype information at critical loci. Mas is especially useful when the target traits have low heritability, the costs of phenotyping are high or if breeders are interested to introgress in elite material just a small part of the genome of a wild relative (i.e. backcrosses). Molecular markers are also crucial in gene cloning, the process that permits the identification of the gene causally controlling a certain phene (Salvi and Tuberosa, 2005). MAS has not faced the same ostracism as other biotech tools. Furthermore, it permits to contemporary track the entire genome and thus to be particulary suitable to complex traits breeding (Tester and Langridge, 2010b) In order to develop markers suitable for MAS, is crucial to identify those QTL controlling the target trait. The QTL discovery strategies are fundamentally statistical regressions where is tested the significance of the association between measured phenes values of a relatively high number of individuals and their genotypic information. As above mentioned, many stresses tolerance mechanisms, notably drought, have a complex genetic and phenotypic architecture. Is therefore crucial to dissect tolerance into component contributory phenes and to identify QTLs controlling them (Araus et al., 2002; Langridge and Reynolds, 2015; Tuberosa, 2012). The high number of individuals needed for QTL discovery jointly with the numerosity of phenes to be collected to dissect complex traits is the origin of what is known as the phenotyping bottleneck (Fiorani and Schurr, 2013; Furbank and Tester, 2011). High throughput phenotyping is the set of technologies developed to permit to obtain with adequate accuracy many phenes on QTL discovery suitable populations.

In the next chapters, we will present two researches where, by use of high throughput phenotyping, we have been able to identify several *loci* involved in drought tolerance-related phenes in maize and durum wheat.

2. High throughput phenotyping of a maize introgression library for water use efficiency and growth-related traits

2.1. Introduction

Water deficit is one of the major factors limiting crop yield potential. Despite this, the genetic basis of drought tolerance remains mostly unknown because of its intrinsic complexity. Modern breeding approaches try to tackle the complexity of drought tolerance first by dissecting it into simpler secondary traits by means of eco-physiological modelling (Abdel-Ghani et al., 2016; Reynolds and Langridge, 2016; Salvi et al., 2011; Szalma et al., 2007; Wei et al., 2015). Each secondary trait is supposed to have a simpler genetic control than yield under drought and, therefore, to be more easily manipulated by breeding. For instance, plant geneticists and physiologists focused on traits such as stomatal conductance, leaf water status and/or osmotic potential, root anatomy and architecture and others (Roy et al., 2011; Vadez et al., 2013).

The capability of plants to uptake water and maintain water use (WU) together with their capability of efficiently use it (water use Efficiency, WUE, defined as the amount of water needed to produce a certain amount of biomass) have been recognized as key components of drought tolerance (Blum, 2009; Reynolds and Tuberosa, 2008; Richards and Passioura, 1989). Several approaches permit to directly or indirectly estimate WUE both at field and plant levels. Despite just a part of the total biomass produced is finally harvested, biomass accumulation rate (BA) in specific growth phases (e.g. early vegetative growth) can be critical for the plant to successfully address later phases such as flowering, fertilization and grain filling. Furthermore, being leaves the main organ of the plant deputed to gas exchange with atmosphere, their extension, together with stomatal density and control, is critical to determine plant water consumption.

One of the major hurdles in working with secondary traits is that their phenotyping can be more time consuming and less repeatable than directly measuring yield. This limitation will likely be mitigated by the advent of high-throughput phenotyping technologies, which appear as particularly suitable for the dissection of abiotic stress tolerance. (Araus and Cairns, 2014; Cabrera-Bosquet et al., 2012; Reynolds et al., 2009; Tuberosa, 2012). One of the advantages of these technologies is the possibility to perform morpho-physiological measurements dynamically, thus enabling to study traits which are usually inaccessible to phenotyping based on single time point (or end-point) measurements.

Several types of populations have been conceptualized and developed to perform phenotype/genotype associations. Among them, introgression libraries (ILs, also referred to as chromosomal substitution lines), allow for the evaluation of chromosomal regions from a donor parent (DP) into a common genetic background from a recurrent parent (RP) (Zamir, 2001). This approach is especially useful for the exploitation of genetic diversity originating from exotic or unadapted plant materials. Indeed, the DP is usually chosen because of the presence of interesting traits despite its overall inadequacy to common farming conditions. On the contrary, the RP is usually a well-characterized highly productive elite line or genotype. Multiple introgression libraries have already been generated in maize (Abdel-Ghani et al., 2016; Salvi et al., 2011; Szalma et al., 2007; Wei et al., 2015).

In this experiment, we used a high-throughput phenotyping strategy to evaluate drought tolerance related traits in a maize IL previously found to segregate for phenology and root system architecture (RSA) (Salvi et al., 2011, 2016). The phenotyping platform PhenoArch (https://www6.montpellier.inra.fr/lepse_eng/M3P/PHENOARCH-platform) is a conveyer based system which permit the dynamic, non-destructive evaluation of biomass and WU and thus to have a direct estimation of WUE (Cabrera-Bosquet et al., 2016; Coupel-Ledru et al., 2014; Lopez et al., 2015). Furthermore, its design allowed for an accurate control of soil water status and atmospheric parameters such as temperature, relative humidity and photoperiod, thus permitting an accurate evaluation of the plant response to water deficit.

We aimed to test whether genetic variation for phenology and RSA would affect BA and WU during the early phase of development, in an elite maize genetic background.

2.2. Materials and methods

Plant material and genetic characterization

A total of 73 lines from a previously developed introgression library (IL) population (Salvi et al., 2011) plus the two parents were tested. The RP of the IL was the elite dent line B73, an inbred line also used as reference for sequencing the maize genome (Schnable et al., 2009) while the DP was the early-flowering north American flint landrace Gaspé Flint (Vigouroux et al., 2008). The IL was obtained through five generation of SSR-marker-assisted backcross followed by two cycles of selfing (Salvi et al., 2011). The IL was previously found to segregate for phenology traits and seminal roots architecture (Salvi et al., 2011, 2016). In this work, the genetic characterization of the IL was refined in respect of the previously available data (Salvi et al, 2011) by means of the 50k SNP ILLUMINA Infinium array (Ganal et al., 2011). A total of 48,361 SNPs were utilized after excluding SNPs with unknown or unclear physical map position on the maize reference

genome (Schnable et al., 2009) and those with >10% of missing data. A graphical genotype of the IL was constructed by creating chromosome BINs of consecutive SNPs with identical genotypic score and labelling the BINs with the first SNP of the BIN. BINs of length < 200 kb and with < 5 SNPs were masked. Linkage Disequilibrium (LD) between BINs was evaluated using TASSEL 5 (Bradbury et al., 2007). LD p-values were estimated by a two-sided Fisher's Exact test (Fisher, 1922). Two BINs were considered in high LD when the calculated p-value was < 0.01.

Experimental design and traits evaluation

The high-throughput phenotyping platform PhenoArch is hosted in a greenhouse of the Laboratory of Plant Eco-physiology under Environmental Stresses (LEPSE) of the French Agricultural Research Institute (INRA) in Montpellier, France. The platform consists of 28 belt conveyers each of which can carry up to 60 pots, for a total throughput of 1680 pots/plants. Conveyers permit the automatic transport of the pots to both watering stations and imaging cabin. The platform hosts two automated watering stations consisting in balances with 1g accuracy (ST-Ex, Bizerba, Balingen, Germany) and high-precision pumps (520U, Watson Marlow, Wilmington, MA, USA). The imaging cabin is provided with two RGB camera (1280×960 px, 3D Scanalyzer, LemnaTec, GmbH, Wüerselen, Germany) and a rotating lift which permits the acquisition of lateral plant pictures from up to 12 angles (0° to 330° with 30° steps) plus a single picture from the top. Biomass was estimated by a four steps process consisting in: 1) image segmentation to isolate the plant from the background and thus estimate the number of pixels it was made of; 2) extrapolation, through image analysis of geometrical properties of the picture of the plants such as width, height, convex hull etc…; 3) selection, among the 12 lateral pictures, of the frontal one (where the plant had the maximum width); 4) estimation of fresh biomass (B) and leaf area (LA) on the base of the number of pixels of the plant in the frontal and the top pictures by means of multiple linear models previously calibrated using destructive measurements. Air temperature, relative humidity and VPD was monitored in eight spots of the greenhouse. Day and night air temperature was maintained at 24 and 18 °C respectively. Natural lighting was integrated with HPS lamps light in order to impose a 18/6-hour (light/dark) photoperiod. Plants where grown in cylindrical pots (55x15 cm) filled with peat-based compost. Pots were weighted twice per day in order to evaluate soil water content and thus, on the base of a previously estimated soil water retention curve, soil water potential. Plants were subjected to two soil water status: well-watered (**WW**) and water deficit (**WD**). In WW, soil water potential was maintained at >1 MPa; in WD, irrigation was suspended when the population was averagely at the 8th leaf stage. When soil water potential was less of the target threshold of -4 MPa, each pot was irrigated dispensing the exact amount of water needed to bring the soil water potential back to -4 MPa. The experimental unit

consisted in a single pot where a single plant was grown. Per each water treatment, eight randomized replicates of the entire IL population and the two parents were grown up to the 13th leaf stage. A lattice design was used to avoid the neighbouring of two replicates of the same genotype.

Thermal Time (TT) was estimated for WW and WD as 20 °C equivalent days as previously suggested (Parent et al., 2010). All time-related traits will be reported as referred to TT. As mentioned above, PhenoArch allows for two classes of automated measurements: ponderal (twice per day) and imaging (once every two days at night). Growth curves for biomass and leaf area were fitted using the package *grofit* (Kahm et al., 2010) in the statistical software R (The R Core Team, 2016). Three possible fitting models were evaluated: *logistic*, *Gompertz*, *modified Gompertz* and *Richards* (Zwietering et al., 1990). For each pot, the model with lower Akaike Information Criterion (AIC) was choose (Akaike, 1974). Ponderal measurements were took twice per day; each time the weight of the plant plus the pot and the tutor was measured immediately before and after watering. The amount of water evapo-transpired (ET) between two consecutive measurement was estimated as follow:

$$ET = W_{ai-1} - W_{bi} - \Delta B$$

Where:

W_{bi} is the weight of the pot plus the plant before watering at the i^{th} measurement

W_{ai-1} is the weight of the plant plus the pot after watering at the measurement preceding the i^{th}

ΔB is the increase in biomass between the two measurements.

In order to obtain comparable observations, we analysed the traits just in an evaluation time window between the imposition of the final target soil humidity in WD and the harvest. Rate of Biomass Accumulation (**BA**) was calculated as the biomass increase between the start and the end of the evaluation window divided for the TT elapsed. Daily Water Use (**WU**) was estimated as the total amount of water evapo-transpired during the evaluation window and its duration expressed in TT. Water Use Efficiency (**WUE**) was estimated as the total biomass increase in the evaluation window and the total amount of evapo-transpired water in the same time. Specific Transpiration (**T**) was calculated as the average amount of water used between two phenotyping points and the average LA of the plant during the same interval. Early Vigor (**EV**) was measured as estimated fresh biomass before the water deprivation treatment (~ 8th leaf stage). BA, WU and T response to water deficit (BA_res, WU_res and T_res) were calculated as the ratio between the standardized phenotypic values of each trait in WW and WD.

The number of visible leaves was scored visually twice per week. An additional score was given to the last visible leaf according to its stage of development as follows:

0.3 – leaf visible just inside the previous leaf sheath

0.5 – leaf blade just emerged the previous one sheath

0.8 – leaf blade fully visible and mostly expanded.

Leaf number was calculated as the number of visible leaves plus the last visible leaf score. Linear fitting was then performed between leaf number and thermal time. We refer to the slope of this fitting as phyllochron (**Phy**). Thus, Phy approximates the number of leaves emitted per thermal day. Since WD affected Phy and just three scores were available in the evaluation period, the results relatives to Phy are referred to the only WW plants.

Micro-environmental effect estimation

In order to evaluate the effects of the micro-environmental variation on the observed traits, a two-step strategy was adopted. First, for each trait the difference from the genotypic mean was calculated for each pot within the experimental design; secondly the micro-environmental effect of the XY position was calculated as the average of the difference of the pots surrounding the XY position. Outliers were detected using the Dixon's Q test (Dixon, 1951) and excluded from further analysis.

Statistical analysis and QTL detection

Statistical analysis was performed using the software R (The R Core Team, 2016). All the graphics and plots were made using the *ggplot2* package (Wickham, 2009). Two-tailed correlation tests were performed using the package *psych* v. 1.6.7 (Revelle, 2017) and the obtained p-values corrected according to Benjamini and Hockenberg (Hochberg and Benjamini, 1990) for false discovery rate. Correlation between traits measured in this experiment and experiments previously conducted on the same materials, were calculated on the BLUPs value of each line calculated by means of the *lme4* package (Bates et al., 2015) using the variable "Genotype" as the only random variable and no other fixed-effect variate. Principal Component Analysis (PCA) was performed on scaled values using the *princomp* function of the *stats* package (The R Core Team, 2016). Dunnett's multiple comparison test was carried out using the package *multcomp* (Dunnett, 1955; Hothorn et al., 2008). Broad sense heritability (h^2) was calculated using the function *repeatability* of the package *repeatability* (Wolak et al., 2012). The genetic position of the markers was assigned according to the nearest marker on the reference map "Genetics" (Coe et al., 2002). Single BIN QTL analysis was performed by t-test comparison between the lines carrying the given introgression and the lines

without the same introgression, and correcting the resulting p-values accordingly to Bonferroni (Bonferroni, 1936). We herein define QTL clusters those BINs or groups of BINs in strong LD (Fisher test p-value < 0.01) that showed evidence of trait-genotype association (p-value Bonferroni corrected <0.01) for at least two traits. In case of genetically linked QTL, QTL were considered as distinct in case of contrasting direction of genetic effect of the donor fragment.

2.3. Results

Effect of water regimes on vegetative growth and water use

The two water regimes (well-watered: WW and water deficit: WD) strongly influenced Biomass accumulation (BA), Daily water use (WU), Transpiration rate (T) and Water use efficiency (WUE), with a reduction of 69%, 46%, 42% and 44%, respectively (Fig. 1; Table 1) in the WD treatment. As an exemplification of the data type and quality collected in this experiment, the time-course (per day) change of BA in the two water regimes for all B73 pots is shown in Fig. 2.

Phy was measured in well-watered plants only. Early vigor (EV) was measured before starting the water deprivation period therefore no response to water regimes was made available. Trait repeatability (h^2) was overall acceptable ranging 0.50 - 0.59 for BA, WU and WUE, and 0.38-0.39 for T (Table 1). EV and Phy showed h^2 values of 0.53 and 0.62, respectively (Table 1).

Correlation among traits

BA, EV, WU, WUE and Phy were positively correlated in both WW and WD conditions (Fig. 4; Table 2). Instead, T generally showed weaker correlation values, with the only significant values observed between T_wd and WU_wd ($r = 0.33$) and with T_ww negatively correlated with BA_res and WU_res ($r = -0.39$ and -0.48, respectively). The three 'response to water deficit traits' (BA_res, T_res and WU_res) resulted positively correlated (r values from 0.58 to 0.82. $P < 0.001$), as expected given their physiological connection (ie. water deprivation is expected to impact in the same negative direction on the three traits). A PCA-based multivariate analysis of platform trait variation showed that the first two principal components (PC1 and 2) explained >80% of total variability (Fig. 3). Overall, vectors for traits collected in platform clustered in a comparable manner in WW and WD. In WW, PC1 was the result of similar loadings assigned to all the five platform traits while PC2 was mainly the result of positive load of WUE and negative load of T. In WD conditions, PC1 had the same composition observed for WW while PC2 mainly showed a contribution from WUE (positive loadings) and EV (negative loadings).

Correlations between platform traits with other morpho-physiological traits collected on the same IL lines in previous experiments (Salvi et al. 2011 and 2016) were also computed. Concerning

root traits, it is interesting to note that Root/Shoot ratio (R/ST) was negatively correlated with BA, EV, WU, WUE and Phy in both WW and WD conditions (r ranging from -0.19 to -0.45. Table 2) while its components (Embryonal Roots Dry Weight and Shoot Dry Weight, ERDWT and STDW, respectively) were not. Phenology-related traits evaluated in the field (Leaf Number and Days to Pollen Shed, LEAN and DPS respectively), showed little correlation with platform traits, except for mild correlations observed between LEAN and WU_ww (r = 0.30, P < 0.05) and between DPS and WUE_ww (r = -0.28, P <0.05).

Water use efficiency and response to water stress of IL lines

In our experiment, the two main components of WUE (BA and WU) were independently assessed, which provided the opportunity to explore physiological and genetic mechanisms responsible for WUE variation.

In WW, 18 IL lines showed higher WUE than B73 and just one line showed lower WUE (Table 3). For the 'high WUEww' lines, higher WUE was associated to higher BA coupled with non-significant difference for WU (seven lines), a non-significant increase in BA coupled with a non-significant reduction of WU (three lines) or an increase of both BA and WU but with a proportionally higher increase in BA (eight lines). The only IL line (IL38) with lower WUE in WW also showed lower WUE in WD; additionally, IL38 showed significantly lower values of WU in both water conditions, and lower BA and Phy, overall suggesting a developmental weakness likely caused by the homozygosity of low performance GF allele(s) not necessarily linked with water balance traits.

In WD, seven lines were characterized by WUE higher than B73 and six by lower WUE. Among the seven with higher WUE, six lines had high WUE associated with either much higher BA matched with unchanged WU (++BA & =WU. IL56, 60, 66 and 72) or by a slightly higher BA matched with a slightly lower WU (+BA & −WU. IL57 and 67. Table 3). The same six lines showed WUE higher than B73 in WW too. However, the seventh line (IL63) showed higher WUE than B73 at WD only. This line reached higher WUE than B73 by reducing WU (−26.99 g; P < 0.01. Dunnet test vs. B73, corrected for multiple tests) without affecting BA accumulation (Table 3). For IL63, a marginally significant reduction of WU was observed in WW too, however this reduction was not enough to impact on WUE in WW. Finally, IL63 showed a negative water use response to water deficit treatment (WU_res < 0. P < 0.001) while did not show any negative response on BA accumulation (BA_res ≈ 0). The same line did not show any significant difference from B73 for other traits such as EV, Phyl and T. Overall, these results suggest that different mechanisms of plant water balance regulation are in place among the different IL lines.

QTL for plant growth-related traits, water use and water use efficiency

A total of 20 QTL clusters and 8 non-overlapping QTL were detected in eight out of ten chromosomes confirming the complex genetic control of the nine physiological traits collected in platform (Fig. 5). Details on all QTL clusters composition and position, and single QTL position, effect, proportion of variance explained and statistical significance are reported in Table 4 also includes QTL for total number of leaf (LEAN), days to pollen shed (DPS), root to shoot ratio (R.ST), embryonic root dry weight (ERDW) and number of seminal roots (SRN) recomputed here using previously collected phenotypes (Salvi et al. 2011, Salvi et al. 2016) and the new 50k-SNP genotype matrix.

Overall, QTL for the tightly physiologically related traits BA, WU, and WUE showed a clear tendency to cluster, supporting the reliability of the results. Additionally, within the same cluster, QTL for these traits were characterized by highly concordant direction of genetic effect (eg. a positive BA genetic effect corresponded to a positive WUE genetic effect, as expected physiologically). In the following, when not specified, the QTL effect is discussed with reference to the Gaspé Flint (GF) allele.

At *Q1* (bin 1.01-02) the GF allele increased BA, WU, and WUE in WW condition and WU in WD condition. Similarly, at *Q4* (bin 2.01-02) the GF allele showed a positive effect on EV, WUE (both WW and WD), BA (in WD) and WU_res. *Q4* was in long-range LD with *Q3* on chromosome 1.

At *Q6* (bin 2.06-08) the GF introgression showed a strong negative effect on BAwd and EV, which likely negatively contributed to the concurrent negative effect on WUwd and WUEwd. This was also confirmed by the negative effect recorded for BA_res and WU_res.

At *Q8* (chr. 3), the GF substitution had a negative effect on most traits (BA, EV, WU and WUE) in both WW and WS conditions. Accordingly, no effect was observed on responsive traits (BA_res and WU_res). *Q8* encompassed a large portion of chromosome 2 (from 32 to 145 cM) due to the presence of very long GF chromosome introgressions and common introgressions among different IL lines.

The GF allele substitution at *Q11* (bin 4.03) induced a strong positive effect on EV (+8.5 g, $P < 1\times10^{-4}$) and had the strongest effect on biomass accumulation throughout the whole experiment (*Q11* BAww genetic effect: +3.97 g, $P < 1\times10^{-8}$). This effect likely drove the positive effect on WUEww and the negative effect on BA_res. It should be noticed that *Q11* seemed to act at WW only and no effect was detected in WD on any of the traits.

Q15 mapped at the bottom of chr. 6 and showed a negative genetic effect on EV and WUwd. The effect on EV was the strongest recorded in this experiment (−10.5 g, $P = 6.4 \times 10^{-9}$). *Q16* (chr. 8) showed a strong reduction in BAwd and WUwd, with a connected effect on WU_res.

At *Q17* (chr. 8), *19* (chr. 9) and *Q20* (chr. 10) GF allele substitutions showed mostly positive effects on BAwd, EV, WUEwd, WUEww and others, with the exception of mild negative effect on WUww at *Q17* only.

Phy QTL were mapped at four QTL clusters (*Q8*, *Q12*, *Q17* and *Q18*) with positive and negative genetic effects. At *Q8* (chr. 3), the GF allele reduced Phy rate (-0.011 leaf × thermal day^{-1}. $P = 3.6 \times 10^{-5}$) in accordance with the negative effect recorded for all other traits at this QTL cluster. At *Q12*, *Q17* and *Q18*, GF allele was associated with positive effects on Phy. Interestingly, at *Q17*, Phy QTL overlapped with the flowering time QTL *Vgt1* and *Vgt2*, known to segregate between GF and B73 (Salvi et al. 2011); more precisely, at this QTL cluster the GF substitution increased Phy rate (0.007 leaf × thermal day^{-1}. $P = 9.3 \times 10^{-3}$) while reducing the number of total nodes and number of days to flowering (Salvi et al. 2011. See Discussion).

2.4. Discussion

Correction for micro-environmental variability

Semi-controlled environments such as a greenhouse provide the possibility to grow plants in relatively ideal conditions strongly reducing the possibility that extreme or uncontrolled environmental events negatively affect the accuracy and repeatability of the experiment. The advanced PhenoArch system additionally allowed for accurate control of the soil water status. Nevertheless, micro-environmental variability was still detectable thus decreasing the heritability (repeatability) of the traits, if left unaccounted for. In order to address this problem, we have applied a correction method (fully explained in Materials and Methods). The method strongly increased h^2 values especially for those traits (T and EV) with low h^2 before the correction (Table 1). The main advantage of the proposed technique as compared to other methods is that it corrects for local non-random spatial effect not intercepted by other explanatory variables such as replicate, XY coordinate etc. Nevertheless, one of the limitation of the method is that while the spatial effect is limited to a specific position on the experimental grid, the moving replicates method extend the effect to the nearby positions owing to the limited number of plants for each moving rep, a problem that we partially addressed by discarding outliers from the moving rep prior to final analysis.

WUE was significantly lower in WD than in WW. This finding can be explained by the way the global evapo-transpiration was estimated. In this experiment, water was poured directly on soil surface hence the transpiration component of ET was affected similarly by the water treatment because evaporation was comparable between WW and WD conditions. Thus, the reduction in rate of biomass accumulation was proportionally higher than the reduction in evapo-transpiration,

resulting in lower WUE in the plants subjected to WD. Indeed, the reduction of BA and WU consequent to water deficit was equal to 69.6 and 46%, respectively while the reduction of WU was of just 46.0%.

Early vigor and its relationship with WUE

Given its importance in field performance and abiotic stress tolerance, genetic variation and control of early vigor in maize have been addressed in several studies (Hund et al., 2004; Jompuk et al., 2005; Liao et al., 2004; Presterl et al., 2007; Ruta et al., 2010; Trachsel et al., 2010, 2016). In our study, EV was one of the more strongly correlated traits with BA and WU in both water regimes. This is explained by the fact that early-vigor plants have also a larger canopy, which can better sustain plant growth. Positive correlation was also found with WUE in both water scenarios. The positive correlation with WUE can be explained by the fact that in plants with larger leaf area, the transpiration component tends to prevail on evaporation, thus reducing the role of water lost through evaporation. This is confirmed by the fact that eight out of eleven lines with significantly higher EV than B73, were more WUE in WW. By contrast, just three of the EV lines were among those more WUE in WD. QTL analysis allowed us to genetically localize the loci affecting EV. In this respect, QTL of EV and WUE often overlapped, like in the case of QTL cluster *Q1* (chromosome 1, BIN1.1) characterized by higher EV (+6.89 g) and WUE (+0.01%) in WW only. A similar effect was detected for *Q11* (chromosome 4, BIN 4.03). In the case of *Q4* and *Q19,* EV was positively associated with WUE in both WW and WD. Given the high LD (p-value <0.01) between these two BINs in our population, it was not possible to map the QTL to a single BIN.

Root shoot ratio measured at seedling stage is negatively correlated with WUE

Several studies have shown the importance of seminal RSA on adaptive capability of plants to abiotic stresses (Bishopp and Lynch, 2015; Hochholdinger and Tuberosa, 2009). In this study we had the opportunity to evaluate a population which was previously characterized for some RSA traits (Salvi et al. 2016). In Figure 4 we report the phenotypic correlations between root traits collected by Salvi et al. by means of the paper roll technique and shoot growth traits collected in this experiment. Unexpectedly, no significant correlation was detected between shoot dry weight at seedling stage and growth components. On the other hand, significant correlations were found between root/shoot ratio and BA and WUE in WW; BA, WU and WUE in WD, other than with EV and Phy. Among the lines used in this experiment, two were found to have a higher R.ST than B73 and six a lower one. Only one of the latter lines showed significantly different EV as compared to the RP while half of them were different in terms of BA in WW and three out of

eight in WD. Interestingly, the embryonal root dry weight was negatively correlated with Phy and not with the other measured traits. These results indicate that those plants preferentially allocate more carbon to the shoot at seedling stage, maintain similar behaviour across the entire vegetative growth. This explains also the negative correlation found between R.ST and WUE: a more shoot-oriented allocation of metabolites resulted in improved shoot growth, water consumption made equal. This hypothesis seems to be confirmed by the colocalization of R.ST and WUE QTL in *Q1* and *Q17*, although the low genetic resolution of this experiment does not permit us to exclude the action of linked but functionally distinct genes underlying the two traits. The confidence interval of *Q1* indeed includes *Rtcs*, a gene previously characterized for its influence on RSA (Taramino et al., 2007) and already proposed as candidate for a QTL for number of seminal roots mapped in the same region (Salvi et al. 2016). Several QTL for RSA were also identified on the *Q17* region in different genetic backgrounds (Burton et al., 2014; Pestsova et al., 2016; Wu et al., 2015; Zurek et al., 2015). This notwithstanding, a constitutively reduced allocation of photosyntates to the RSA might be detrimental in case of nutrient/water limited field conditions. Notably, yield QTL have been detected in the same region of *Q1* in WW field conditions but not in WD (Millet et al., 2016).

Among the 73 IL lines, IL63 showed the higher WUE and could be considered an example of "conservative WUE" line. IL63 line showed lower WU and similar BA when compared to the RP (B73) in WD conditions. Interestingly, this line did not show lower T as compared to B73. IL63 carries a 27.2 cM Gaspé Flint introgression between the BINs 3.04 and 3.05 (69.8 cM – 97.03 cM of the Genetics reference map) and was previously shown to be early flowering when compared with B73 due to a major QTL, named *Vgt3* (Salvi et al. 2011), similarly mapped in several independent experiments (Romay et al. 2013; Hirsch et al. 2014; Millet et al. 2016). Additionally, the same line develops a higher proportion of juvenile leaves (Salvi et al. 2011) which are characterized by a much higher leaf epicuticular wax than adult leaves ((Poethig, 1990; Vega et al., 2002). In IL63, transition occurs at leaf-10 rather than at leaf-7- 8 as in B73. Thus, the higher WUE of this line (and of the corresponding QTL) could be due to the fact that this line allocated less of its photosyntetates to canopy expansion than to other shoot sinks (e.g. stem, leaves thickness) thus maintaining low water use at the same time.

Flowering time genes and WUE

The IL lines studied in this experiment were formerly characterized for phenology traits such as DPS, LEAN and others (Salvi et al., 2011). Specifically, this population is known to segregate for *vgt1* and *vgt2* (Bouchet et al., 2013; Chardon et al., 2005; Salvi et al., 2002) and these two strong flowering time QTL map within the confidence interval of *Q17*, a QTL cluster where the Gaspé

Flint allele shortened flowering time and increased WUE in both WW and WD, with a significant effect on BA in both conditions. It is also interesting to notice that within the QTL cluster *Q17*, *Vgt1* coincided with the peak of a Phy QTL (Bin 8.05, 104.6 - 138.2 Mb. Supp Tab. 2) where Gaspé Flint again contributed for the positive effect allele (in this case, increaed pace of leaf emission). Additionally, a large GWA study recently identified a major flowering time QTL (SNP marker AX-91405380, 159.5 Mb) near but distinct from *Vgt1*, characterized by a positive effect on yield in many water regimes (Millet et al. 2017). A simple, although still speculative explanation is that *vgt1* (or perhaps the combination of different flowering time QTL at bin 8.05-06, in strong LD in this population) might act on flowering time not only by affecting the time of transition of the apical meristem to the reproductive phase, but also by acting on the vegetative developmental pace (either plastochron or Phy, or both), providing the opportunity for the early-Gaspé Flint allele to accumulate more biomass per unit of time. The use of the PhenoArch platform was instrumental for the detection of the genetic effect on Phy.

2.5. Conclusions

This study identified and characterized several maize IL lines with well-defined contrasting physiological responses to water regimes, in the B73 elite genetic background, the most extensively investigated line in maize from genetic and physiological standpoints. For the first time, we observed a correlation between root/shoot ratio at seedling stage and WUE at full vegetative growth. Indeed, it seems that the tendency of certain genotypes to preferentially allocate resources to the shoot results in an increase in WUE, especially in WW conditions. In the case of QTL cluster *Q1*, the presence within the confidence interval of a strong candidate gene such as *Rtcs* could indicate it as candidate gene for the reduced root/shoot ratio. In the other case, further fine mapping efforts are needed in order to identify the causal genes. As regard to phenology traits, a QTL for delayed juvenile to adult transition was shown to affect WUE in WD conditions and it is possible that this association is linked to an augmented number of wax-coated juvenile leaves. Additionally, for the first time a significant effect of a major flowering time QTL (*Vgt1*) was detected on maize Phy, with the early flowering allele also contributing to faster Phy and thus positively affecting biomass accumulation and WUE. Although the presence of more than one introgression in the same IL line often limited the capability to accurately localize the QTL, this study provided clear evidence of the power of high-throughput phenomics investigation on well characterized elite genetic materials, towards the genetic dissection of physiological processes of agronomic impact such as plant response to water deficit.

2.6. Tables and figures

Table 1 Mean values of the observed traits for the entire population and the RP (B73) in both the experimental conditions. Broad sense heritability is reported both before and after the moving replicates correction.

Variable ID	Variable description	Unit	Population average WW	B73 WW	Population average WD	B73 WD	H^2 before correction WW	H^2 after correction WW	H^2 before correction WD	H^2 after correction WD
BA	Daily biomass accumulation	g/20°C day	11.15	11.08	3.422	3.55	0.32	0.57	0.33	0.55
WU	Daily water use	g/20°C day	186.2	180.9	101.08	106.7	0.35	0.59	0.29	0.53
T	Specific transpiration rate	g/m^{2}20°C day	113.8	115.2	66.51	69.74	0.33	0.38	0.20	0.39
WUE	Water use efficiency	g/g	0.0594	0.053	0.0335	0.0329	0.37	0.50	0.34	0.52
EV	Early Vigor	g	48.06	46.58	NA	NA	0.22	0.53	NA	NA
Phy	Phyllochron	Leaves/20°C day	0.27	0.27	NA	NA	0.43	0.62	NA	NA
BA_res	BA response to water deficit	Standard BA_ww/ Standard BA_wd	NA	NA	0.857	0.947	NA	NA	NA	0.40
WU_res	WU response to water deficit	Standard WU_ww/ Standard WU_wd	NA	NA	0.979	1.169	NA	NA	NA	0.57
T_res	Transpirative response to water deficit	Standard T_ww/ Standard T_wd	NA	NA	0.831	0.951	NA	NA	NA	0.47

Table 2 Correlation matrix reporting in the bottom left corner Pearson's correlation among traits and in the top right corner significance of the correlation. Correlations between the following traits are reported: daily biomass accumulation (BA, g/20°C day), daily evapo-transpired water (WU, g/20°C day), early vigor measured as estimated fresh weight at eight leaves (EV, g), specific transpiration measured as WU per cm2 of leaf area(T, WU/cm2), water use efficiency, (WUE, BA/WU, g/g), Phyllochron (leaves emitted per 20 °C day). Suffixes "ww" and "wd" indicate whether the QTL was detected on well-watered or water deficit conditions respectively. Traits measured by Salvi et al. 2011 and Salvi et al. 2016 are reported as DPS (days per pollen shed), LEAN (leaf number), R.ST (root-shoot ratio, g/g), ERDW (embryonal root dry weight, g) and STDW (shoot dry weight, g).

	WU_ww	T_ww	Phy	WUE_ww	BA_ww	WU_wd	T_wd	WUE_ wd	BA_wd	WU_res	BA_res	T_res	LEAN	DPS	ERDW	STDW	SRN	R.ST	EV
WU_ww		***	***	***	***	***		*	***	***	***	**	*						***
T_ww	0.47						*			***	**	***							
Phy	0.61	0.01		***	***	**		***	***	*	*				*			***	***
WUE_ww	0.41	0.03	0.63		***	**		***	***		*			*				***	***
BA_ww	0.80	0.26	0.71	0.87		***		***	***	*	***							**	***
WU_wd	0.63	0.09	0.40	0.40	0.60		*	***	***	*	*							*	***
T_wd	0.03	0.33	-0.19	-0.03	-0.02	0.33						***							
WUE_wd	0.30	-0.09	0.54	0.79	0.65	0.48	0.09		***						*			**	***
BA_wd	0.52	0.02	0.54	0.70	0.73	0.83	0.25	0.88										**	***
WU_res	-0.48	-0.48	-0.31	-0.12	-0.31	0.31	0.19	0.06	0.20		***	***							
BA_res	-0.41	-0.39	-0.30	-0.30	-0.41	0.28	0.26	0.17	0.26	0.82		***							
T_res	-0.36	-0.49	-0.18	-0.07	-0.24	0.23	0.64	0.14	0.21	0.62	0.58								
LEAN	0.30	0.06	0.08	-0.24	0.01	0.14	0.16	-0.19	-0.05	-0.24	-0.09	0.06		***	**		***	**	
DPS	0.18	0.08	-0.12	-0.28	-0.08	0.05	0.20	-0.22	-0.10	-0.22	-0.11	0.08	0.78		**		***	***	
ERDW	-0.07	0.11	-0.32	-0.28	-0.21	-0.16	0.16	-0.30	-0.27	-0.05	-0.01	0.03	0.43	0.39		***	***	***	
STDW	0.15	0.12	0.10	0.16	0.21	0.15	0.06	0.08	0.13	0.03	-0.01	-0.07	0.08	-0.07	0.56				
SRN	0.07	-0.03	-0.17	-0.14	-0.06	0.02	0.16	-0.01	0.00	-0.12	0.03	0.11	0.52	0.54	0.53	0.05		***	
R.ST	-0.19	0.04	-0.45	-0.45	-0.41	-0.31	0.15	-0.40	-0.41	-0.09	-0.02	0.10	0.37	0.48	0.71	-0.17	0.58		*
EV	0.71	0.14	0.59	0.71	0.83	0.60	-0.03	0.64	0.73	-0.22	-0.21	-0.16	-0.04	-0.07	-0.21	0.07	0.02	-0.29	

Table 3 Differences between the observed values of the IL lines vs. B73. Asterisks indicate significance levels calculated by the Dunnett's multiple comparison test and indicate the following p-value: ""≤ 0.05, "**" ≤ 0.01 and "***" ≤ 0.001*

	WW						WD				Response to WD		
	BA	WU	EV	T	WUE	Phy	BA	WU	T	WUE	BA	WU	T
B73_ita	9.781	180.855	35.526	0.023	0.053	0.268	3.55	106.735	0.014	0.032	1.34	1.235	1.132
NILG01	0.775	7.991	1.933	0	0.002	0.005	-0.706	-14.286*	0	-0.002	-0.579**	-0.571**	-0.36.
NILG03	3.141**	28.448**	4.692	0	0.009	0.005	0.127	9.099	-0.001.	-0.001	-0.477*	-0.191	-0.403*
NILG05	1.682	10.993	1.712	0	0.006	0.006	-0.493	-12.633*	-0.001***	-0.001	-0.583**	-0.553**	-0.404*
NILG07	3.117**	23.087.	1.638	0	0.008	0.002	0.039	-1.824	-0.001***	0.001	-0.509**	-0.427.	-0.565***
NILG09	0.91	-4.613	-1.774	0	0.006	0.006	-0.718	-17.093**	-0.001***	-0.002	-0.604**	-0.522*	-0.452*
NILG10	0.021	-9.504	-1.87	0	0.002	0.003	-0.225	-12.044*	0	0.001	-0.151	-0.249	-0.205
NILG12	0.691	8.486	0.816	-0.001*	0.003	0.003	-0.033	-3.033	-0.001*	0.001	-0.186	-0.191	-0.036
NILG13	3.856***	22.082	10.038***	0	0.014***	0.007	-0.298	-11.904.	-0.002***	0.001	-0.701***	-0.627***	-0.814***
NILG14	1.959	0.282	3.235	0	0.011*	-0.001	-0.635	-7.744	-0.001***	-0.002	-0.679***	-0.266	-0.602***
NILG15	1.947	35.261***	2.84	0.002***	0.001	0.011	0.343	8.579	0	0	-0.225	-0.245	-0.429**
NILG16	2.961**	31.878**	7.697***	0	0.006	0.003	0.32	6.495	0	0.001	-0.379	-0.288	-0.289
NILG17	-0.097	-14.381	-8.297***	0	0	-0.01	-0.779*	-18.535***	0	-0.002	-0.482*	-0.432.	-0.427**
NILG18	-0.585	-10.723	-6.414*	0	0	-0.002	-0.916**	-21.531***	-0.001***	-0.002	-0.491*	-0.615***	-0.608***
NILG19	2.004	1.776	3.846	0	0.009	0.002	0.069	-5.755	-0.001*	0.004.	-0.36	-0.224	-0.278
NILG20	1.887	1.426	4.741	0	0.011*	0.014**	0.305	-3.14	-0.001.	0.004.	-0.291	-0.132	-0.145
NILG21	1.437	3.475	2.703	0	0.007	-0.001	-0.326	-7.029	-0.001*	0	-0.47.	-0.292	-0.375
NILG23	-2.153	-16.611	-7.821***	0	-0.008	-0.021***	-1.173***	-13.839**	0	-0.007***	-0.295	-0.17	0.004
NILG24	-1.594	-31.132**	-8.281***	0	-0.002	-0.034***	-1.393***	-21.933***	0	-0.007***	-0.688***	-0.198	-0.228
NILG25	-1.822	-18.84	-1.912	0	-0.003	-0.009	-1.07***	-23.642***	-0.001**	-0.004	-0.303	-0.478.	-0.567***
NILG26	0.701	11.805	-0.255	0	0	0.004	-1.33***	-26.291***	-0.001***	-0.004.	-0.904***	-0.936***	-0.546***
NILG27	-0.497	-14.208	2.737	0	0	-0.01	-0.98***	-17.155***	-0.002***	-0.004	-0.519**	-0.352	-0.699***
NILG28	2.043	20.999	7.446**	0	0.005	0.004	-0.172	-6.773	-0.001**	0	-0.476*	-0.5*	-0.58***
NILG29	-0.189	-11.526	-4.121	0	0.002	0	-0.56	-12.598*	-0.001**	-0.001	-0.323	-0.231	-0.428**
NILG30	1.341	2.941	3.436	0	0.006	0.009	-0.479	-9.753	-0.001*	-0.001	-0.534**	-0.372	-0.468*
NILG31	2.973**	43.206***	4.368	0	0.005	0.013*	-0.07	-0.896	-0.001***	0	-0.538**	-0.521*	-0.645***

	WW						WD				Response to WD		
	BA	WU	EV	T	WUE	Phy	BA	WU	T	WUE	BA	WU	T
NILG32	3.06**	32.652***	4.967	0	0.007	0.012.	0.058	3.221	0	0	-0.495**	-0.367	-0.397*
NILG34	3.278**	19.784	4.107	0	0.008	-0.001	0.125	4.517	0	0	-0.492*	-0.193	-0.359.
NILG37	-1.254	-16.439	-7.342**	0.001.	-0.002	-0.02***	-0.874**	-8.664	0	-0.006***	-0.295	0.067	-0.133
NILG38	-2.85**	-32.345***	-13.596***	-0.002***	-0.013**	-0.014*	-0.904**	-4.319	-0.002***	-0.006***	0.493*	1.151***	-0.068
NILG40	1.116	26.523*	5.856*	0	0	0.007	0.254	-3.774	0	0.003	-0.1	-0.439	-0.321
NILG42	1.907	7.043	0.512	0	0.008	0.006	-0.159	-10.871	0	0.002	-0.494**	-0.482*	-0.339
NILG43	-0.172	6.839	1.63	0	-0.002	-0.009	0.072	-4.052	-0.001***	0.001	-0.02	-0.25	-0.692***
NILG44	2.252.	9.308	5.689*	0	0.009.	0	0.608	5.423	0	0.003	-0.197	-0.036	-0.122
NILG45	1.665	6.94	-3.873	0	0.005	0.006	-0.395	-10.781	-0.001.	0	-0.533**	-0.455*	-0.434**
NILG46	2.175	17.177	3.358	0	0.009	0.007	0.023	-1.572	0	0.001	-0.445.	-0.318	-0.386*
NILG47	2.849**	26.489*	2.321	0	0.007	0.013*	0.013	3.981	-0.001**	0	-0.49*	-0.287	-0.459**
NILG48	2.174	2.502	5.254	0	0.012**	0.012.	0.28	-1.349	-0.001**	0.003	-0.29	-0.093	-0.168
NILG49	3.891***	30.512**	6.538*	0	0.012**	0.015**	0.299	5.61	-0.001	0.001	-0.453*	-0.271	-0.317
NILG50	0.816	17.649	-1.348	0.001	0	0.008	-1.135***	-19.179***	-0.001**	-0.005*	-0.823***	-0.782***	-0.577***
NILG51	0.446	-19.915	1.793	-0.001	0.008	-0.005	-0.613	-19.259***	-0.001.	0	-0.477*	-0.356	-0.022
NILG52	2.883**	14.859	5.386	0	0.01*	0.009	0.109	-2.437	0	0.002	-0.455	-0.312	-0.278
NILG53	1.734	13.149	0.38	0	0.009	-0.005	0.271	-3.666	-0.001*	0.004	-0.224	-0.241	-0.448**
NILG54	-3.177***	-38.258***	-7.157**	0	-0.01.	-0.034***	-1.128***	-16.088***	0	-0.006***	0.431.	0.701***	-0.161
NILG55	0.371	-1.821	-0.994	0	0.003	0.005	-0.393	-13.231*	-0.001**	0.001	-0.421.	-0.422	-0.328
NILG56	4.157***	-0.176	0.532	0	0.023***	0.021**	0.866**	2.261	0	0.007***	-0.317	0.08	-0.386*
NILG57	1.695	-6.893	1.752	0	0.015***	0.009	0.222	-7.668	-0.001*	0.005**	-0.241	-0.096	-0.097
NILG58	-0.989	-36.934***	-3.709	-0.001**	0.005	-0.003	-0.303	-13.204*	-0.001***	0	0.097	0.844***	0.049
NILG59	3.243***	9.968	3.388	0	0.014***	0.019***	-0.31	-9.991	-0.002***	0	-0.658***	-0.466*	-0.731***
NILG60	2.991**	-20.018	5.752	0	0.018***	0.01	0.916**	-0.782	-0.001.	0.006***	-0.023	0.354	-0.175
NILG61	0.459	-6.284	-1.075	0	0.004	0.007	-0.585	-12.308*	-0.001*	-0.001	-0.462*	-0.319	-0.138
NILG62	-0.993	-16.93	-1.672	-0.001	-0.001	-0.005	-0.544	-17.121***	-0.001***	0	-0.097	-0.338	-0.383*
NILG63	-0.092	-25.552*	-3.436	0	0.007	0.002	-0.424	-26.991***	0	0.005**	-0.254	-0.676***	-0.276
NILG64	4.237***	32.065**	10.309***	0	0.014***	0.022***	0.831*	12.194.	0	0.003	-0.338	-0.164	-0.045
NILG65	2.109	37.392***	8.288***	0	0.004	0.004	0.733.	6.264	0	0.001	-0.094	-0.346	-0.403*

	WW						WD				Response to WD		
	BA	WU	EV	T	WUE	Phy	BA	WU	T	WUE	BA	WU	T
NILG66	1.522	-16.242	4.64	0	0.015***	-0.003	0.755*	-1.576	0	0.007***	0.051	0.52*	0.177
NILG67	2.087	-2.816	9.615***	0	0.014***	-0.001	0.711.	-0.872	-0.001.	0.006***	-0.125	0	-0.378.
NILG68	3.364***	7.107	6.737**	0	0.015***	0.005	0.352	-5.575	0	0.004.	-0.406.	-0.363	-0.119
NILG70	2.886**	7.965	6.363*	0	0.014***	0	0.263	-3.229	0	0.003	-0.421.	-0.229	-0.168
NILG71	0.838	0.105	0.497	0	0.005	0.003	-0.217	-4.216	-0.001**	0	-0.318	-0.144	-0.4*
NILG72	4.616***	40.934***	16.353***	0	0.011**	0.002	1.071***	11.081	-0.001.	0.005*	-0.298	-0.281	-0.327
NILG75	4.332***	30.049**	9.304***	0.001.	0.014***	0.007	0.428	-2.608	-0.001*	0.004	-0.486*	-0.473.	-0.584***
NILG76	6.227***	25.86*	9.552***	0	0.023***	0.003	0.364	0.229	0	0.003	-0.65***	-0.39	-0.339
NILG77	1.342	9.582	-1.645	0.001	0.004	-0.01	-0.238	-5.961	0	-0.001	-0.357	-0.344	-0.474**

Table 4. QTL clusters detected by single BIN regression for the following traits: daily biomass accumulation (BA, g/20°C day), daily evapo-transpired water (WU, g/20°C day), early vigor measured as estimated fresh weight at eight leaves(EV, g), specific transpiration measured as WU per cm2 of leaf area(T, WU/cm2), water use efficiency, (WUE, BA/WU, g/g), Phyllochron (leaves emitted per 20 °C day). Suffixes "ww" and "wd" indicate whether the QTL was detected on well-watered or water deficit conditions respectively. The suffix "res" indicate the response of the trait to water deficit. QTL for traits measured by Salvi et al. 2011 and Salvi et al. 2016 are reported as DPS (days per pollen shed), LEAN (leaf number), R.ST (root-shoot ratio, g/g), ERDW (embryonal root dry weight, g).

Cluster[a]	Chr.	Position[b]		Marker	Effect[c]	r2	Phenotype	p_Bonferroni[d]	Left[e]		Right[e]		BIN[f]	BIN left[g]	BIN right[g]
		cM	Mbp						Mbp	cM	Mbp	cM			
Q1	1	25.75	10.54	PZE.101018057	-3.674	0.11	DPS	5.65E-06	10.54	25.75	10.54	25.75	1.01	1.01	1.01
Q1	1	25.75	9.43	SYN14147	6.692	0.02	EV	3.79E-03	9.43	25.75	9.43	25.75	1.01	1.01	1.01
Q1	1	25.75	10.54	PZE.101018057	-1.599	0.08	LEAN	4.06E-04	10.54	25.75	10.54	25.75	1.01	1.01	1.01
Q1	1	25.75	10.54	PZE.101018057	-0.239	0.13	R.ST	4.96E-03	10.54	25.75	12.26	28.50	1.01	1.01	1.01
Q1	1	25.75	9.43	SYN14147	-1.570	0.13	SRN	2.58E-03	9.43	25.75	42.92	61.58	1.01	1.01	1.03
Q1	1	25.75	9.43	SYN14147	16.808	0.06	WUwd	9.79E-06	9.43	25.75	9.43	25.75	1.01	1.01	1.01
Q1	1	25.75	9.43	SYN14147	25.977	0.03	WUww	5.24E-03	9.43	25.75	9.43	25.75	1.01	1.01	1.01
Q1	1	28.50	12.43	PZE.101021574	-2.146	0.08	LEAN	9.98E-04	12.43	28.50	12.43	28.50	1.02	1.02	1.02
Q1	1	37.20	19.24	PZE.101031377	3.313	0.06	BAww	2.98E-06	19.24	37.20	24.69	42.50	1.02	1.02	1.02
Q1	1	37.20	19.24	PZE.101031377	6.899	0.02	EV	9.85E-04	19.24	37.20	35.58	54.94	1.02	1.02	1.03
Q1	1	37.20	19.24	PZE.101031377	0.010	0.03	WUEww	6.44E-03	19.24	37.20	19.24	37.20	1.02	1.02	1.02
Q2	1	40.15	20.11	SYN35792	-0.064	0.05	BA_res	3.50E-05	20.11	40.15	35.58	54.94	1.02	1.02	1.03
Q2	1	40.15	20.11	SYN35792	-3.314	0.06	DPS	3.90E-03	20.11	40.15	35.58	54.94	1.02	1.02	1.03
Q2	1	40.15	20.11	SYN35792	-1.824	0.08	LEAN	4.53E-04	20.11	40.15	42.92	61.58	1.02	1.02	1.03
Q2	1	61.58	42.92	SYN11249	-0.061	0.04	BA_res	2.01E-04	42.92	61.58	42.92	61.58	1.03	1.03	1.03
Q2	1	61.58	42.92	SYN11249	-0.580	0.03	BAwd	3.89E-03	42.92	61.58	42.92	61.58	1.03	1.03	1.03
Q2	1	61.58	42.92	SYN11249	-2.812	0.06	DPS	6.92E-03	42.92	61.58	42.92	61.58	1.03	1.03	1.03
Q2	1	61.58	42.92	SYN11249	-0.398	0.09	T_res	6.19E-10	35.58	54.94	42.92	61.58	1.03	1.02	1.03
Q2	1	61.58	42.92	SYN11249	-4.466	0.07	T_wd	1.19E-07	35.58	54.94	42.92	61.58	1.03	1.02	1.03
Q2	1	61.58	42.92	SYN11249	-0.072	0.05	WU_res	5.15E-05	42.92	61.58	42.92	61.58	1.03	1.03	1.03
Q2	1	61.58	42.92	SYN11249	-9.350	0.03	WUwd	6.62E-03	42.92	61.58	42.92	61.58	1.03	1.03	1.03

Cluster[a]	Chr.	Position[b]		Marker	Effect[c]	r2	Phenotype	p_Bonferroni[d]	Left[e]		Right[e]		BIN[f]	BIN left[g]	BIN right[g]
		cM	Mbp						Mbp	cM	Mbp	cM			
Q3	1	231.85	278.71	PZE.101229026	0.063	0.03	WU_res	3.17E-03	278.71	231.85	280.98	241.01	1.10	1.10	1.10
Q3	1	228.35	274.71	SYN19653	0.003	0.03	WUEwd	8.36E-03	274.71	228.35	276.25	231.85	1.10	1.10	1.10
Q3	1	228.35	274.71	SYN19653	0.253	0.04	T_res	5.20E-04	265.45	220.76	280.98	241.01	1.10	1.10	1.10
Q3	1	242.00	283.39	PZE.101235852	0.467	0.09	T_res	6.74E-10	283.09	242.00	285.06	243.25	1.11	1.11	1.11
Q3	1	242.00	283.39	PZE.101235852	4.253	0.04	T_wd	1.57E-04	283.39	242.00	285.06	243.25	1.11	1.11	1.11
Q3	1	242.00	283.39	PZE.101235852	0.078	0.04	WU_res	4.40E-04	283.39	242.00	285.06	243.25	1.11	1.11	1.11
S1	1	257.75	289.06	PZE.101242552	-5.241	0.12	ERDWppr	8.71E-03	289.06	257.75	289.57	258.58	1.11	1.11	1.11
Q4	2	7.73	3.39	PZE.102006513	5.651	0.02	EV	1.71E-03	3.39	7.73	3.39	7.73	2.01	2.01	2.01
Q4	2	20.58	6.00	PZE.102013873	0.757	0.04	BAwd	3.55E-04	6.00	20.58	9.13	23.51	2.02	2.02	2.02
Q4	2	20.58	6.00	PZE.102013873	5.921	0.02	EV	5.81E-04	6.00	20.58	6.00	20.58	2.02	2.02	2.02
Q4	2	20.58	6.00	PZE.102013873	0.006	0.06	WUEwd	8.03E-07	6.00	20.58	9.13	23.51	2.02	2.02	2.02
Q4	2	20.58	6.00	PZE.102013873	0.010	0.04	WUEww	2.37E-04	6.00	20.58	6.00	20.58	2.02	2.02	2.02
Q4	2	23.51	9.13	SYN1141	0.088	0.03	WU_res	6.74E-03	9.13	23.51	9.13	23.51	2.02	2.02	2.02
Q5	2	42.00	16.78	SYN9947	-0.091	0.04	BA_res	3.36E-04	16.78	42.00	20.39	54.13	2.03	2.03	2.03
Q5	2	42.00	16.78	SYN9947	-0.391	0.04	T_res	1.04E-03	16.78	42.00	20.39	54.13	2.03	2.03	2.03
Q5	2	61.00	28.05	PZE.102050267	-0.066	0.03	BA_res	7.01E-03	28.05	61.00	28.05	61.00	2.03	2.03	2.03
S2	2	54.13	20.52	PZE.102040935	9.698	0.02	EV	9.58E-04	20.52	54.13	20.52	54.13	2.03	2.03	2.03
Q6	2	95.75	177.44	PZE.102127663	-7.445	0.03	EV	7.84E-07	177.44	95.75	194.63	113.45	2.06	2.06	2.07
Q6	2	103.53	186.27	PZE.102137410	-0.686	0.04	BAwd	1.55E-04	186.27	103.53	205.94	126.85	2.06	2.06	2.08
Q6	2	103.53	186.27	PZE.102137410	0.001	0.03	Tww	2.52E-03	186.27	103.53	194.63	113.45	2.06	2.06	2.07
Q6	2	103.53	186.27	PZE.102137410	-0.004	0.03	WUEwd	2.70E-03	186.27	103.53	194.63	113.45	2.06	2.06	2.07
Q6	2	103.53	186.27	PZE.102137410	-11.229	0.05	WUwd	1.36E-04	186.27	103.53	205.94	126.85	2.06	2.06	2.08
Q6	2	120.18	203.63	SYN10567	-0.053	0.04	BA_res	1.21E-03	203.63	120.18	205.94	126.85	2.07	2.07	2.08
Q6	2	120.18	203.63	SYN10567	-0.278	0.05	T_res	3.94E-05	203.63	120.18	205.94	126.85	2.07	2.06	2.08
Q6	2	120.18	203.63	SYN10567	-0.074	0.06	WU_res	1.08E-06	186.27	103.53	205.94	126.85	2.07	2.06	2.08
Q6	2	150.23	220.83	PZE.102178234	-0.053	0.04	BA_res	1.21E-03	220.83	150.23	220.83	150.23	2.08	2.08	2.08
Q6	2	150.23	220.83	PZE.102178234	-0.585	0.04	BAwd	5.02E-04	220.83	150.23	220.83	150.23	2.08	2.08	2.08

Cluster[a]	Chr.	Position[b]		Marker	Effect[c]	r2	Phenotype	p_Bonferroni[d]	Left[e]		Right[e]		BIN[f]	BIN left[g]	BIN right[g]
		cM	Mbp						Mbp	cM	Mbp	cM			
Q6	2	150.23	221.24	PZE.102178542	-6.037	0.03	T_wd	4.47E-03	221.24	150.23	221.24	150.23	2.08	2.08	2.08
Q6	2	150.23	220.83	PZE.102178234	-0.278	0.05	T_res	3.94E-05	220.83	150.23	220.83	150.23	2.08	2.08	2.08
Q6	2	150.23	220.83	PZE.102178234	-0.074	0.06	WU_res	1.08E-06	220.83	150.23	220.83	150.23	2.08	2.08	2.08
Q6	2	150.23	220.83	PZE.102178234	-10.366	0.05	WUwd	5.20E-05	220.83	150.23	220.83	150.23	2.08	2.08	2.08
Q7	2	126.85	206.50	PZE.102160379	9.698	0.02	EV	9.58E-04	206.50	126.85	206.50	126.85	2.08	2.08	2.08
Q7	2	126.85	206.50	PZE.102160379	-6.037	0.03	T_wd	4.47E-03	206.50	126.85	206.50	126.85	2.08	2.08	2.08
Q7	2	134.70	210.31	PZE.102165681	9.698	0.02	EV	9.58E-04	210.31	134.70	213.21	140.81	2.08	2.08	2.08
Q7	2	134.70	210.31	PZE.102165681	-6.037	0.03	T_wd	4.47E-03	210.31	134.70	213.21	140.81	2.08	2.08	2.08
Q7	2	150.23	221.24	PZE.102178542	9.698	0.02	EV	9.58E-04	221.24	150.23	221.24	150.23	2.08	2.08	2.08
Q8	3	32.35	12.13	PZE.103019668	-0.730	0.06	BAwd	7.94E-07	12.13	32.35	113.35	69.83	3.03	3.03	3.04
Q8	3	32.35	12.13	PZE.103019668	-2.399	0.07	BAww	4.24E-08	12.13	32.35	170.46	100.30	3.03	3.03	3.06
Q8	3	32.35	12.13	PZE.103019668	-0.011	0.05	Phy	3.64E-05	12.13	32.35	170.46	100.30	3.03	3.03	3.06
Q8	3	32.35	12.13	PZE.103019668	-0.005	0.07	WUEwd	3.19E-07	12.13	32.35	97.37	63.65	3.03	3.03	3.04
Q8	3	32.35	12.13	PZE.103019668	-0.009	0.06	WUEww	2.97E-06	12.13	32.35	170.46	100.30	3.03	3.03	3.06
Q8	3	32.35	12.13	PZE.103019668	-8.864	0.03	WUwd	5.99E-03	12.13	32.35	170.46	100.30	3.03	3.03	3.06
Q8	3	32.35	12.13	PZE.103019668	-18.491	0.04	WUww	3.91E-04	12.13	32.35	169.11	98.70	3.03	3.03	3.06
Q8	3	41.73	17.18	PZE.103024586	-1.186	0.07	LEAN	3.68E-03	17.18	41.73	28.62	47.70	3.04	3.04	3.04
Q8	3	45.43	20.74	PZE.103028239	-4.131	0.02	EV	5.11E-05	20.74	45.43	154.66	86.76	3.04	3.04	3.05
Q8	3	53.56	38.60	PZE.103041877	-1.630	0.09	LEAN	2.44E-04	38.60	53.56	67.70	61.27	3.04	3.04	3.04
Q8	3	69.83	113.35	SYN1588	-1.690	0.07	LEAN	2.73E-03	113.35	69.83	169.11	98.70	3.04	3.04	3.06
Q8	3	86.76	157.02	PZE.103097269	-0.781	0.10	BAwd	1.25E-11	157.02	86.76	170.46	100.30	3.05	3.05	3.06
Q8	3	86.76	157.02	PZE.103097269	-0.004	0.06	WUEwd	5.76E-06	157.02	86.76	176.33	105.90	3.05	3.05	3.06
Q8	3	100.30	170.46	PZE.103109970	-1.124	0.07	LEAN	1.47E-03	170.46	100.30	176.33	105.90	3.06	3.06	3.06
Q8	3	105.90	176.33	SYN7426	2.740	0.04	T_ww	9.58E-04	176.33	105.90	176.33	105.90	3.06	3.06	3.06
Q8	3	112.85	178.15	PZE.103119393	-0.564	0.05	BAwd	2.36E-05	178.15	112.85	202.95	145.00	3.06	3.06	3.07
Q8	3	112.85	178.15	PZE.103119393	-1.615	0.04	BAww	2.84E-04	178.15	112.85	202.95	145.00	3.06	3.06	3.07
Q8	3	112.85	178.15	PZE.103119393	-0.003	0.04	WUEwd	6.75E-04	178.15	112.85	188.67	126.80	3.06	3.06	3.06

Cluster[a]	Chr.	Position[b]		Marker	Effect[c]	r2	Phenotype	p_Bonferroni[d]	Left[e]		Right[e]		BIN[f]	BIN left[g]	BIN right[g]
		cM	Mbp						Mbp	cM	Mbp	cM			
Q8	3	112.85	178.15	PZE.103119393	-0.007	0.05	WUEww	3.32E-05	178.15	112.85	188.67	126.80	3.06	3.06	3.06
Q8	3	112.85	178.15	PZE.103119393	-9.003	0.05	WUwd	7.55E-05	178.15	112.85	202.95	145.00	3.06	3.06	3.07
Q8	3	120.58	184.31	PZE.103127310	-1.567	0.09	LEAN	7.92E-05	184.31	120.58	205.03	149.50	3.06	3.06	3.07
Q8	3	120.58	184.12	PZE.103126743	-0.009	0.04	Phy	1.15E-03	184.12	120.58	188.67	126.80	3.06	3.06	3.06
Q8	3	120.58	184.31	PZE.103127310	-0.225	0.03	T_res	7.25E-03	184.31	120.58	184.31	120.58	3.06	3.06	3.06
Q8	3	123.50	187.01	PZE.103130290	-2.878	0.10	DPS	3.68E-05	187.01	123.50	202.95	145.00	3.06	3.06	3.07
Q8	3	123.50	187.01	PZE.103130290	-1.068	0.18	SRN	7.69E-05	187.01	123.50	202.95	145.00	3.06	3.06	3.07
Q8	3	123.50	187.01	PZE.103130290	-19.426	0.05	WUww	1.08E-05	187.01	123.50	188.67	126.80	3.06	3.06	3.06
Q8	3	128.18	191.37	PZE.103136011	-3.293	0.04	T_wd	2.07E-04	191.37	128.18	202.95	145.00	3.07	3.07	3.07
Q8	3	128.18	191.37	PZE.103136011	-0.240	0.04	T_res	1.89E-03	191.37	128.18	202.95	145.00	3.07	3.07	3.07
Q9	3	149.50	204.47	PUT.163a.60346254.2548	-6.473	0.04	T_ww	1.40E-03	204.47	149.50	205.03	149.50	3.07	3.07	3.07
Q9	3	149.50	204.47	PUT.163a.60346254.2548	-42.400	0.05	WUww	6.43E-05	204.47	149.50	205.03	149.50	3.07	3.07	3.07
Q10	4	9.38	2.65	PZE.104002805	-0.061	0.04	BA_res	6.23E-04	2.65	9.38	2.65	9.38	4.01	4.01	4.01
Q10	4	9.38	2.65	PZE.104002805	-0.614	0.04	BAwd	2.26E-03	2.65	9.38	2.77	9.51	4.01	4.01	4.01
Q10	4	9.38	2.65	PZE.104002805	-0.061	0.03	WU_res	7.63E-03	2.65	9.38	2.65	9.38	4.01	4.01	4.01
Q10	4	9.38	2.65	PZE.104002805	-10.637	0.04	WUwd	8.24E-04	2.65	9.38	2.77	9.51	4.01	4.01	4.01
Q10	4	9.51	2.77	PZE.104003099	-0.051	0.04	BA_res	5.65E-04	2.77	9.51	2.77	9.51	4.01	4.01	4.01
Q10	4	9.51	2.77	PZE.104003099	-3.205	0.05	T_wd	6.45E-05	2.65	9.38	2.77	9.51	4.01	4.01	4.01
Q10	4	9.51	2.77	PZE.104003099	-0.280	0.06	T_res	3.38E-06	2.65	9.38	2.77	9.51	4.01	4.01	4.01
Q11	4	36.78	14.04	PZE.104014780	-0.074	0.03	BA_res	8.32E-03	14.04	36.78	14.04	36.78	4.03	4.03	4.03
Q11	4	36.78	14.04	PZE.104014780	3.965	0.08	BAww	1.36E-09	14.04	36.78	14.04	36.78	4.03	4.03	4.03
Q11	4	36.78	14.04	PZE.104014780	8.185	0.03	EV	1.46E-05	14.04	36.78	14.04	36.78	4.03	4.03	4.03
Q11	4	36.78	14.04	PZE.104014780	0.013	0.06	WUEww	3.36E-06	14.04	36.78	14.04	36.78	4.03	4.03	4.03
Q12	4	59.45	31.25	PZE.104026198	21.465	0.03	WUww	2.49E-03	31.25	59.45	31.25	59.45	4.04	4.04	4.04
Q12	4	70.00	66.29	PZE.104044698	21.465	0.03	WUww	2.49E-03	66.29	70.00	177.35	109.00	4.05	4.05	4.07
Q12	4	109.00	177.35	PZE.104100589	0.011	0.03	Phy	9.13E-03	177.35	109.00	177.35	109.00	4.07	4.07	4.07
Q13	5	0.00	0.08	PZE.105000063	-5.496	0.12	DPS	3.84E-07	0.08	0.00	0.08	0.00	5.00	5.00	5.00

Cluster[a]	Chr.	Position[b]		Marker	Effect[c]	r2	Phenotype	p_Bonferroni[d]	Left[e]		Right[e]		BIN[f]	BIN left[g]	BIN right[g]
		cM	Mbp						Mbp	cM	Mbp	cM			
Q13	5	0.00	0.08	PZE.105000063	-2.859	0.12	LEAN	1.13E-06	0.08	0.00	0.08	0.00	5.00	5.00	5.00
Q13	5	0.00	0.08	PZE.105000063	0.006	0.04	WUEwd	1.61E-04	0.08	0.00	0.08	0.00	5.00	5.00	5.00
Q13	5	0.00	0.08	PZE.105000063	0.013	0.05	WUEww	9.18E-05	0.08	0.00	0.08	0.00	5.00	5.00	5.00
Q14	5	116.80	188.83	SYN35847	9.698	0.02	EV	9.58E-04	188.83	116.80	188.83	116.80	5.05	5.05	5.05
Q14	5	116.80	188.83	SYN35847	-6.037	0.03	T_wd	4.47E-03	188.83	116.80	188.83	116.80	5.05	5.05	5.05
Q14	5	119.15	192.13	SYN31647	-0.077	0.03	BA_res	7.27E-03	192.13	119.15	192.13	119.15	5.05	5.05	5.05
Q14	5	119.15	192.13	SYN31647	-0.087	0.03	WU_res	4.52E-03	192.13	119.15	192.13	119.15	5.05	5.05	5.05
S3	5	160.90	212.76	SYN35270	0.081	0.03	BA_res	4.73E-03	212.76	160.90	212.76	160.90	5.08	5.08	5.08
S3	5	169.18	215.84	ZM013240.0409	0.081	0.03	BA_res	4.73E-03	215.84	169.18	215.84	169.18	5.09	5.09	5.09
S4	6	69.28	132.83	PZE.106077504	2.960	0.07	DPS	2.36E-03	132.83	69.28	147.93	79.75	6.05	6.05	6.05
S4	6	79.75	148.25	SYN37017	-2.333	0.15	SRN	6.50E-04	148.25	79.75	150.46	79.75	6.05	6.05	6.05
S4	6	79.75	148.25	SYN37017	13.457	0.04	WUwd	1.75E-03	148.25	79.75	148.25	79.75	6.05	6.05	6.05
Q15	6	132.95	166.18	SYN7865	-10.463	0.04	EV	3.38E-09	166.18	132.95	166.18	132.95	6.07	6.07	6.07
Q15	6	132.95	166.18	SYN7865	-14.633	0.04	WUwd	1.14E-03	166.18	132.95	166.18	132.95	6.07	6.07	6.07
Q16	8	13.75	4.85	SYN12530	-1.105	0.05	BAwd	9.91E-06	4.85	13.75	4.85	13.75	8.01	8.01	8.01
Q16	8	13.75	4.85	SYN12530	-0.097	0.04	WU_res	1.05E-03	4.85	13.75	4.85	13.75	8.01	8.01	8.01
Q16	8	13.75	4.85	SYN12530	-19.766	0.07	WUwd	3.46E-07	4.85	13.75	4.85	13.75	8.01	8.01	8.01
Q16	8	28.83	11.66	PZE.108011210	-10.300	0.05	WUwd	1.30E-04	11.66	28.83	12.99	32.32	8.02	8.02	8.02
Q16	8	28.83	11.66	PZE.108011210	-16.942	0.03	WUww	6.32E-03	11.66	28.83	13.62	32.32	8.02	8.02	8.02
Q16	8	20.78	7.62	SYN9898	-1.714	0.11	LEAN	1.03E-05	7.62	20.78	164.01	115.20	8.01	8.01	8.06
Q16	8	28.83	9.88	PZE.108009251	-2.467	0.07	DPS	2.11E-03	9.88	28.83	164.01	115.20	8.01	8.01	8.06
Q17	8	32.32	12.99	PZE.108012841	-1.022	0.17	SRN	9.89E-05	12.99	32.32	142.37	95.43	8.02	8.02	8.05
Q17	8	40.20	17.87	PZE.108019899	-0.152	0.12	R.ST	9.56E-03	17.87	40.20	17.87	40.20	8.02	8.02	8.02
Q17	8	44.50	20.82	PZE.108021947	-0.176	0.14	R.ST	1.52E-03	20.82	44.50	48.80	50.51	8.02	8.02	8.03
Q17	8	44.50	20.52	SYN16954	0.050	0.05	WU_res	2.09E-05	20.52	44.50	20.52	44.50	8.02	8.02	8.02
Q17	8	44.50	20.52	SYN16954	0.005	0.03	WUEww	4.83E-03	20.52	44.50	20.52	44.50	8.02	8.02	8.02
Q17	8	44.50	20.52	SYN16954	-12.642	0.03	WUww	3.46E-03	20.52	44.50	20.52	44.50	8.02	8.02	8.02

Cluster[a]	Chr.	Position[b]		Marker	Effect[c]	r2	Phenotype	p_Bonferroni[d]	Left[e]		Right[e]		BIN[f]	BIN left[g]	BIN right[g]
		cM	Mbp						Mbp	cM	Mbp	cM			
Q17	8	71.15	101.96	PZE.108056925	-0.225	0.17	R.ST	2.06E-04	101.96	71.15	138.22	95.43	8.03	8.03	8.05
Q17	8	71.15	101.96	PZE.108056925	0.007	0.05	WUEww	4.98E-05	101.96	71.15	138.22	95.43	8.03	8.03	8.05
Q17	8	72.50	104.62	PZE.108058577	-6.929	0.17	ERDWppr	1.34E-04	104.62	72.50	138.22	95.43	8.03	8.03	8.05
Q17	8	72.50	104.62	PZE.108058577	0.007	0.03	Phy	9.27E-03	104.62	72.50	138.22	95.43	8.03	8.03	8.05
Q17	8	77.60	113.07	PZE.108063246	0.003	0.05	WUEwd	1.23E-04	113.07	77.60	138.22	95.43	8.04	8.04	8.05
Q17	8	81.00	118.42	PZE.108066752	0.457	0.03	BAwd	4.04E-03	118.42	81.00	118.42	81.00	8.04	8.04	8.04
Q17	8	81.00	118.19	SYN27931	1.356	0.03	BAww	5.71E-03	118.19	81.00	118.42	81.00	8.04	8.04	8.04
Q17	8	81.00	119.04	PZE.108067299	-2.891	0.04	T_ww	1.35E-03	118.42	81.00	138.22	95.43	8.04	8.04	8.05
Q17	8	95.43	138.91	PZE.108082144	0.071	0.04	WU_res	3.04E-03	119.04	81.00	138.91	95.43	8.05	8.04	8.05
Q17	8	95.43	138.91	PZE.108082144	-22.441	0.03	WUww	3.76E-03	138.91	95.43	142.37	95.43	8.05	8.05	8.05
Q17	8	103.30	149.15	PZE.108092139	-0.226	0.13	R.ST	3.54E-03	149.15	103.30	164.01	115.20	8.06	8.06	8.06
Q18	9	0.00	1.73	PZE.109001250	25.044	0.03	WUww	5.82E-03	1.73	0.00	6.47	6.08	9.00	9.00	9.01
Q18	9	0.00	0.07	PZE.109000332	6.196	0.03	T_ww	3.62E-03	0.07	0.00	0.07	0.00	9.00	9.00	9.00
Q18	9	2.95	3.08	SYN36188	2.037	0.03	BAww	5.47E-03	3.08	2.95	3.08	2.95	9.00	9.00	9.00
Q18	9	2.95	3.08	SYN36188	0.012	0.03	Phy	5.90E-03	3.08	2.95	3.08	2.95	9.00	9.00	9.00
Q18	9	2.95	3.08	SYN36188	13.874	0.05	WUwd	1.24E-05	3.08	2.95	6.47	6.08	9.00	9.00	9.01
Q18	9	6.08	6.47	PZE.109005850	6.368	0.01	EV	1.00E-02	6.47	6.08	6.47	6.08	9.01	9.01	9.01
Q19	9	6.08	6.47	PZE.109005850	4.939	0.04	T_wd	3.95E-04	3.08	2.95	6.47	6.08	9.01	9.01	9.01
Q19	9	48.93	23.54	SYN5266	0.547	0.04	BAwd	1.82E-03	23.54	48.93	23.54	48.93	9.03	9.03	9.03
Q19	9	48.93	23.54	SYN5266	4.075	0.01	EV	9.40E-03	23.54	48.93	23.54	48.93	9.03	9.03	9.03
Q19	9	48.93	23.54	SYN5266	0.004	0.04	WUEwd	4.12E-04	23.54	48.93	133.70	96.27	9.03	9.03	9.05
Q19	9	48.93	23.54	SYN5266	0.007	0.04	WUEww	1.55E-04	23.54	48.93	133.70	96.27	9.03	9.03	9.05
Q19	9	48.93	23.54	SYN5266	2.921	0.03	T_wd	3.50E-03	23.54	48.93	23.54	48.93	9.03	9.03	9.03
Q19	9	48.93	23.54	SYN5266	0.247	0.04	T_res	9.40E-04	23.54	48.93	23.54	48.93	9.03	9.03	9.03
Q19	9	51.10	27.09	SYN32275	0.652	0.06	BAwd	1.17E-06	27.09	51.10	133.70	96.27	9.03	9.03	9.05
Q19	9	51.10	27.09	SYN32275	6.912	0.05	EV	1.06E-12	27.09	51.10	135.46	129.38	9.03	9.03	9.05
Q20	9	131.50	142.66	PZE.109097083	8.837	0.03	EV	6.05E-07	142.66	131.50	147.67	146.98	9.06	9.06	9.06

Cluster[a]	Chr.	Position[b]		Marker	Effect[c]	r2	Phenotype	p_Bonferroni[d]	Left[e]		Right[e]		BIN[f]	BIN left[g]	BIN right[g]
		cM	Mbp						Mbp	cM	Mbp	cM			
Q20	9	141.83	146.92	PZE.109103626	1.219	0.04	BAwd	2.46E-03	146.92	141.83	147.67	146.98	9.06	9.06	9.06
Q20	9	141.83	146.92	PZE.109103626	3.305	0.03	BAww	9.77E-03	146.92	141.83	146.92	141.83	9.06	9.06	9.06
Q20	9	141.83	146.92	PZE.109103626	36.602	0.03	WUww	2.54E-03	146.92	141.83	147.67	146.98	9.06	9.06	9.06
S5	10	133.00	148.50	PZE.110109364	38.907	0.04	WUww	6.28E-04	148.50	133.00	148.50	133.00	10.07	10.07	10.07

[a] QTL clusters are defined as groups of QTL in high LD (p-value <0.01), contiguous on the genome and with comparable direction of the effects; singleton QTL are indicated by the prefix "S" while QTL clusters by "Q".

[b] Position of the most associated SNP; genetic positions refer to the positions of the closest marker on the genetics consensus map.

[c] Effect of the Gaspé flint introgression with respect to the population mean.

[d] p-value of the comparison between Gaspé flint and B73 alleles corrected for multiple comparisons using the Bonferroni method.

[e] Left and right positions of the QTL peak; QTL peak are defined as physically contiguous chromosomal positions for which de Bonferroni corrected p-value was <0.01.

[f] Classical BINs of the maize genome.

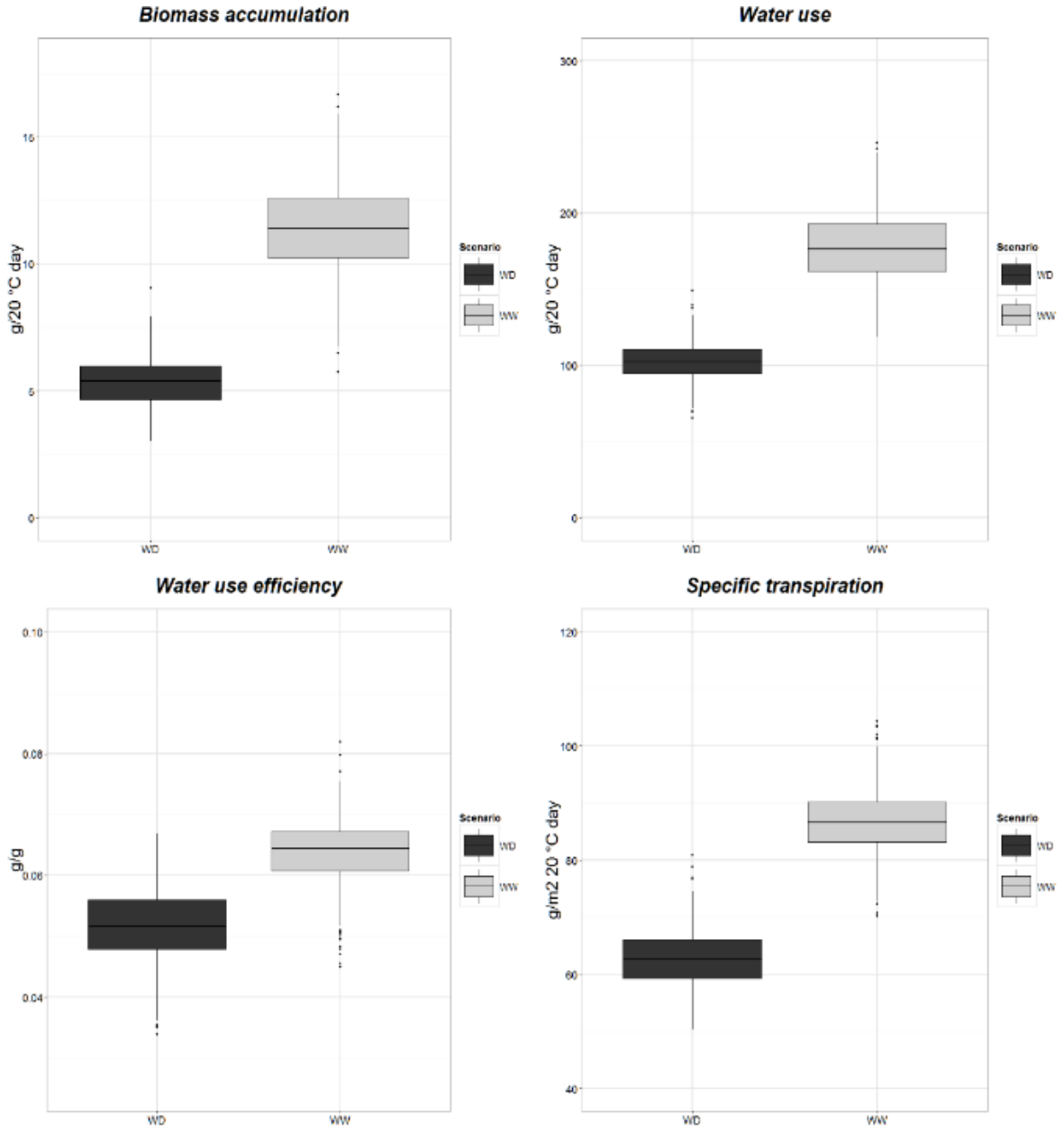

Figure 1 Box plots showing the distribution of the phenotypic values of the four traits, in the 73 IL line collection, under two water regimes (WW: well-watered; WD: water deficit).

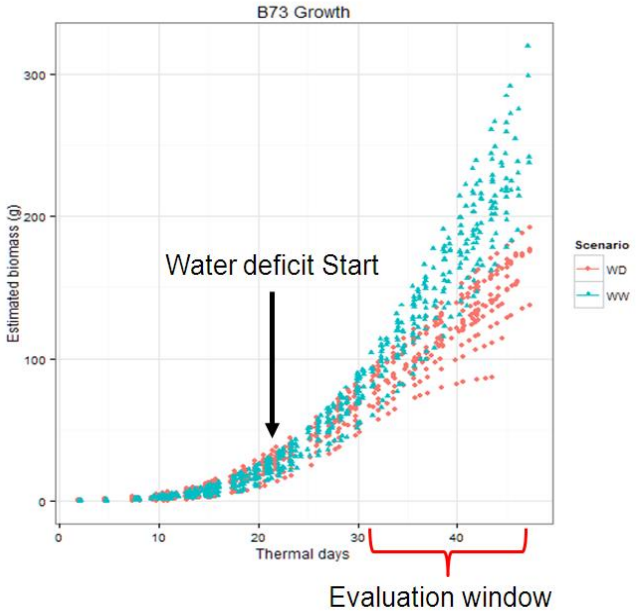

Figure 2 Trend of rate of Biomass accumulation (BA) throughout the whole experiment. Values for B73 only are shown, as representative of the entire IL population. Each point represents a single BA estimate as detailed in Materials and Methods and each line of dots represent a single plant BA evolution throughout the experiment. Ten plants in WD and ten plants in WW were utilized. 'Evaluation window' indicates the time period when trait values utilized for QTL analysis were collected.

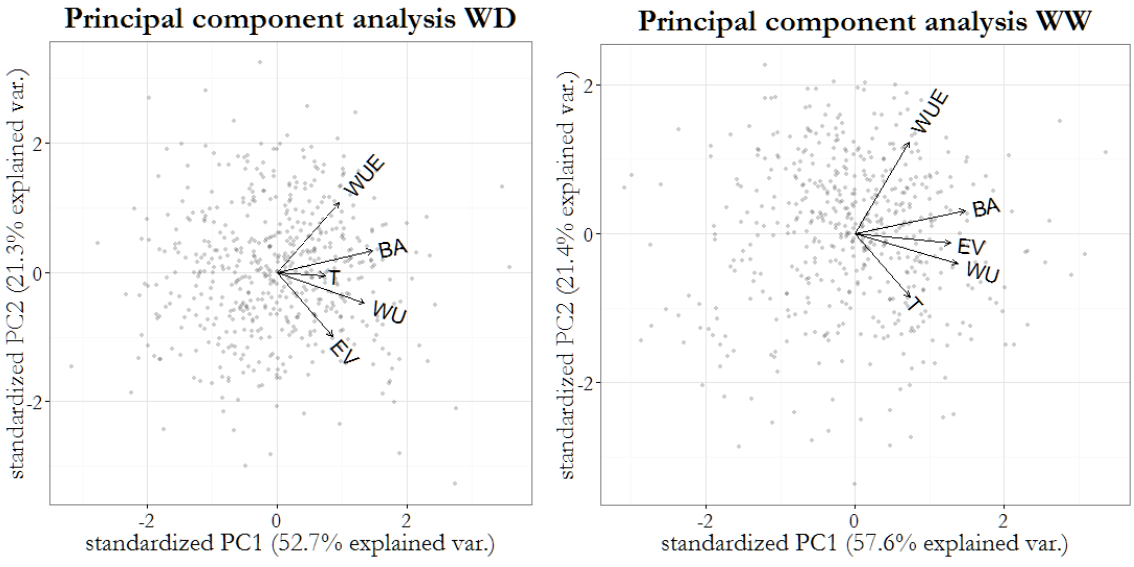

Figure 3 Plots of principal component analysis in WW and WD.

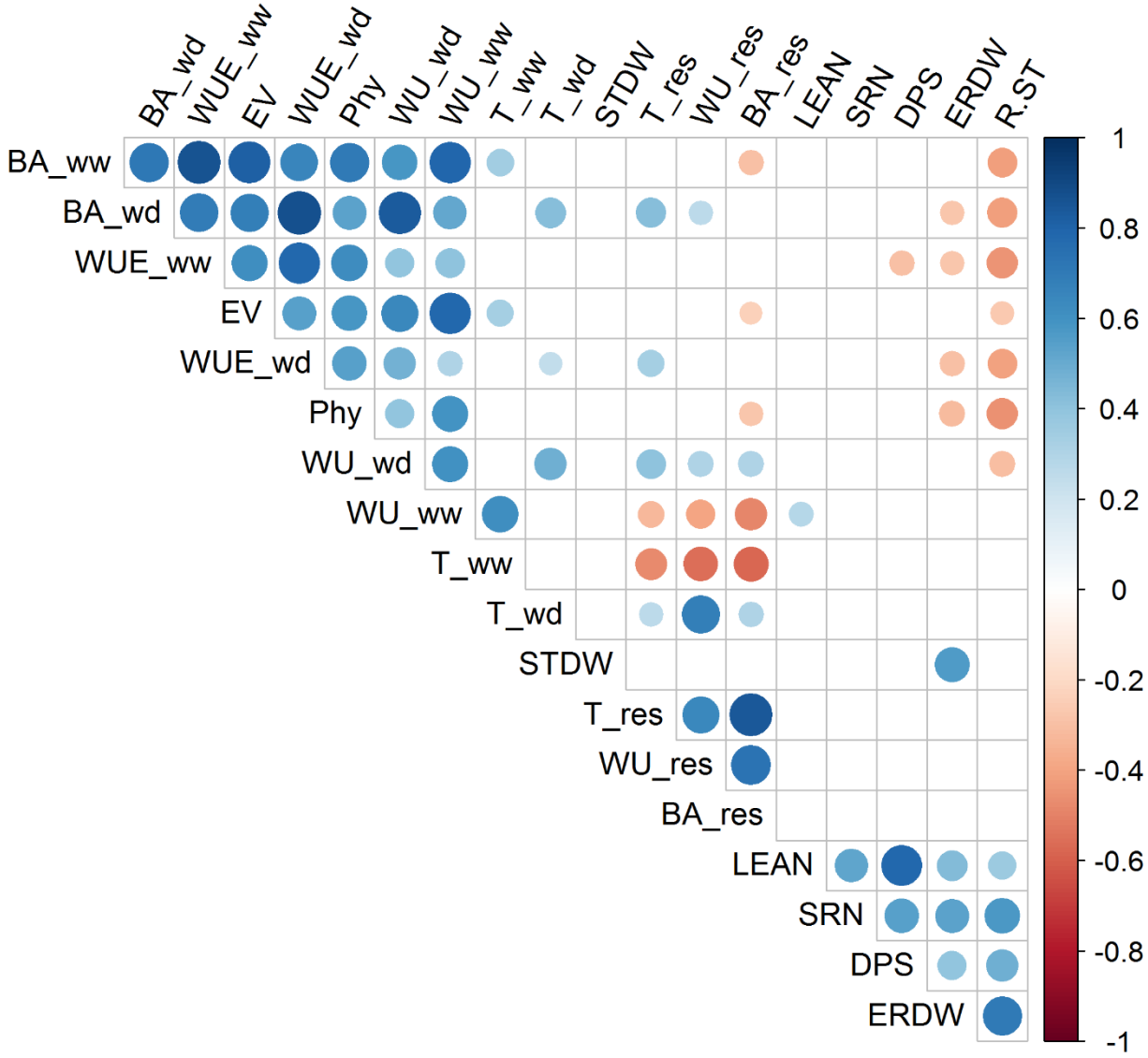

Figure 4 Correlations between platform and previously measured traits

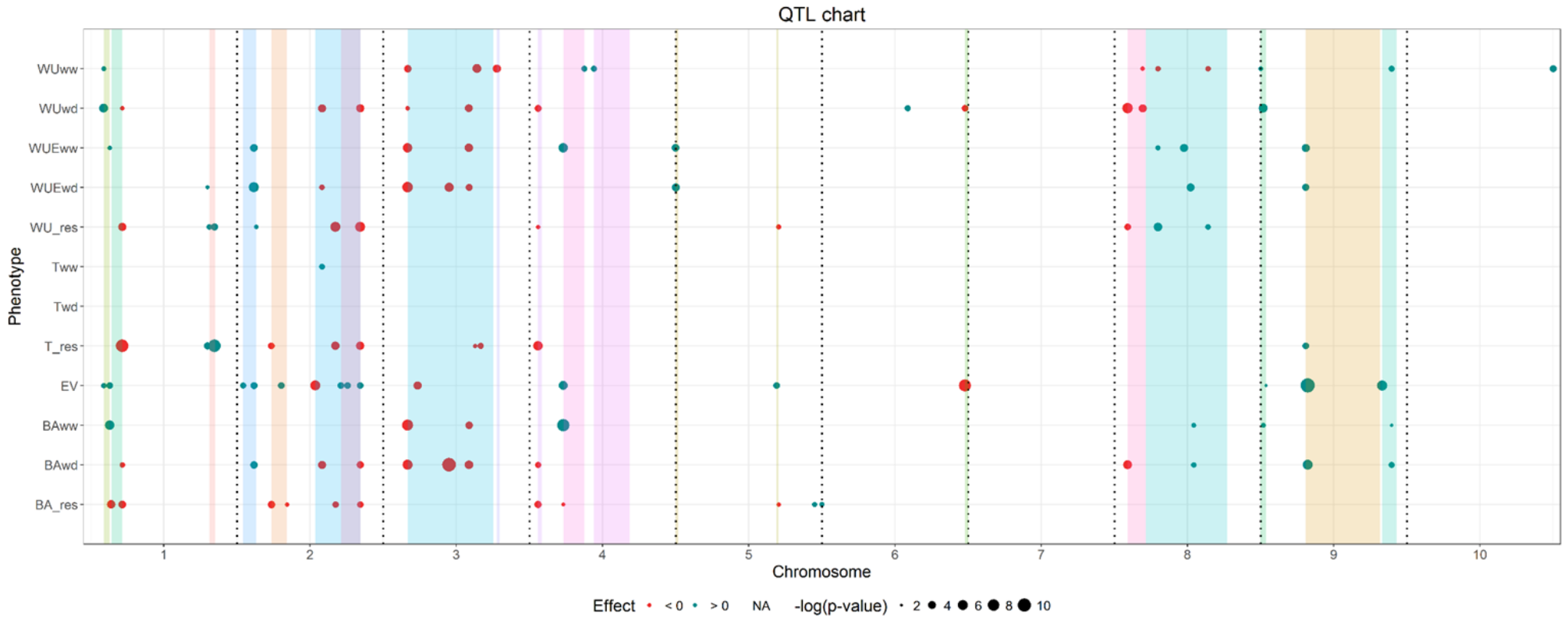

Figure 5 QTL for the observed traits. Dot dimension is proportional to the –log10 of the Bonferroni corrected p-value of the difference between Gaspé flint and B73 allele. Colours indicate positive or negative effect of the Gaspé flint introgression. Coloured rectangles represent different QTL clusters

3. Morphological characterization of a durum wheat association panel for root and shoot traits in a high-throughput phenotyping platform

3.1. Introduction

Durum wheat: botany, genomic and economical relevance

Wheat (*Triticum* spp.) is one of the three major staple food crops. It is the main source of carbohydrates for one third of the global population (Shewry, 2009). All the wheats belong to the *Triticeae* tribe of the *Poaceae* family. The great majority of wheat production comes from two species: bread wheat (*Triticum aestivum* L., 2n = 6x = 42) and durum wheat (*Triticum durum* Desf., 2n = 4x = 28). Bread and durum wheat are alloheaxaploid and allotetraploid species. Because of their size (17 and 12 Gbp, respectively) and richness in repetitive elements, sequencing of wheat genomes has been one of the major challenges in plant genomics (Ganal and Röder 2007; Mayer et al. 2014). Durum wheat (genome formula: AABB), evolved from the allo-polyploidization of *Triticum uratu*, donor of the pivotal genome A, and a species of the *Aegilops* genus strictly related to the modern *Aegilops speltoides*, donor of the homoeologous B genome (Sarkar and Stebbins 1956; Marcussen et al. 2014). A secondary allo-polyploidization of the durum wheat wild relative *T. dicoccoides* with *Aegilops tauschii* originated the wild relative of bread wheat (genome formula AABBDD) which therefore share two third of the genome with durum wheat (Marcussen et al., 2014). As mentioned before, size and complexity of wheat genomes make their sequencing an ongoing challenge. This notwithstanding, several useful genomic tools have been made available from the scientific community. Up to date, several consensus genetic maps have been developed, the most advanced of which are based on high-throughput genotyping technologies (Maccaferri et al., 2014, 2015; Marone et al., 2012; Somers et al., 2004; Wen et al., 2017). As regard to physical maps, several bread wheat draft assemblies have been released, none of which might be considered as reference (International Wheat Genome Sequencing Consortium (IWGSC), 2014; Zimin et al., 2017). An important available genomic tool is the assembly of the wild relative of durum wheat *T. dicoccoides* (Avni et al., 2017) which, beside its direct usefulness in gene discovery, together with the assembly of durum wheat might shade light on the domestication dynamics from a genomic standpoint.Durum wheat is the second most important wheat species, representing 5% of the total wheat production (Peng et al., 2013). Global production of durum wheat was more than 37

millions of tonnes versus a global wheat production of almost 750 millions of tonnes (FAOSTAT 2016, http://www.fao.org/faostat/en/#data/QC). Durum wheat is the most important humans' carbohydrates source in the Mediterranean basin, where more than half of the global acreage of this crop is grown. Durum wheat kernels are the base of semolina, a high protein and gluten flour used for cous-cous and pasta production. The production of durum wheat is concentrated in Italy, Spain, France and Greece in Europe, Canada, Mexico and USA in America, Algeria, Morocco and Tunisia in Africa, Turkey, Kazakhstan, Syria and India in Asia. Because its importance in the local cuisine, durum wheat is the most cultivated wheat in Italy. Since durum wheat is traditionally cultivated in rainfed conditions in drought prone environments, tolerance to drought is pivotal in most durum wheat genetic improvement programs (Araus et al. 2002, 2003a,b; Condon et al. 2004).

Importance of drought stress tolerance in wheat production

There is increasing recognition that the optimization of root architecture is an important component in designing new crop ideotypes, which should enable to increase productivity and/or to maintain acceptable yield performance under low-input management systems or stressed environments (Collins et al., 2008; Zhu et al., 2011)

Unexpectedly, wheat grain yield which has steadily increased for almost a century has started to stall (Ray et al., 2012). The yield plateau phenomenon has been recorded across many different countries and environments, including the highest yielding locations, and in industrialized countries such as Great Britain, France, US and others. The actual causes have not been identified yet, and exhausted genetic variation, new restrictions on use of agronomic inputs (eg. N fertilizers), economic disincentives to increase productivity and/or climate change effects have been proposed (Hochman et al., 2017). However, there is accumulating evidence that global climate change could be one of the most importance challenges to face in order to maintain or increase wheat productivity. For instance, there is already evidence that increasing global temperatures are negatively affecting grain yield (Asseng et al., 2015).

Drought stress has been and will be the most important negative factor contributing to yield reduction in crops, including wheat. A recent meta-analysis-based estimate of the effect of drought episodes on wheat production confirmed their severity (21% yield reduction with 40% water reduction) and indicated that the most negative effects are usually experienced in relatively dry environments (Daryanto et al., 2016). Additionally, almost 50% of wheat cultivated in the developing world (50 million ha) is sown under rain-fed systems, which receive less than 600 mm of precipitation per annum and which could be as low as less than 350 mm per annum in areas

inhabited by the poorest and most disadvantaged farmers (Gupta et al., 2017), worsening the social effect of drought episodes.

Phenotypic and genetic analysis of root traits

Among the different options available to the breeders to develop more drought tolerant wheat cultivars, selection for optimized root traits appears one of the most promising (Fleury et al., 2010; Reynolds and Tuberosa, 2008). However, selection for root traits has so far been clearly left behind as compared to other physiological or morphological traits. One of the reasons is that root traits (anatomical, morphological, and general architectural) are intrinsically difficult to evaluate. Indeed, roots are i) hidden from direct non-destructive investigation and ii) extremely sensitive to environmental conditions (Hodge, 2004) and prone to unpredictable developmental responses to changing conditions (Malamy, 2005; Topp, 2016). Additionally, root phenotyping can be particularly cumbersome in genetic and breeding contexts where several thousands of plants are normally required to be screened to obtain information useful for genetic analysis and selection decisions. To circumvent these constraints, several phenotyping techniques in controlled environment conditions have been proposed and applied, in the perspective of a substantial correlation with root trait expression in field conditions (Kuijken et al., 2015). More recently, advances in root trait phenotyping directly in the field have also been made. In the following section, the main root phenotyping techniques and methods of some relevance to cereals and specifically to wheat, will be briefly presented. More extensive reviews can be found elsewhere (Fiorani and Schurr, 2013; Gregory et al., 2009; Tardieu et al., 2017; Zhu et al., 2011).

Root phenotyping methods can be grouped in controlled environment (1) and field methods (2). The controlled-environment methods can be further subdivided in soil-based (1.1) and soil-free systems (1.2). Further distinctions include whether systems are destructive or enable real-time multiple inspections, or whether the imaging systems are based on optical (visual) access to roots or non-optical systems.

Soil based systems in controlled environments

Soil-filled rhizoboxes having at least one transparent (glass) plate-wall are being largely used in order to access root growth in real time and in a non-destructive manner (Nagel et al., 2012). Rhizoboxes are usually utilized in combination with digital imaging and analysis technologies and enable to perform relatively large-scale screens of plant populations. Not secondarily, thanks to the soil-based substrate, rhizoboxes represent a phenotyping system relatively close to field conditions and enable to acquire several shoot traits too (this depending on the species and on the developmental window under target). Similarly to rhizoboxes, transparent rhizotubes with

inner core of soil allow growing several plants simultaneously, at a maximum height of little more than 1 m and up to approximately two months, depending on plant species (Jeudy et al., 2016). Plastic (non-transparent, polyvinyl chloride - PVC - or similar) pots or pipes have also been utilized for growing plants followed by root inspection at the end of the growing (or treatment) phase, however these approaches are destructive and thus do not allow repeated analysis on the same plant (Becker et al., 2016; Tomar et al., 2016)

A different type of approach is the investigation of root architecture in soil-filled pot without direct optical imaging, which is replaced by X-ray micro-computed tomography (X-ray μCT) or magnetic resonance imaging (MRI). X-ray μCT is a non-destructive imaging technique that can visualize the internal structure of opaque objects and can produce a 3D image of the sample (eg. roots in soil-filled pot) in which each image element contains a value proportional to the molecular density of the imaged object (Mairhofer et al., 2013; Millet et al., 2016). The target object (ie. the pot containing a growing plant) is placed on a rotating stage inside the imaging device. An emitter projects X-rays through the rotating sample to a detector on the other side of the device. The system acquires a series of projections by measuring the attenuation of ionizing radiation passing through the target object. These projections are combined to reconstruct a three-dimensional image. Thus, μCT is not subject to the constraints facing light-based imaging techniques and enables non-invasive, non-destructive imaging of roots growing in soil. MRI is another non-destructive medical-derived imaging technology suitable for 3D root system reconstruction (Borisjuk et al., 2012). MRI enables spatially resolved nuclear magnetic resonance (a phenomenon where a strong magnetic field induces hydrogen nuclei to absorb and emit radio frequency signals, which can be recorded) to image water protons based on their local magnetic environment. Currently root imaging based on MRI does not reach the results obtained with μCT but remains a promising technique. In all, both μCT and MRI appear useful techniques for detailed non-invasive 3D reconstruction of root apparatus, however they both currently lack the resolution power to detect smaller, finer roots and, because of costs of analysis and infrastructure, can realistically be applied to small number of plants.

Soil-free systems

Soil-free protocols are among the most popular because they usually enable to address large number of plants, although mostly at the seedling stage of development only, at least for species like wheat. These systems include:

- transparent agarose gel (gel chamber) or gellan gum (Bengough et al., 2004; Clark et al., 2011; Iyer-Pascuzzi et al., 2010). In these approaches, different types of transparent or semi-

transparent gel-like substrates have been utilized in order to sustain plant growth and root development and, at the same time, enable optical investigation of root traits. While extremely informative and suitable for high-throughput setups, some of these systems can induce abnormal root growth responses when compared with real soil or field experiment-based results.

- paper rolls, growth pouches or germination paper on (Gioia et al., 2017; Hund et al., 2009; Maccaferri et al., 2016; Salvi et al., 2016; Watt et al., 2013; Zhu et al., 2005). In this systems, seeds or young seedlings are placed in humid filter or germination paper, sometime supported in plastic bags (pouches) or acrylic screens and let grow for a limited time (up to 10 days without nutrients, or for longer if nutrient solution is provided). At the end, root phenotypes are collected both manually and/or by digital imaging.
- hydroponic and semi-hydroponic systems (Chen et al., 2017; Jones, 1982; Tuberosa et al., 2002). These systems enable high-throughput non-destructive analysis of large number of seedlings or even adult plants and testing the response to different nutrient concentrations or other type of conditions. However, these systems do not provide effective 3D root architecture information; additionally, the correlation between genetic variation observed in hydroponics with that present in field condition should be verified on a case-by-case basis.

Field- based approaches

Approaches enabling to carry out root phenotyping directly in the field have also been applied and are continuously improved. Traditional approaches based on excavation included soil coring, trenching and shovelomics (Wasson et al., 2014; Zhu et al., 2011). Shovelomics (Trachsel et al., 2011), which has recently become relatively popular, consists of the excavation of single plants in order to access the above portions of the root stocks, which are cleaned by residual soil and subsequently phenotyped (most often through digital image acquisition and/or other methods. Trachsel et al. 2011). Although of proven utility for capturing several important root architectural traits, shovelomic-like approaches are labor-intensive, destroy or leave in the ground a large portion of the root system (including most of the lateral finer roots), and measurements cannot be repeated. Complementary to these approaches, tubular minirizothones are available. Minirhizotrons are transparent tubes which are installed vertically or at various angles in the ground, near plants. Roots growing outside the tube walls can be imaged by a digital camera inserted down the tube length. A number of different root traits can be observed or estimated such as root number per unit of soil volume, root density, depth etc, during a relatively long growing period. This notwithstanding, minirhizotrons only capture a very small portion of the

root systems (Zhu et al., 2011).

Ground-penetrating radar (GPR) is a method based on pulses of high frequency radio waves, which cause differential responses of belowground structures (roots vs soil). GPR is rapid and relatively inexpensive, however detection power is limited to thick roots (> 5 mm) and in the shallow portion of the soil. It has so far been applied for measuring root biomass of woody species only (Zhu et al., 2011). Electrical resistivity is another method that is primarily useful for biomass measurements. This technique uses electrode arrays distributed on the area under investigation to measure soil resistivity upon application of an electric current. Under favorable conditions, soil resistivity appears function of root biomass (Wasson et al., 2012). A related approach is the recording of electric capacitance of the soil-plant system at the plant under investigation (Dalton, 1995; Postic and Doussan, 2016), given that a correlation between capacitance and root dry mass in the soil was also demonstrated. This method has already been applied in wheat (Nakhforoosh et al., 2014). Capacitance values are relatively simple and fast to collect; however, they are strongly influenced by soil water content and therefore have inherently low heritability; thus, this method needs further refinement.

More recently, DNA analysis of soil samples has been proposed and tested to quantify root mass in the field (Steinemann et al., 2016). The approach is based on representatively sampling soil portions in the area under investigation, followed by DNA extraction and PCR (or direct DNA sequencing using next generation methods). The extension of root apparatus in the soil can be estimated by the proportion of samples including the DNA of the target species. This approach will likely be further developed in the near future.

The search of modified and improved root ideotypes

Unfortunately, there is currently too limited information on root genetic control and on physiological relationship across traits (and between traits and yield) in order to easily propose new, more efficient root ideotypes (Collins et al., 2008; Comas et al., 2013). However, some consensus is emerging across studies. First, the main challenges ahead of modern agriculture (and specifically, cereals) appear to be increasingly more frequent and harsher drought episodes, decline in soil nutrient availability due to nutrient depletion, change in soil microflora and/or the necessity to reduce chemical fertilization, adapting wheat cultivation to new growing environments. Therefore, these should be the challenges to be addressed while breeding for new root (and crop) wheat ideotypes. Among the challenges above, drought has so far received the main attention, and studies addressing the physiological and genetic design of more efficient root systems are now proliferating.

The species where the most innovative root ideotype for improved water acquisition has been

proposed is maize. The work of Jonathan Lynch at Penn U (Lynch, 2013) demonstrated, in a number of different theoretical and experimental papers, how a root system with narrow insertion angle on the stem axes, a lower number and longer axial crown roots and root with a simplified (less expensive) anatomy and rich in empty spaces (aerenchyma) (Chimungu et al., 2015) can be favorable at least in stressed (eg. water limited) environments (Saengwilai et al., 2014). This ideotype has been named "Steep, cheap and deep".

Newer wheat ideotypes and specifically new root ideotypes possibly more adapted to water limited cropping systems have also been proposed. Based on a first study, these new varieties should be characterized by a deeper root system, a higher density of lateral root density at deeper soil layers and a greater radial hydraulic conductivity at depth, which should be achieved by reducing xylem size and lowering axial resistance to water movement (Wasson et al., 2012). The same study suggested a positive effect of longer and denser root hairs. Similar conclusions were reached in a different study (Meister et al., 2014).

At least in cereals, root morphological and architectural plasticity can be a favorable trait per se. In efforts to evaluate the magnitude of root plasticity across crop germplasm collections, it has been repeatedly reported (or suggested based on modeling analysis) a positive correlation between the degree of root plasticity and yield stability across environments (Sandhu et al., 2016; Topp, 2016; Wissuwa et al., 2016). In wheat, relatively strong root plasticity was already shown in response to varying N fertilization regimes, where cultivars, on average, responded to low N supply by expanding their root surface area through increased total root number and/or length of lateral roots (Melino et al., 2015). At the same time, in a different study, it was shown that plasticity in stele and xylem diameter, and xylem number along the root length in wheat cultivars facilitates efficient use of available moisture under water-deficit stress (Kadam et al., 2015).

Genetic dissection of root traits in wheat by QTL mapping

Almost any breeding, marker-assisted and biotechnological approaches can be deployed to reach the target ideotypes. Therefore, once identified the most promising such root ideotypes, the challenge shifts to the identification of the source of useful allelic variation, mapping genes and QTL responsible for the target traits and finally to the implementation of experimental crosses, marker-selection and breeding schemes in order to transfer useful genetic variant to the future crop varieties. A number of studies have recently reviewed the use of genomic assisted approaches in breeding cereals and annual species (Barabaschi et al., 2016; Gupta et al., 2010).

Biotechnological approaches to specifically improve root traits based on genetic engineering and aiming to increased tolerance to stress have also been reviewed (Ghanem et al., 2011). These

authors prioritized the following traits and/or genes to be modified using biotech tools: aquaporins and hormonal regulation of their expression, nutrient transporters, root morphology and architecture by modifying both developmental genes, expression level of hormones such as ABA, auxins and cytokinins (the latters being largely involved in lateral root formation) or genes which are hormones' immediate target of regulation. Additionally, the need to identify and make available to genetic engineering highly efficient and specific (even at the level of specific tissue and sub-tissue) promoters was emphasized (Ghanem et al., 2011).

Objectives of the study

In this study we used a well characterized durum wheat association panel to dissect the genetic bases of both hypo and epigeal wheat morphology at vegetative stage. We used a high-throughput approach to evaluate the dynamics of plant growth thus dissecting final data point measures in their simpler components. This approach was expected to dramatically increase our QTL detection power by reducing the confounding effect of several segregating secondary traits. Furthermore, we wanted to know to what extent, if any, results from soil based root phenotyping are comparable with those from previous experiments conducted in soil-free systems (Maccaferri et al., 2016). Last but not least, we wanted to know if segregation for secondary source-related morphological traits correspond to segregation for yield in field condition by comparing our results with those from a multi-environmental trial conducted on the same plant material (Maccaferri et al., 2011).

3.2. Materials and methods

Plant material

The population consisted of 183 durum wheat cultivars from Italy, Spain, Morocco, Tunisia, Southern USA, CIMMYT and ICARDA selected in order to sample the genetic diversity of the elite durum wheat germplasm and to limit heading date variation within a ten days window in Mediterranean environments. The 183 cvs thoroughly genotyped with SSRs and DARTs (Maccaferri et al. 2011) and with a 90k wheat SNP array genetically positioned in the genome projecting the SNPs in a durum wheat consensus map constructed using the same genotyping technologies (Maccaferri et al., 2015). The association panel (DP) was previously phenotypically characterized for root system architecture (RSA) at the seedling stage (Canè et al., 2014; Maccaferri et al., 2016) using polycarbonate screening plates in growth chamber. Importantly, the same genetic material was used by Maccaferri et al. for an association study on grain yield, yield

components and other phenological, morphological and physiological traits evaluated directly in field trials throughout different locations of the Mediterranean basin (Maccaferri et al., 2011). Based on the characterization of simple sequence repeat (SSR) markers, the population structure of the Unibo-DP accessions herein considered appeared to be structured into five main subgroups representing the main breeding lineages present in the germplasm, identified by well-defined breeding ideotypes (and corresponding hallmark founders developed and widely cultivated in subsequent decades of breeding). These subgroups corresponded to: S1, ICARDA and Italian accessions for dryland areas from the native Syrian and North African germplasm (from Haurani and related landraces); S2, ICARDA accessions bred for temperate areas (from Cham 1); S3, Italian cultivars related to Valnova and Creso founders and subsequently bred with CIMMYT and Southwestern US accessions (Desert Durum®); S4, widely adapted early CIMMYT germplasm introduced to several Mediterranean countries (from Yavaros 79, Karim, Duilio); S5, more recent high yield potential CIMMYT germplasm (from Altar84). Details are reported in Maccaferri et al. (2011) and in Letta et al. (2013).

The GROWSCREEN-Rhizo phenotyping platform

Plants were grown in the GROWSCREEN-Rhizo phenotyping facility at the *Institut für Bio- und Geowissenschaften Pflanzenwissenschaften* (IBG-2), *Jülich forschungszentrum* in Jülich, Germany. The phenotyping facility has been described by Nagel et al. (Nagel et al., 2012) and used for tetraploid wheat phenotyping (Gioia et al., 2015). Briefly, GROSCREEN-Rhizo consists of two rows of 36 frames, for a total of 72 slots in which rhizotrons (90 × 70 × 5 cm) are inserted. The rhizotrons consist of polycarbonate boxes having one of the two sides made from transparent polycarbonate. The transparent side is shielded from light by mean of a black plastic plate combined with, black brush curtains. Each row of the platform is split into two blocks. Imaging was carried out by an automated moving cabinet provided with lights and RGB camera. The cabinet moves between the two rows of the platform. The rhizotrons are individually drew inside the imaging cabinet by a mechanical swivel arm. Images of the whole transparent rhizotrons surface were acquired with a high-resolution camera (16 MP camera, IPX-16M3-VMFB, Imperx, Inc., Boca Raton, FL, USA; combined with Zeiss Distagon T 2,0/28 ZF-I lens, Jena, Germany). The whole procedure is automated and driven by a custom software program implemented with LabVIEW (National Instruments, Austin, TX, USA). Plants are automatically irrigated by mean of drippers positioned at the top of each frame of the platform.

Experimental design and growing conditions

In order to screen the entire population, three distinct and sequential sub-experiments were conducted. Four plants of two different cultivars had been transplanted in each rhizotron and each cultivar was replicated in two different rhizotron for a total of four plants per cultivar. The most representative lines of the five population structure groups had been replicated in the three sub-experiments as control lines. Thus, in each sub-experiment 63 cultivars plus the five controls were screened. The 63 cultivars were selected in order to uniformly sample the genetic diversity arisen from the population structure study. Within each of the main population structure subgroups, accessions were randomly sampled and assigned to each of the three sub-experiments. For each accession, healthy seeds with uniform size were pre-germinated on filter paper into individual petri dishes. In order to guarantee germination uniformity, seeds were allowed to pre-germinate in dark and cold room (4 °C) for a week. After the pre-germination step, vital seedlings were transplanted into the rhizotrons. Rhizotrons were filled with ~ 18 l of black and nutrient rich peat-based compost. Each rhizotron was watered twice per day using 100 ml of tap water. Plants were grown for four weeks under semi-controlled conditions in the Phytec Greenhouse, with 16 h photoperiod, day/night temperatures of 24/18 °C. Plants were allowed grown for four to five weeks after transplanting up to the stage at which longest roots reached the bottom of the rhizotrons (corresponding to the Zadock scale 16, on average).

Phenotyping and image analysis

Picture of the visible root system were taken daily from transplanting to harvest. Leaf area (**LA**) was scored by manually measure the length (**LL**) and width (**LW**) of each leaf of the plants. LA per each leaf was than calculated according to the well-known formula (Kemp, 1960; Masle and Passiowa, 1987):

$$LA = LL * LW * 0.858$$

Number of tillers (**Tillers**) and leaves (**Leaves**) were measured as well. These measurements were taken twice a week in the first two weeks of growth and once a week in the last weeks of the experiment as well as the day before harvest. At harvest the root system was separated from the shoot at the ground level and dry biomass was measured for both.

Images of the root system were analysed by mean of the in-house software *GrowScreen Root*. Briefly, this software allows digitally drawing the root system, discriminating among three different root classes. In this experiment we classified the roots as seminal, nodal and lateral. The output provided by the software are the single root length, maximum depth and width of the root system, area under the convex hull, root length density for each chosen root level/layer at different depths.

Since multiple measurements were taken along the experiments, we were able to fit the root and shoot growth curves in order to retrieve dynamical growth parameters. Leaf chlorophyll content was estimated twice using the SPAD-502 chlorophyll meter (Minolta Corp., Ramsey, NJ, USA) at stages Z13 and Z14 of the Zadok scale. A summary of mean, range, heritability and description of the evaluated traits is reported in **Table 1.**

Data analysis

Data analysis was mainly carried out using the R statistical software (The R Core Team, 2016).
Since phenotypes distributions were not always normal, all the data was transformed using the quantile normalization technique (Hicks et al., 2017). In order to remove the effects due to the subsequent sub-experiments, best linear unbiased estimators (BLUES) were calculated using the line ID as fixed effect and different sub-experiments as random effect variate. The mixed models were fitted using the *lme4* R package (Bates et al., 2015).
Mean cultivar repeatability was calculated using the formula:

$$h2=\sigma G2(\sigma G2+\sigma E2/r)$$

where: σG^2=genetic variance, σE^2=residual variance, r=number of reps.
Data for heritability estimation were first corrected for the sub-experiment effect. Calculations were conducted using the package "Heritability" (Wolak et al., 2012).
Growth curves were fitted using the package "growfit" and using the Gompertz's growth model (Kahm et al., 2010; Zwietering et al., 1990).

GWAS

Multi-locus mixed-model algorithm (MLMM) as implemented into the "mlmm" package (Segura et al., 2012) was used for phenotype/genotype association using both the kinship and population structure matrices as covariates. Briefly, this algorithm performs phenotypes correction for kinship and population structure and include associated markers, on the base of a certain *p*-value threshold, as covariates for further association tests until no improvement is gained in terms of explained heritability. Kinship was calculated as identity by state between informative markers. Non-redundant, informative markers were selected using the "tagger" function implemented in software *Haploview* (Barrett et al., 2005), setting an R^2 threshold of 1.0. We chose to select just the non-redundant, informative markers in order to avoid biases due to uneven sampling of the genome based on the available SNPs from the iSelect array.

LD decay analysis

We fitted the SNP decay curve according to Rexroad and Vallejo (Rexroad and Vallejo, 2009) and Sved et al. (1971), who based the analysis on the known relationship between LD as measured by r2 (squared correlation of allele frequencies at a pair of loci) and effective population size Ne,.

$$E(r^2) = \frac{1}{(\alpha + kN_e c)} + 1/n$$

where:

c is the recombination rate between loci, n is the experimental sample size. The constant $\alpha = 1$ in the absence of mutation (Sved et al. 1971). The constant k was set to $k = 4$ for autosomes. Knowing r^2 LD values and c, we estimated N_e by fitting this nonlinear regression model,

$$y_{ij} = \frac{1}{(\alpha_j + \beta_j c_{ij})} + e_{ij}$$

Where $y_{ij} = (r^2 - 1/n)$ is the observed LD (adjusted for chromosome sample size n) for marker pair i in chromosome j, c_{ij} is the recombination rate from two-point linkage analysis for marker pair i in chromosome j. The parameter β_j is the estimator of effective population size for chromosome j where $\hat{N}_e = \beta_j / k$. The parameters a_j and β_j were estimated iteratively by using non-linear modeling.

The decline of linkage disequilibrium with distance (recombination rate in Morgans) was estimated by fitting again

$$y_{ij} = \frac{1}{(1 + kb_j d_{ij})} + e_{ij}$$

Where $y_{ij} = (r^2 - 1/n)$ is, as above, the observed LD between markers, the constant $k = 4$ for autosomes, d_{ij} is the recombination rate from two-point linkage analysis for marker pair i in chromosome j, bj is the estimate of effective population size for chromosome j, and e_{ij} is a random residual. The estimates of r2 for pairs of markers were adjusted for experimental sample size.

In order to assess the significance threshold to include a marker in the QTL model, we first calculated the upper LD threshold for the background LD caused by population structure by inspecting the distribution of LD values for unlinked marker-pairs (>50 cM genetic distance in the consensus maps) and by selecting as threshold the r^2 corresponding to the 95th percentile

distribution. This r^2 value was used to set a *tagger* function in Haploview in order to retrieve an estimate of the genome-wide number of independent association tests, considering only those SNPs not in LD according to the r^2 threshold. Bonferroni correction for multiple tests on the MLMM was applied to allow the alghorithm to include the markers in the GWAS-QTL model. Confidence intervals were assessed by inferring the genetic distance at which, on average, LD decayed to r^2 value ≤ 0.3. The tag-markers associated to phenotypes falling within the same confidence interval were considered and discussed as belonging to a unique QTL cluster. We also reported those QTL which significance p.value was higher than the genome wide threshold but lower than 0.001 considering them as putative QTL (Maccaferri et al., 2016). QTL effect direction was reported according the sign of the effect of the QTL which showed higher average LD with other markers of the same cluster. QTL effects are reported as percentage of the mean population value.

3.3. Results

Root and shoot Trait variation, heritability and correlations

The use of the GROWSCREEN-Rhizo phenotyping facility allowed us to assess the root system architecture of the 183 durum elite panel accessions in greater details as compared to previous root system phenotyping conducted at seedling stage in paper-filter screen sheets (Canè et al. 2014; Maccaferri et al 2016). In total, 32 root traits and 18 shoot-related traits were measured and phenotypic data were subsequently subjected to GWAS analysis (Table 1). In particular, the GROWSCREEN-Rhizo platform allowed us to discriminate and specifically measure the three main distictinct components of the root system, i.e. seminal, nodal and laterals roots. Based on the root trait features, root phenotypes could be further distinguished and grouped according to: (i) root length, (ii) root depth and width, (iii) root dry weight and root to shoot ratio, (iiii) root dynamic traits (growth speed and day of occurrence of flex points). Shoot traits included (i) estimates of total shoot biomass at the end of the observation cycles, (jj) leaf length and width, leaf area and specific leaf weight, total leaf number, (iii) cholorophyll content, (iiii) tiller count and tiller emission rate.

In **Table 5** we report summary statistics for the analysed traits. A wide range of variation was observed for most root and shoot traits as well as for the three main root categories (seminal, nodal and lateral). Heritability ranged between 0.12 and 0.77 for maximum seminal density (**Seminal_dmax**) and average leaf length (**Leafl_ave**). Most of traits showed h2 values comprised between 0.45 and 0.75, with a mean value of 0.55.

Plant growth cycle in rhizotrons was terminated at GS16 (Zadock scale) for root and shoot

biomass harvesting. At that stage, the seminal root apparatus extended through most of the allowed vertical space in rhizothrons (**Depth** ranging from 34.09 to 75.91 cm) while the nodal roots were mostly limited to the top 35-cm layer. Considering root length, the seminal apparatus reached a maximum of 555.01 cm compared to a maximum of 366.67 cm (66.07%) and 187.85 cm (33.84%) for the nodal and lateral apparatus, respectively. As expected from these statistics, the nodal/seminal ratio averaged across all accessions was equal to 0.26; however, the ratio varied widely among accessions, ranging from zero (no nodal roots emission, at least in the explored time-frame) up to 2.36. The width of the total root apparatus also showed a wide range of variation, from very narrow to wide root distributions in horizontal plane (from 5cm to 55.26 cm). Another trait that showed ample variation among accessions was the shoot to root ratio (from 0.54 to 17.68 g/g). Considering the shoot-related traits, shoot development at the end of the growth cycle varied considerably among accessions (from 0.03 to 0.91 g/plant), mainly concomitantly with the number of tillers (from 1 to 11 tillers/plants). Other shoot traits of interest that varied considerably among accessions were the mean leaf area (from 1.99 to 13.50 cm2/leaf) and the chlorophyll content (from 23.92 to 50.15 SPAD units).

Frequency distribution and correlations for the most relevant and discussed traits are reported in Figure 6. Shoot and root traits showed distributions approaching the normality in most cases, indicating quantitative inheritance for most of traits. For several traits, distributions were positively skewed or highly skewed (total Lateral root length, total nodal root length, maximum nodal root density, maximum lateral root density, root width), indicating that only relatively few genotypes showed extreme trait values at the top of the distribution (elongated tail at the right portion of the distribution). At least to some extent, in addition to genetic/inheritance reasons, the positively skewed trait distributions could have been caused by the still limited growth cycle length allowed to the plants grown in the rhizotrons, not reaching the physiological maturity and thus the maximum development. On the contrary, root system depth showed a negatively skewed distribution most probably due to some extent to the rhizotrons' vertical space constrains. Most of the root traits were inter-related to some extent. Interestingly, nodal, seminal and lateral total root length were scarcely correlated to each other (seminal vs. nodal, r= 0.25***; seminal vs. lateral, r= 0.23***; nodal vs. lateral, r=-0.034 NS), indicating that a partially different genetic control is at the basis of the inheritance of the three root types. Root system width showed limited correlations to all other root and shoot traits (r values ranging from NS to 0.28***) thus indicating its genetically distinct and unique inheritance features. Shoot and root dry weight were correlated at r=0.62***, indicating a partial common inheritance of the two traits, as expected. Chlorophyll content is another vegetative trait that showed limited correlation *vs.* the other shoot traits.

However, some significant relationships were observed between SPAD and root dry weigth (r= 0.38***) and, in particular, with nodal root apparatus traits (SPAD vs Nodal length, *r*=0.33 and SPAD vs. Nodal_dmax, *r*=0.31***), suggesting a possible relationship between the capacity to accumulate photosynthates and the subsequent growth of nodal roots, or viceversa.

QTL models

A total of 211 QTL were detected for the 41 analysed traits, with an average of 5.14 QTL per trait.

In **Table 6** we report details on the R2 of the QTL model and number of significant QTL detected, considering the QTL and population structure effects separately. We also report minimum, mean and maximum adjusted R^2 of the QTL detected per each phenotype. The variance explained by the QTL model was firstly affected by the number of QTL included in the model (Pearson's r = 0.89) and secondly by the maximum R^2 explained by a single QTL in the model (r = 0.81). Based on the medium-to- high number of QTL identified for several traits (**Table 6**) and based on the global R2 fit of the multiple QTL models, MLMM proved to be an efficient QTL search method for quantitative root and shoot traits obtained from the rhizotron phenotyping platform.

For some traits including root nodal length, total root length in the top layer, seminal deep, depth, shoot dry weight, leaf area, despite their medium-to-high h2, it was possible to identify two-to-three QTL only, with global QTL models not exceeding R2 = 0.20. This could be interpreted as a consequence of relatively high-complexity in the genetic control of those traits, with a substantial absence of major QTL segregating in the germplasm considered and multiple alleles at the causal genes. Therefore the GWAS results for these traits could be considered as cases of missing heritabilities (Manolio et al., 2009).

In other cases, such as the total root length, seminal root length in top layer, lateral roots in the top layers, lateral deep, root width, leaf length and leaf width, SPAD, tiller emission rate, GWAS identified seven up to 14 QTL, and total R^2 models of 0.35-0.66, indicating the presence of major QTL (**Table 6**). Correlation between trait heritability and R2 of the QTL model (without population structure) was moderate (r = 0.3), indicating substantial effect of kinship and/or population structure or, again, the presence of several minor effect QTL that did not reached significance. In **Table 7** and figures 7-22 we report the results of the GWAS for the analysed traits. Overall, the cumulative number of QTL identified for the dissected traits was higher than the number of QTL identified for their respective primary order traits (i.e. six QTL were spotted for **Total_lenght** while ten QTL were detected for its secondary traits **Seminal, Lateral** and

Nodal). GWASs for lateral and seminal roots related traits explained more variance than nodal roots traits GWASs in terms of both length and distributions. As regard to shoot traits, leaf morphology-related traits were better explained by the QTL models as compared to tiller-related traits, indicting a tight genetic control for the former traits as compared to the latter.

QTL clusters

QTL positioned at genetic distances less than 3.52 cM (double of LD decay at r^2 0.3) with respect to each other were grouped into QTL cluster. A summary of the detected QTL clusters is reported in **Table 8**. A total of 156 QTL out of 211 was grouped in 49 clusters including at least two QTL/phenotypes. The number of QTL in each cluster ranged from 2 to 11. Twenty-four clusters consisted of two QTL, 10 of three, 9 of four QTL, three clusters contained 5 QTL and three single clusters were composed by six, ten and eleven markers. A cluster was detected in the sub-centromeric region of chromosome 1A, four in chromosome 1B, four on 2A, six on 2B, five on 3A, one on 3B and 4A, two on 4B, four on 5A, two on 5B and 6A, four, nine and five on chromosomes 6B, 7A and 7B respectively. Detailed information of position, number of QTL, phenotypes with indication of the hypothetical sign of the effect, confidence interval and max significance is reported on **Table 8**. Only three QTL clusters did not contain at least a major QTL (-log10 p-value > 3.7). We define as major clusters those clusters comprising, within their confidence interval, more than four QTL for four distinct traits.

For several cases, the QTL-clusters included single QTL for both root and shoot traits, particularly leaf area, leafw or leafL, indicating major QTL clusters for whole plant vigour of architecture. Q1, a major QTL cluster at position 75.1 – 80.9 cM on chr. 1A, was essentially a cluster for whole-plant vigour, positively affecting maximum root system depth (Depth), seminal and total roots below 35 cm (Seminal_deep, Total_ deep), total root length (Total_length), tiller emission rate (Tiller_emission_rate) and maximum root system width (Width). A second major QTL cluster (Q2) located on chromosome 1B between 74.1 and 87.1 cM, influenced, with concordant effect direction, depth of the deepest lateral root (Lateral_d), lateral roots length below 35 cm (Lateral_deep), seminal and total root length (Seminal and Total_length respectively), Seminal_deep and Total_deep, root dry weight (Root_dry), day of root deeping flex point (T0_dep), and average leaf area (Ave_leaf). A major QTL cluster (Q14) was detected on chr. 2B, c.i. 165.7 – 166.3 cM; it positively affected the depth of the deepest nodal root (Nodal_d) and Total_deep while it had a negative effect on total and lateral root length above 35 cm (Total_top and Lateral_top), and Total_length. A QTL clusters affecting shoot dry weight (Shoot_dry), shoot and roots dry biomass (Total_biomass), Lateral_d, Lateral_deep and leaf specific weight (LSW) was positioned on chromosome 3A at position 102.7 – 105.3 cM. Two major QTL clusters were

located on chromosome 7A. Q37 was located in a relatively wide c.i. (50.4 – 62.1 cM) and positively affected Lateral_d while had a deleterious effect on Shoot_dry, Total_biomass, Width, and nodal to seminal length ratio (Nod_Sem_ratio). The QTL cluster containing more QTL was Q40, on chr. 7A at position 112.6 – 114 cM. It affected negatively Depth, Lateral_deep, maximum root length speed (Mu_rlen), Seminal, Total, Seminal_deep, Total_deep while had a positive effect on shoot/root dry biomass ratio (Shoot_root), root specific weight (RSW) and maximum leaf expansion rate (Mu_LA).

For a few traits showing unique inheritance features, mostly not related to other traits, though major QTL were identified, they were not included into QTL-clusters. One example is root system width. As much as seven single significant and highly significant QTL were found for root system width. Among those, four on chromosomes 2A, 5B, 6A and 7A showed R^2 values ≥ 0.10 (10%) and were thus considered as major GWAS-QTL, including the one on chromosome 6A explaining up to 23% PEV. Only three of them were included into QTL-clusters (one QTL on 6A and two on 7A).

3.4. Discussion

Trait correlations

Unexpectedly, root system maximum width (**Width**) was not negatively correlated with root system depth (**Depth**). Despite it might seems counterintuitive, the cause of this discrepancy could be related to the adopted experimental conditions. Indeed, a wider root system is associated to a weak gravitropic response from the root system. Gravitropism acts by slowing down the activity of the down oriented part of the root tip meristem zone (Young et al., 1990) thus causing the curvature of the root. In the growing conditions of this experiment, roots were artificially and constantly exposed to gravitropic stimuli to allow them to grow on the transparent part of the rhizotrons. This might had caused the constant and experiment-wide slowdown of the more gravitropic root system and, therefore, compensate the favourable effect of a narrower root growth angle on root depth.

Shoot_dry and **Root_dry** showed a moderate/high correlation ($r = 0.62^{***}$) indicating an autocatalytic effect of plant vigor on both root system and shoot. Indeed, both shoot and root are totally dependent each other in terms of water and nutrient for the shoot and of metabolized carbon the root system. An increase in **LA** (tightly correlated with **Shoot_dry**) guarantee to the entire plant a higher light interception and, therefore, increased carbon metabolization for all the organs including roots. On the other hand, increase in root length guaranty a better nutrient and water caption thus sustaining a larger shoot. This nonetheless, is well-known that **LA** is tightly

correlated with water consumption causing a detrimental effect of wider **LA** in the most drought prone environments. Is therefore crucial to study their reciprocal relationships in order to understand to what extent, if any, is possible to tune root system independently to shoot. As logical, **Shoot_root** was positively correlated with **Shoot_dry** and negatively with **Root_dry** (r = 0.42*** and r = -0.38 respectively). L**ateral** showed the highest correlation (r = -0.38***) with **Shoot_root** among root classes, with **Seminal** and **Nodal** showing much weaker r coefficients (-0.14*** and -0.01 respectively). This could appear in contrast with the fact that visible lateral roots represented in this experiment only 6.8 % of **Total_length**, with **Seminal** and **Nodal** representing the 76.0 and 17.2 % respectively. Furthermore, **Root_dry** showed moderate and comparable correlations with the length of all the root classes (r = 0.47***, 0.39***, 0.40*** for **Seminal, Lateral** and **Nodal** respectively). This could be explained by the fact that **Lateral** did not correlated with **Shoot_dry** (r = 0.06) while, as above mentioned, **Lateral** and **Root_dry** did. Seemingly, **Lateral** was independent of the vigor-loop (+**LA** = more nutrients for the roots, +roots = more water and nutrients for the shoot) by pulling the carbon partitioning to root system with no beneficial effect on shoot. Our hypothesis is that lateral roots, since numerous and directly connected to roots phloem (Yu et al., 2016), are very strong metabolites sinks in the competition against shoot meristems for organic carbon, more than seminal and nodal roots. As consequence of that, the advantages of a better soil exploration are equally counterbalanced by the higher carbon demand due to a greater number of carbon absorbing tips. It should be said that lateral root emission is stimulated by low nutrient content in the soil and, thus, that in not optimal growing conditions the prevalence of **Lateral** on total root length might be dramatically different from what was observed in this experiment. Furthermore, at least in early stages, lateral roots are not well differentiated from a histological standpoint and, therefore, they miss a proper gravity response apparatus, which results in a low gravitropism. This make us infer that **Lateral** underestimates the actual total lateral root length and prevalence on other root classes. This nonetheless, the moderate correlation with **Root_dry** makes us suppose that, in spite of its bias, **Lateral** is a good estimator of actual lateral root length. If more the higher investment in lateral roots drove the higher carbon partitioning to the root system, we would expect the same for **Nodal**. It was not the case, since **Nodal**, contrary to **Lateral** and to a lesser extent **Seminal**, did not correlated with **Shoot_root**. This might be because, as confirmed by this study, nodal root density is notoriously positively correlated with tillering (Belford et al., 1987; Klepper et al., 1984). As consequence of that, the nodal roots sink strength is counterbalanced by the highest amount of vegetative tips due to the increased number of tillers, resulting in no effect on carbon partitioning.

QTL modelling

None of the detected QTL explained more than 30% of variance, indicating the quantitative nature of all the analysed phenotypes. Despite moderate correlation (r = 0.3*) was found between traits heritability and the variance explained by the QTL, the linearity between the h2 and R2 varies dramatically among phenotypes. This is a well-known issue in GWAS, referred as "missing heritability". Several mechanisms have been proposed to explain this power constrain of GWAS. One of the possibility is the poor genome coverage of the SNP chip. This is for sure not the case of this study since the average genetic distance between subsequent markers was much lower than the LD decay at R2 = 0.3. Another possible explanation is that SNP chips only permit to detect two allelic forms of a certain *locus* thus ignoring the possibility of multiple haplotypes. No specific studies have been conducted to evaluate this possibility on the tested genetic material. This nonetheless, we cannot exclude this hypothesis given that an average of 5.1 alleles per locus was observed among the SSR markers. Another possible cause of missing heritability might be the extremely complex genetic architecture of the traits. This results in an extremely high number of minor effect QTL underling the studied trait and therefore in a lack of power of the association analysis. Epistatic interactions, might also undermine the chances of QTL discovery. Last but not least, strong kinship relationships or population structure may account for most of the explained variance thus limiting its QTL explained portion. All these hypotheses need further investigation in order to increase the statistical power and thus the capability to identify QTL for root and shoot morphological traits. This said, we would like to remark how the dissection of complex traits into simpler ones allowed us to increase our QTL discovery capability. Indeed, we detected just two major QTL for total **LA**, while, its secondary traits (**Leaves** and **LA_ave**) were explained by 13 QTL. Same for root traits, were **Total_length** was explained by six QTL whereas 3, 4 and 3 QTL were detected for **Seminal**, **Lateral** and **Nodal** respectively. Among root classes, QTL for **Nodal** explained less variance as compared to **Seminal** and **Lateral** with the first globally explaining 0.15 of the variance versus 0.24 and 0.25 of the QTL models of the latter. This might be due to stronger genotype/sub-experiment interaction for **Nodal**. Since **Nodal** and **Tillers** are correlated and being the latter notoriously affected by light intensity and quality (Casal, 1988), it might be that differences in these environmental parameters between sub-experiments might had differentially affected the trait expression resulting in lower QTL detection capability.

QTL discovery and comparison with previous experiments

In this experiment we had the chance to morphologically characterize roots of a durum wheat association panel at a growth stage and phenotypic resolution that had never been explored before. Furthermore, we could dynamically investigate root classes development end their reciprocal relationships and effects on shoot growth. This nonetheless, it is important to compare the results obtained from this experiment with those obtained using cheaper and quicker phenotyping technique. It is indeed crucial, for geneticists and breeders, to know to what extent cheap and quick phenotypes are maintained in later growth stages and, thus, choose the proper phenotyping technology for population screening or QTL fine mapping. As expected, at least for the main QTL, is possible to find a certain degree of correspondence between RSA measured at seedling stage with paper-roll or paper-non-roll techniques and RSA traits observed at late tillering stage in rhizotrons. Q2 on chr. 1B at 74.1 - 87.1 cM, i.e. is one of the QTL cluster which have a correspond cluster in the work of Maccaferri et al. 2016 acting on comparable traits. Indeed, it was found in this study that this QTL affect the global plant vigour both below and above ground. In the paper-roll experiment, the authors found, in the same chromosomal region of Q2, QTL for total root number, average root length, primary root length and thousand kernel weight. The same could be said for Q14, a major QTL cluster for **Lateral_top, Nodal_d, Total_length, Total_deep, Total_top** which colocalized with major QTL for average root length, primary root length and total root length in found in paper roll. Q18 did not found any clear correspondence in the paper roll experiment but this could be expected since this QTL cluster affect lateral root traits which were not measured in paper-roll. It is interesting to notice that the QTL which had the highest R2 for root growth angle in paper roll, located on chr. 6A c.i. 119.9 – 124.9, corresponded to the QTL with the highest R2 (0.22) for width in the rhizotron experiment. We did not observe deeper roots in correspondence of this QTL but this might explained by the fact that, as we mentioned before, more gravitropic roots are slightly disadvantaged in terms of growth speed in rhizotron growing condition.

As expected, several QTL clusters discovered in this experiment were not found in previous experiments, demonstrating the complementarity of the used strategies. The most interesting of this is Q40, the QTL cluster including more phenotypes (11). Located in the centromere of chr. 7A, it is involved in most of the deep rooting traits (**Depth2, Lateral_deep, Mu_rlen, Seminal, Seminal_deep, Total_deep, Total_Length, Seminal_top**) and, importantly, it also affects Shoot_**Root** by inducing a more root oriented phenotype in accordance with deep rooting allelic form. In the study of Maccaferri et al. 2016, in the same region was found only a putative QTL for seminal root number. What make this QTL cluster particularly interesting is that the deep-

rooting allelic form is clearly prevalent in the two sub populations from ICARDA and the Italian germplasm (S1, S2 and S3, deep rooting allele frequencies of 0.72, 0.80 and 0.92 respectively) while it is underrepresented in CIMMYT breeding program material (sub-populations S4 and S5, deep rooting allele frequency 0.37 for both the sub-groups). ICARDA breeding programs are specifically focused on the adaptation of durum wheat to dryland conditions. Italian material is traditionally cultivated in rainfed conditions. On the other hand, CIMMYT breeding programs are traditional run in optimal growing conditions in order to fully understand the genetic potential of a certain line. Our hypothesis is that, by providing artificial watering, CIMMYT breeders did not selected for deep rooting traits and on the contrary, privileged the allelic form which permit a more shoot-oriented carbon partitioning. The fact that this chromosomal region was not of particular interest in the paper-roll experiment might be a caused by the late display of the QTL, which could be linked to lateral roots appearance.

3.5. Conclusions

We have been able to perform an extremely detailed morphological characterization of a wheat association panel for both roots and shoot at full vegetative phase. Trait dissection permitted us to increase our QTL detection capability. Comparison with previously conducted experiments using other techniques, permit us to identify the most valuable strategy to adopt for QTL fine mapping. A detailed plant modelling approach will permit us to better understand the physiological mechanisms underlying important drought adaptive traits such as shoot/root carbon partitioning. GWAS allowed us to identify novel loci which may had had a critical role in the durum wheat breeding history. The most interesting loci will be tested in bi-parental and homogeneous genetic backgrounds to better understand the environmental and farming conditions at which a certain allelic form may result in higher yield or better yield stability.

3.6. Tables and figures

Table 5 Trait description, summary statistics, and heritability

Phenotype	Description	GWAS analysis in details	Min	Mean	Max	h2
Root traits						
Length of root apparatus						
Total_Length	Total root length (cm)		80.96	331.03	833.34	0.60
Seminal	Seminal root length (cm)	**x**	50.01	246.38	555.01	0.47
Nodal	Nodal root length (cm)	**x**	0.00	61.75	366.67	0.66
Lateral	lateral root length (cm)	**x**	0.00	23.13	187.85	0.68
Nod_Sem_ratio	Nodal/seminal ratio (cm/cm)		0.00	0.26	2.36	0.59
Depth and width						
Nodal_d	Maximum nodal root depth (cm)		1.89	21.40	62.45	0.46
Depth	Root system depth (cm) maximum	**x**	34.09	61.91	75.91	0.67
Depth2	Depth at the last but one phenotyping point (cm)		30.75	57.30	75.91	0.65
Width	Root system width (cm)	**x**	5.51	16.46	55.26	0.45
Root_Dry	Root Dry weight (g)	**x**	0.00	0.05	0.11	0.54
Density of root apparatus						
Total_top	Density of roots above 35 cm (cm/cm2)		0.10	0.42	1.12	0.67

Phenotype	Description	GWAS analysis in details	Min	Mean	Max	h2
Seminal_top	Density of seminal roots above 35 cm (cm/cm2)		0.03	0.27	0.58	0.51
Nodal_top	Density of nodal roots above 35 cm (cm/cm2)		0.00	0.13	0.69	0.65
Lateral_top	Density of lateral roots above 35 cm (cm/cm2)		0.00	0.02	0.20	0.54
Total_deep	Density of roots below 35 cm (cm/cm2)		0.00	0.16	0.52	0.60
Seminal_deep	Density of seminal roots below 35 cm (cm/cm2)		0.00	0.15	0.44	0.60
Nodal_deep	Density of nodal roots below 35 cm (cm/cm2)		0.00	0.00	0.10	0.35
Lateral_deep	Density of lateral roots below 35 cm (cm/cm2)		0.00	0.02	0.24	0.65
Total_dmax	Maximum root density measured in the rhizotron (cm/cm2)	**x**	0.21	0.54	1.31	0.66
Seminal_dmax	Maximum seminal roots density measured in the rhizotron (cm/cm2)		0.07	0.35	0.79	0.12
Nodal_dmax	Maximum nodal root density measured in the rhizotron (cm/cm2)	**x**	0.00	0.23	0.90	0.62
Lateral_dmax	Maximum lateral root density measured in the rhizotron (cm/cm2)	**x**	0.00	0.09	0.78	0.62
Total_dmaxdep	Depth of the maximum density of the root apparatus (cm)		1.89	14.71	70.02	0.25
Seminal_dmaxdep	Depth of the maximum density of seminal roots (cm)		1.89	20.55	70.02	0.29
Nodal_dmaxdep	Depth of the maximum density of nodal roots (cm)		1.89	5.13	43.53	0.21
Lateral_dmaxdep	Depth of the maximum density of the lateral roots (cm)		1.89	25.75	70.02	0.51
Root dynamic traits						
Mu_dep	maximal deeping speed (cm/day)		1.45	3.50	6.30	0.45
T0_dep	flex point in the deeping curve (day)		2.24	6.05	15.80	0.53
Mu_rlen	Maximum root length speed (cm/day)		2.74	14.34	30.44	0.39
T0_rlen	flex point total root length (day)		3.26	8.15	22.75	0.55

Phenotype	Description	GWAS analysis in details	Min	Mean	Max	h2
First_Nodal_day	Day of apparence of the first nodal root		1.00	16.28	28.00	0.45
RSW	root specific weight (g/cm2)	**x**	0.00	0.00	0.00	0.41
Shoot traits						
Shoot_fresh	Shoot fresh weight (g)		0.04	2.86	6.98	0.55
Shoot_Dry	shoot dry weight (g)	**x**	0.03	0.36	0.91	0.50
Shoot_Root	Shoot/root ratio (g/g)	**x**	0.54	7.34	17.68	0.59
Leaves	Final Total leaves (nb)		6.00	16.94	37.00	0.44
LA	Final leaf area (cm2)		22.87	99.51	204.84	0.64
Ave_LA	Mean leaf area of the measured leaves (cm2/leaf)	**x**	1.99	5.98	13.50	0.72
Leafl_max	Max leaf length scored in a plant (cm)		13.80	24.65	38.50	0.78
Leafl_ave	mean length of the leaves measured in a plant (cm)		7.23	12.86	17.69	0.77
Leafw_max	Max leaf width scored in a plant (cm)		0.50	0.74	1.10	0.60
Leafw_ave	mean width of the leaves measured in a plant (cm)		0.27	0.44	0.60	0.76
Mu_LA	Maximum leaf expansion rate (cm2/day)		1.18	8.60	183.15	0.05
Tillers	Final number of tillers (nb)	**x**	1.00	5.31	11.00	0.45
First_tiller_day	Day of apparence of the first tiller (day)		1.00	11.87	27.00	0.48
Tiller_emission_rate	Tillers emitted per day		0.00	0.40	0.80	0.34
LSW	Leaf specific weight (g/cm2)		0.00	0.00	0.01	0.31

Phenotype	Description	GWAS analysis in details	Min	Mean	Max	h2
SPAD	Chlorophyl content	**x**	23.92	36.40	50.15	0.74
Water_content	Water content in the plant ((Shoot_fresh-shoot_dry)/shootdry)		0.33	7.17	25.04	0.51
Total_biomass	Shoot + roots dry biomass		0.03	0.41	1.02	0.50

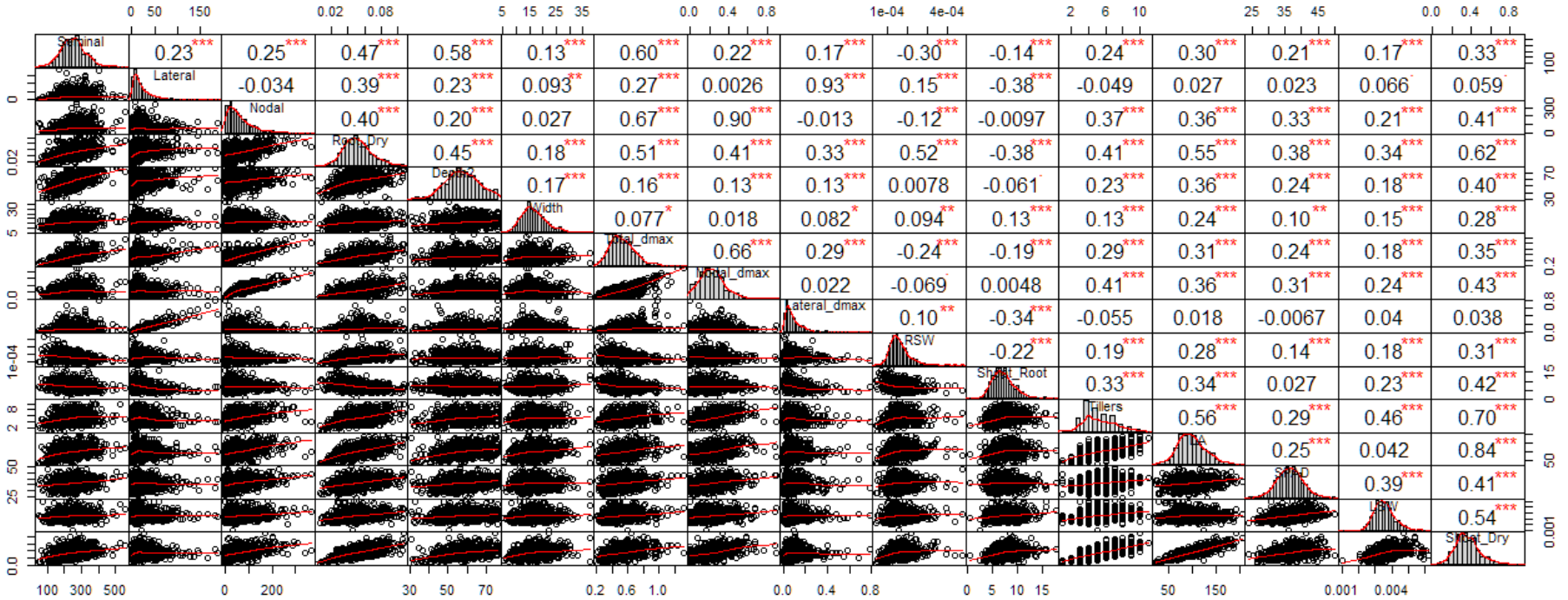

*Figure 6 Correlation and distribution of the principal, untransformed row traits. In the top corner are reported the Spearman's correlation coefficients and the significance level is reported as: p-value <0.05 *, <0.01 ** and <0.0001 ****

Table 6 Summary of the fitted QTL models; R2 values of the QTL model without the population structure, of the population structure and of the model including both. Summary statistics of R2 values of single QTL within each QTL model

	QTL model (QTL+structure) R^2			**Single QTL R^2**			
Phenotype	QTL	Structure	Global	Min.	Mean	Max	nb.
Ave_LA	0.46	0.01	0.53	0.10	0.15	0.22	8
Depth	0.21	0.07	0.26	0.05	0.08	0.13	3
First_Nodal_day	0.12	0.01	0.17	0.04	0.06	0.10	3
First_tiller_day	0.15	0.00	0.24	0.06	0.09	0.13	4
LA	0.14	-0.01	0.16	0.09	0.10	0.10	2
Lateral	0.25	0.01	0.30	0.07	0.10	0.16	4
Lateral_d	0.48	-0.01	0.53	0.04	0.13	0.23	11
Lateral_deep	0.51	0.00	0.54	0.07	0.12	0.16	10
Lateral_dmax	0.27	0.00	0.27	0.08	0.12	0.19	4
Lateral_top	0.46	0.01	0.46	0.06	0.11	0.21	7
Leafl_ave	0.66	0.02	0.66	0.05	0.15	0.29	14
Leafw_ave	0.54	0.02	0.68	0.04	0.17	0.30	13
Leaves	0.31	-0.01	0.33	0.07	0.10	0.16	5
LSW	0.44	0.15	0.50	0.09	0.13	0.16	7
Mu_LA	0.28	0.00	0.28	0.07	0.09	0.13	4
Mu_rlen	0.13	0.00	0.13	0.06	0.08	0.09	2
Nodal	0.15	-0.02	0.14	0.05	0.06	0.09	3
Nodal_d	0.20	-0.02	0.20	0.05	0.07	0.13	4
Nodal_dmax	0.10	-0.01	0.11	0.07	0.08	0.09	2
Nodal_top	0.08	-0.02	0.09	0.05	0.05	0.05	2
Nod_Sem_ratio	0.16	-0.02	0.15	0.03	0.04	0.04	4
Root_Dry	0.16	0.00	0.18	0.02	0.04	0.05	4
RSW	0.20	0.01	0.23	0.03	0.06	0.11	4
Seminal	0.24	0.02	0.25	0.07	0.10	0.15	3
Seminal_deep	0.22	0.06	0.27	0.06	0.09	0.14	3
Seminal_dmax	0.28	-0.01	0.35	0.04	0.08	0.11	7
Seminal_top	0.47	0.01	0.51	0.08	0.11	0.16	9
Shoot_Dry	0.17	0.02	0.23	0.06	0.09	0.12	3
Shoot_Root	0.29	0.01	0.31	0.07	0.10	0.11	5
SPAD	0.53	0.24	0.59	0.09	0.15	0.20	7
T0_dep	0.33	0.01	0.32	0.04	0.08	0.13	6
Tiller_emission_rate	0.17	0.01	0.36	0.03	0.06	0.13	7
Tillers	0.11	0.00	0.21	0.07	0.08	0.10	3
Total_biomass	0.17	0.02	0.22	0.06	0.09	0.11	3

	QTL model (QTL+structure) R^2			Single QTL R^2			
Phenotype	QTL	Structure	Global	Min.	Mean	Max	nb.
Total_deep	0.35	0.04	0.39	0.03	0.09	0.18	6
Total_dmax	0.06	-0.01	0.07	0.08	0.08	0.08	1
Total_dmaxdep	0.19	0.03	0.20	0.06	0.08	0.10	3
Total_Length	0.35	0.00	0.38	0.06	0.10	0.16	6
Total_top	0.19	-0.01	0.28	0.08	0.12	0.17	4
Water_content	0.15	0.00	0.32	0.09	0.11	0.13	4
Width	0.48	0.02	0.47	0.05	0.11	0.23	7

Table 7 QTL analysis results. QTL are sorted according chromosomal position on the durum wheat consensus map. QTL within 3.5 cm were considered to belong to the same QTL cluster. The central marker of each cluster is reported as tag SNP. Significance is reported as -log_{10} of the p-value of the association. Effects are reported as percentage of the population mean

SNP	-log_{10} pvalue	Phenotype	Chr	Pos (cM)	Left (cM)	Right (cM)	Cluster	Effect %	R^2
IWB35897	3.18	Depth2	1A	75.1	72.1	78.1	Q1	-0.16	0.05
IWB35039	3.25	Width	1A	75.1	72.1	78.1	Q1	-0.13	0.05
IWA5174	3.47	Tiller_emission_rate	1A	77.5	74.5	80.5	Q1	-0.17	0.06
IWA3419	3.44	Seminal_deep	1A	80.9	77.9	83.9	Q1	-0.17	0.07
IWA3419	4.08	Total_Length	1A	80.9	77.9	83.9	Q1	-0.12	0.07
IWA3419	3.84	Total_deep	1A	80.9	77.9	83.9	Q1	-0.13	0.05
IWB884	4.24	Tiller_emission_rate	1A	102.8	99.8	105.8	S1	0.24	0.13
IWB41745	4.12	Lateral_d	1A	132.7	129.7	135.7	S2	0.18	0.08
tPt-7724	10.41	Leafw_ave	1A	140	137	143	S3	0.20	0.26
IWB59696	3.41	Nod_Sem_ratio	1B	3	0	6	S4	-0.06	0.04
IWB47566	4.96	Lateral_d	1B	74.1	71.1	77.1	Q2	0.11	0.10
IWB71349	6.20	Lateral_deep	1B	79.6	76.6	82.6	Q2	0.12	0.16
IWB71349	3.21	Root_Dry	1B	79.6	76.6	82.6	Q2	0.06	0.03
IWB12327	3.86	T0_dep	1B	81.2	78.2	84.2	Q2	0.10	0.13
IWA7317	5.84	Total_Length	1B	82.2	79.2	85.2	Q2	0.08	0.10
wPt-3579	3.70	Seminal	1B	87	84	90	Q2	0.11	0.08
IWA4090	7.18	Ave_LA	1B	87.1	84.1	90.1	Q2	0.14	0.19
IWA2041	4.10	Total_deep	1B	87.1	84.1	90.1	Q2	0.12	0.13
IWA2041	3.13	Seminal_deep	1B	87.1	84.1	90.1	Q2	0.09	0.06
IWA2041	3.01	Root_Dry	1B	87.1	84.1	90.1	Q2	0.05	0.02
IWB35875	8.59	First_tiller_day	1B	93.4	90.4	96.4	Q3	-0.11	0.10
IWB65872	8.90	Leafw_ave	1B	93.5	90.5	96.5	Q3	-0.20	0.23
wPt-2257	3.30	Leafw_ave	1B	115.7	112.7	118.7	S5	-0.07	0.07
IWB72561	8.60	Lateral_dmax	1B	140.1	137.1	143.1	Q4	-0.18	0.19

SNP	-log10 pvalue	Phenotype	Chr	Pos (cM)	Left (cM)	Right (cM)	Cluster	Effect %	R^2
IWB72561	5.79	Lateral	1B	140.1	137.1	143.1	Q4	-0.15	0.16
IWB72561	5.99	Lateral_top	1B	140.1	137.1	143.1	Q4	-0.14	0.12
IWB66474	3.38	First_tiller_day	1B	152	149	155	Q5	0.15	0.08
IWB72247	8.35	SPAD	1B	156.3	153.3	159.3	Q5	0.12	0.18
IWA1563	3.94	Lateral_dmax	2A	7.8	4.8	10.8	Q6	0.16	0.08
wPt-7175	4.15	RSW	2A	8.6	5.6	11.6	Q6	-0.09	0.05
IWB69417	4.46	Lateral_d	2A	53.4	50.4	56.4	S6	-0.10	0.09
IWB70278	5.33	Lateral_deep	2A	101.6	98.6	104.6	Q7	0.11	0.12
IWB1896	4.92	Water_content	2A	102	99	105	Q7	0.20	0.13
IWB66894	5.02	Width	2A	117.6	114.6	120.6	S7	-0.16	0.11
IWB12196	9.44	Leafl_ave	2A	193.4	190.4	196.4	Q8	0.13	0.18
IWA4870	5.14	LSW	2A	197.6	194.6	200.6	Q8	0.11	0.11
IWA5978	6.11	Leaves	2A	204.3	201.3	207.3	Q9	-0.08	0.16
IWB9316	4.02	Leafl_ave	2A	208.7	205.7	211.7	Q9	-0.08	0.08
IWB10465	3.26	Nod_Sem_ratio	2A	208.7	205.7	211.7	Q9	-0.05	0.04
IWB28973	6.39	Lateral_deep	2B	12.2	9.2	15.2	Q10	-0.10	0.11
IWB42208	3.87	Lateral_dmax	2B	12.2	9.2	15.2	Q10	-0.11	0.08
IWB39434	4.01	Width	2B	17.7	14.7	20.7	Q10	-0.11	0.09
IWB55339	3.00	Lateral_d	2B	51.8	48.8	54.8	Q11	-0.07	0.04
IWB46470	4.92	Total_Length	2B	55.3	52.3	58.3	Q11	-0.09	0.11
IWB66226	3.83	Seminal_dmax	2B	103.5	100.5	106.5	Q12	-0.18	0.11
IWB66226	4.45	Seminal_top	2B	103.5	100.5	106.5	Q12	-0.14	0.10
IWB68216	5.92	LSW	2B	108.2	105.2	111.2	Q12	-0.19	0.13
IWA6122	4.36	Mu_rlen	2B	140.3	137.3	143.3	Q13	-0.15	0.09
IWB22762	3.19	Seminal	2B	144.8	141.8	147.8	Q13	-0.15	0.07
IWB22762	3.22	Total_deep	2B	144.8	141.8	147.8	Q13	-0.10	0.03
IWB28961	4.36	Shoot_Root	2B	146.5	143.5	149.5	Q13	0.17	0.11
IWB57663	4.06	Seminal_dmax	2B	156.6	153.6	159.6	S8	0.09	0.09
IWB19170	3.74	Nodal_d	2B	165.7	162.7	168.7	Q14	-0.19	0.13
IWB19170	3.07	Total_deep	2B	165.7	162.7	168.7	Q14	-0.17	0.07
IWB36286	7.63	Total_top	2B	166.3	163.3	169.3	Q14	-0.18	0.17
IWB39104	4.50	Lateral_top	2B	166.3	163.3	169.3	Q14	-0.18	0.09
IWB36286	3.04	Total_Length	2B	166.3	163.3	169.3	Q14	-0.09	0.06
IWB28826	5.77	Leafw_ave	2B	181.6	178.6	184.6	Q15	0.17	0.16
IWB28826	3.71	Leafl_ave	2B	181.6	178.6	184.6	Q15	0.13	0.13
IWB28826	3.81	Ave_LA	2B	181.6	178.6	184.6	Q15	0.14	0.10
IWA2946	4.69	Seminal_dmax	2B	187.9	184.9	190.9	S9	0.15	0.11
IWB44601	3.93	First_Nodal_day	3A	43.7	40.7	46.7	Q16	0.21	0.10
IWB44601	3.76	Nodal	3A	43.7	40.7	46.7	Q16	-0.09	0.09
IWB44601	3.51	Nod_Sem_ratio	3A	43.7	40.7	46.7	Q16	-0.06	0.04
IWB48828	4.09	Leafw_ave	3A	49.9	46.9	52.9	Q17	-0.10	0.12

SNP	-log10 pvalue	Phenotype	Chr	Pos (cM)	Left (cM)	Right (cM)	Cluster	Effect %	R^2
IWB72544	3.23	Mu_LA	3A	54.5	51.5	57.5	Q17	-0.08	0.07
IWB67653	4.77	Shoot_Dry	3A	102.7	99.7	105.7	Q18	-0.08	0.10
IWB67653	4.39	Total_biomass	3A	102.7	99.7	105.7	Q18	-0.07	0.09
IWA1260	7.44	LSW	3A	105.3	102.3	108.3	Q18	-0.17	0.16
IWB58656	7.38	Lateral_d	3A	105.3	102.3	108.3	Q18	-0.16	0.14
IWB58656	4.97	Lateral_deep	3A	105.3	102.3	108.3	Q18	-0.13	0.12
wPt-3133	4.41	Tillers	3A	123.5	120.5	126.5	Q19	-0.09	0.08
wPt-3133	4.14	Leaves	3A	123.5	120.5	126.5	Q19	-0.08	0.08
IWB5363	6.60	Leafl_ave	3B	30.2	27.2	33.2	Q20	-0.11	0.09
wPt-1691	8.83	Lateral_d	3B	33.12	30.12	36.12	Q20	-0.21	0.19
wPt-1349	3.79	Tillers	3B	36.64	33.64	39.64	Q20	0.07	0.10
IWA3426	3.98	Lateral_deep	3B	43.2	40.2	46.2	S10	-0.11	0.10
IWA4218	3.02	T0_dep	3B	100.9	97.9	103.9	S11	0.08	0.05
IWB8243	3.31	Seminal_dmax	3B	144.8	141.8	147.8	S12	-0.06	0.04
IWB67339	3.88	Shoot_Root	3B	191.8	188.8	194.8	S13	-0.18	0.10
IWB70884	3.33	Tiller_emission_rate	3B	209.7	206.7	212.7	S14	-0.09	0.04
IWB68749	7.80	Leafl_ave	4A	15.02	12.02	18.02	S15	-0.15	0.20
IWB74418	3.44	T0_dep	4A	22.2	19.2	25.2	S16	-0.07	0.06
IWB53508	4.65	Total_top	4A	51.3	48.3	54.3	S17	0.18	0.10
IWA5123	3.30	Lateral_top	4A	64.1	61.1	67.1	Q21	0.10	0.06
IWB26362	6.60	LSW	4A	68.4	65.4	71.4	Q21	0.12	0.15
IWA6733	4.42	Total_Length	4A	91.1	88.1	94.1	S18	-0.09	0.09
IWB1056	3.81	Water_content	4A	160.2	157.2	163.2	S19	0.11	0.09
IWB24513	5.09	Seminal_top	4A	173.6	170.6	176.6	S20	0.09	0.11
IWB34327	6.76	Seminal_top	4B	0	0	3	S21	0.17	0.16
IWB73001	3.03	Lateral_deep	4B	26.4	23.4	29.4	Q22	0.10	0.07
IWB12149	4.66	Leafl_ave	4B	30.8	27.8	33.8	Q22	0.12	0.05
IWB11925	6.13	SPAD	4B	34.4	31.4	37.4	Q22	-0.08	0.13
IWB51614	4.84	Mu_LA	4B	34.4	31.4	37.4	Q22	-0.10	0.11
IWB35101	5.46	T0_dep	4B	44.3	41.3	47.3	S22	0.10	0.13
IWB73006	3.49	Total_dmaxdep	4B	64.4	61.4	67.4	S23	0.09	0.06
IWA1382	3.04	Tiller_emission_rate	4B	77	74	80	Q23	-0.13	0.05
IWB7783	3.78	RSW	4B	80.6	77.6	83.6	Q23	-0.11	0.03
IWB10847	3.40	Total_deep	4B	82.3	79.3	85.3	Q23	0.12	0.05
IWB1109	3.41	Depth2	4B	83.1	80.1	86.1	Q23	0.13	0.05
IWB66445	5.04	Ave_LA	4B	115.5	112.5	118.5	S24	0.12	0.14
IWB39067	5.79	Leafw_ave	4B	135.5	132.5	138.5	S25	-0.15	0.16
IWB50844	10.82	Leafw_ave	5A	14.3	11.3	17.3	Q24	0.22	0.30
IWB25728	3.08	Leaves	5A	14.3	11.3	17.3	Q24	-0.08	0.07
IWB30321	4.46	Mu_LA	5A	37.7	34.7	40.7	S26	-0.15	0.13
IWB71919	3.17	Nodal_top	5A	67.3	64.3	70.3	Q25	-0.06	0.05
IWB69492	3.35	Leafw_ave	5A	73	70	76	Q25	-0.06	0.04

SNP	-log10 pvalue	Phenotype	Chr	Pos (cM)	Left (cM)	Right (cM)	Cluster	Effect %	R^2
IWB65371	3.35	Nodal_d	5A	102.2	99.2	105.2	S27	0.08	0.05
IWB46815	3.05	Nodal_d	5A	136.3	133.3	139.3	S28	0.07	0.06
IWA3887	4.02	Leaves	5A	146.5	143.5	149.5	S29	0.09	0.08
IWB35863	3.18	Total_biomass	5A	160	157	163	Q26	0.07	0.06
IWB35863	3.01	Shoot_Dry	5A	160	157	163	Q26	0.06	0.06
IWB23336	3.35	Lateral	5A	196.2	193.2	199.2	Q27	0.17	0.07
IWA3335	8.02	Ave_LA	5A	199.6	196.6	202.6	Q27	-0.24	0.22
IWA420	6.20	Leafl_ave	5B	16.7	13.7	19.7	S30	0.09	0.11
IWB69059	9.10	Leafl_ave	5B	40.3	37.3	43.3	S31	0.10	0.17
IWB28778	9.73	SPAD	5B	47.4	44.4	50.4	Q28	-0.11	0.20
IWB28778	4.09	Shoot_Root	5B	47.4	44.4	50.4	Q28	0.11	0.10
IWB72812	6.32	SPAD	5B	112.5	109.5	115.5	S32	-0.15	0.13
tPt-1253	3.22	Seminal_dmax	5B	144.98	141.98	147.98	Q29	-0.07	0.05
wPt-3329	8.18	Lateral_d	5B	146.1	143.1	149.1	Q29	-0.20	0.13
wPt-3329	3.95	Lateral_deep	5B	146.1	143.1	149.1	Q29	-0.15	0.09
IWB9424	5.87	Width	5B	171.2	168.2	174.2	S33	0.16	0.16
IWB60548	3.11	Leafl_ave	5B	192.7	189.7	195.7	S34	-0.07	0.06
IWA6578	7.96	Leafl_ave	5B	206.2	203.2	209.2	S35	-0.10	0.15
wPt-1377	4.15	Ave_LA	6A	0	0	3	S36	0.10	0.11
IWB12224	3.20	Nodal_d	6A	16.6	13.6	19.6	S37	-0.06	0.05
IWB38287	4.28	LSW	6A	43.1	40.1	46.1	S38	-0.10	0.09
IWB30925	3.81	Nodal_dmax	6A	62.1	59.1	65.1	Q30	0.09	0.09
IWB30925	3.50	Nodal_top	6A	62.1	59.1	65.1	Q30	0.07	0.05
IWB30925	3.22	Nodal	6A	62.1	59.1	65.1	Q30	0.06	0.05
IWA399	7.04	LSW	6A	62.6	59.6	65.6	Q30	0.16	0.15
IWB57644	3.98	LA	6A	118.2	115.2	121.2	Q31	0.10	0.10
IWA7572	6.96	Leafw_ave	6A	119	116	122	Q31	0.13	0.18
IWB57413	4.26	Total_dmaxdep	6A	122.1	119.1	125.1	Q31	0.12	0.10
IWB35245	9.59	Width	6A	122.4	119.4	125.4	Q31	0.18	0.23
IWB60756	5.55	Lateral_top	6B	7.5	4.5	10.5	S39	0.25	0.13
IWB54801	4.40	SPAD	6B	20.4	17.4	23.4	S40	-0.08	0.09
IWB59107	3.78	Lateral	6B	29.5	26.5	32.5	S41	-0.11	0.09
wPt-3309	4.95	Leafw_ave	6B	36	33	39	S42	-0.11	0.13
IWB26976	3.00	T0_dep	6B	58.6	55.6	61.6	S43	-0.06	0.05
IWA2975	6.05	Leafl_ave	6B	65.9	62.9	68.9	Q32	-0.07	0.06
IWB33924	3.34	Lateral_top	6B	67.8	64.8	70.8	Q32	-0.10	0.06
IWB29294	6.05	Leafw_ave	6B	74.9	71.9	77.9	Q33	-0.13	0.16
IWA1501	5.50	Water_content	6B	77.6	74.6	80.6	Q33	-0.19	0.12
IWB13090	3.22	Shoot_Root	6B	90.1	87.1	93.1	Q34	-0.15	0.07
IWB73374	4.54	Leaves	6B	92.9	89.9	95.9	Q34	0.08	0.10
IWB52227	3.05	Tiller_emission_rate	6B	124.4	121.4	127.4	S44	-0.10	0.03

SNP	-log10 pvalue	Phenotype	Chr	Pos (cM)	Left (cM)	Right (cM)	Cluster	Effect %	R^2
IWB48362	4.53	Seminal_top	6B	134	131	137	S45	0.10	0.10
IWB13062	3.51	Tiller_emission_rate	6B	145.3	142.3	148.3	S46	-0.06	0.03
IWB2096	5.01	Seminal_top	6B	152.2	149.2	155.2	Q35	-0.15	0.11
IWB2096	4.81	Seminal_dmax	6B	152.2	149.2	155.2	Q35	-0.17	0.10
IWB52925	4.18	LA	6B	154.6	151.6	157.6	Q35	-0.13	0.09
IWB52925	3.22	Root_Dry	6B	154.6	151.6	157.6	Q35	-0.10	0.05
IWB67175	14.26	Leafl_ave	7A	14.1	11.1	17.1	Q36	-0.13	0.25
IWB13845	8.48	Leafw_ave	7A	14.1	11.1	17.1	Q36	-0.15	0.24
IWB67174	6.11	Ave_LA	7A	14.2	11.2	17.2	Q36	-0.12	0.15
IWB68559	9.12	SPAD	7A	43.5	40.5	46.5	S47	-0.11	0.20
IWB74024	4.49	Lateral_d	7A	50.4	47.4	53.4	Q37	-0.15	0.11
IWB27639	5.03	Shoot_Dry	7A	53.1	50.1	56.1	Q37	-0.09	0.12
IWB27639	4.76	Total_biomass	7A	53.1	50.1	56.1	Q37	-0.09	0.11
IWB47149	3.18	Width	7A	58.9	55.9	61.9	Q37	-0.07	0.05
IWB12626	3.05	Nod_Sem_ratio	7A	62.1	59.1	65.1	Q37	0.05	0.03
IWB46670	3.22	First_Nodal_day	7A	82.2	79.2	85.2	Q38	-0.16	0.05
IWB23424	3.11	Nodal	7A	82.6	79.6	85.6	Q38	-0.07	0.06
IWB53919	3.49	Nodal_dmax	7A	89.6	86.6	92.6	Q39	-0.08	0.07
IWB72815	9.60	Lateral_d	7A	89.8	86.8	92.8	Q39	0.19	0.23
IWB70728	7.08	Total_deep	7A	112.6	109.6	115.6	Q40	-0.15	0.18
IWB51612	7.03	Seminal	7A	112.6	109.6	115.6	Q40	-0.16	0.15
IWB70728	5.68	Seminal_deep	7A	112.6	109.6	115.6	Q40	-0.14	0.14
IWB70728	6.48	Lateral_deep	7A	112.6	109.6	115.6	Q40	-0.11	0.14
IWB70728	5.83	Depth2	7A	112.6	109.6	115.6	Q40	-0.16	0.13
IWB51612	3.09	Mu_rlen	7A	112.6	109.6	115.6	Q40	-0.09	0.06
IWA3579	6.88	Total_Length	7A	112.7	109.7	115.7	Q40	-0.11	0.16
IWB43420	7.14	Seminal_top	7A	113.1	110.1	116.1	Q40	-0.11	0.15
IWB57877	4.25	Shoot_Root	7A	113.4	110.4	116.4	Q40	0.13	0.10
IWB69251	3.30	RSW	7A	113.4	110.4	116.4	Q40	0.11	0.06
IWB71893	4.11	Mu_LA	7A	114	111	117	Q40	0.08	0.07
IWA2752	4.31	Width	7A	130.5	127.5	133.5	Q41	-0.16	0.11
IWB11768	3.00	Tillers	7A	136.2	133.2	139.2	Q41	-0.08	0.07
IWB57762	6.41	Lateral_d	7A	157.3	154.3	160.3	Q42	0.17	0.19
IWB10093	5.79	First_tiller_day	7A	157.3	154.3	160.3	Q42	-0.13	0.13
IWA7046	7.08	SPAD	7A	159.2	156.2	162.2	Q42	0.16	0.15
IWB35048	15.04	Leafl_ave	7A	168.6	165.6	171.6	S48	-0.15	0.28
IWB28062	6.25	Lateral_d	7A	181.8	178.8	184.8	Q43	0.21	0.13
IWB28062	3.13	Total_dmaxdep	7A	181.8	178.8	184.8	Q43	-0.16	0.06
IWB72649	6.91	Lateral_deep	7A	192.9	189.9	195.9	S49	0.17	0.16
IWB61376	4.90	Seminal_top	7A	203.4	200.4	206.4	Q44	-0.10	0.11
IWB49295	3.93	Total_top	7A	203.4	200.4	206.4	Q44	-0.08	0.08
IWB61376	3.07	Root_Dry	7A	203.4	200.4	206.4	Q44	-0.07	0.05

SNP	-log10 pvalue	Phenotype	Chr	Pos (cM)	Left (cM)	Right (cM)	Cluster	Effect %	R^2
IWB61376	3.56	Seminal_dmax	7A	203.4	200.4	206.4	Q44	-0.07	0.04
IWB8973	4.15	Ave_LA	7B	0	0	3	Q45	0.10	0.11
IWB25853	3.09	First_Nodal_day	7B	0	0	3	Q45	-0.11	0.04
IWB72147	3.82	First_tiller_day	7B	58.4	55.4	61.4	S50	0.09	0.06
IWB47779	6.19	Ave_LA	7B	90	87	93	Q46	0.24	0.14
IWB47779	4.01	Leafw_ave	7B	90	87	93	Q46	0.20	0.13
IWB72641	3.28	T0_dep	7B	92.9	89.9	95.9	Q46	-0.08	0.04
IWB58920	4.99	Seminal_top	7B	96.1	93.1	99.1	Q46	-0.13	0.11
IWB41721	5.92	Lateral_dmax	7B	114.2	111.2	117.2	Q47	0.15	0.13
IWB54467	3.23	Lateral	7B	114.2	111.2	117.2	Q47	0.10	0.07
IWB73754	4.44	Water_content	7B	120.4	117.4	123.4	Q48	0.21	0.09
IWB65673	4.66	Lateral_deep	7B	122.1	119.1	125.1	Q48	0.13	0.11
IWB25295	4.55	Tiller_emission_rate	7B	132.8	129.8	135.8	S51	-0.12	0.07
IWB64809	5.53	RSW	7B	150.8	147.8	153.8	S52	0.16	0.11
wPt-4814	3.94	Seminal_top	7B	161.7	158.7	164.7	Q49	0.07	0.08
IWB68493	5.43	Total_top	7B	165	162	168	Q49	0.09	0.12
IWB73409	3.02	Total_dmax	7B	166.2	163.2	169.2	Q49	0.08	0.08
IWB72241	7.35	Lateral_top	7B	169.8	166.8	172.8	Q49	0.26	0.21
wPt-6156	17.02	Leafl_ave	7B	175.9	172.9	178.9	S53	0.16	0.29
IWB10818	4.90	LSW	7B	186	183	189	S54	-0.12	0.11
IWB13260	4.05	Lateral_top	7B	208.1	205.1	211.1	S55	0.10	0.07

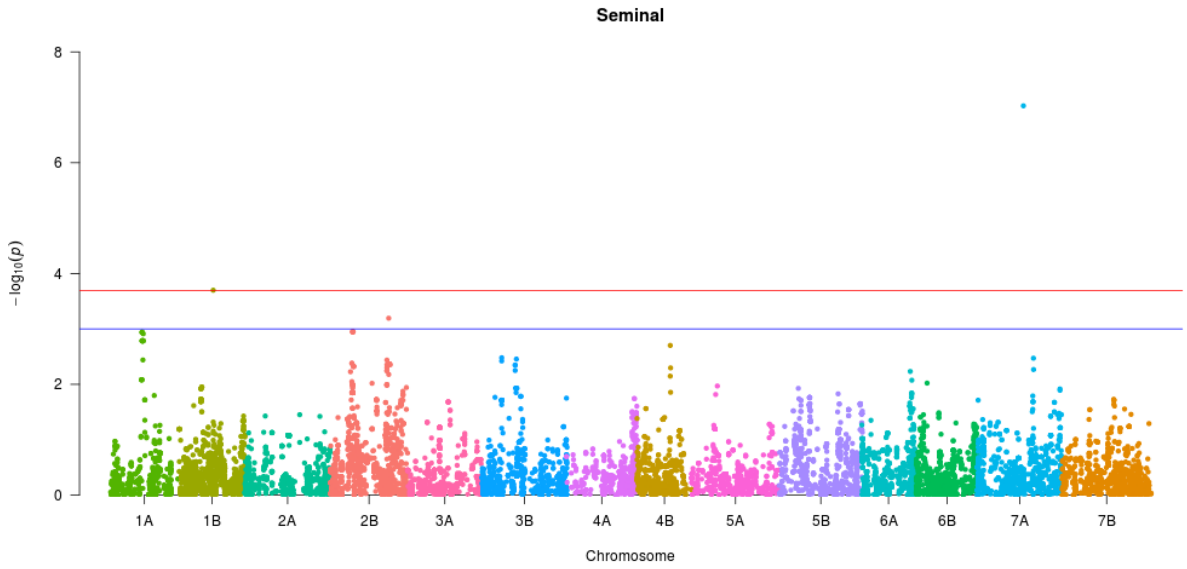
Seminal
−log10(p)
8
6
4
2
0
1A
1B
2A
2B
3A
3B
4A
4B
5A
5B
6A
6B
7A
7B
Chromosome

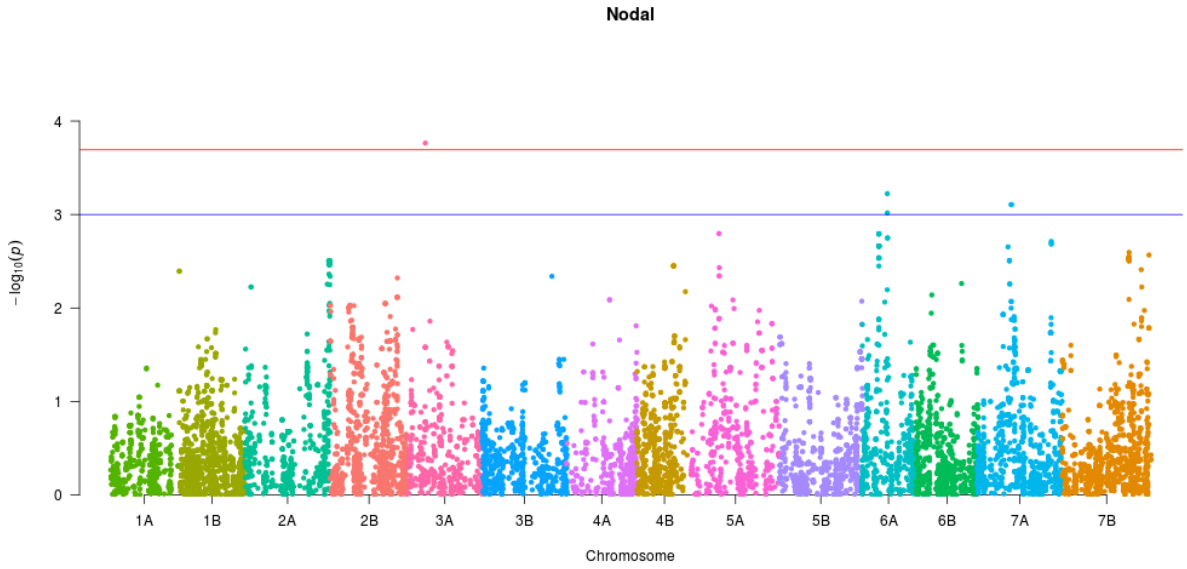
Nodal
−log10(p)
4
3
2
1
0
1A
1B
2A
2B
3A
3B
4A
4B
5A
5B
6A
6B
7A
7B
Chromosome

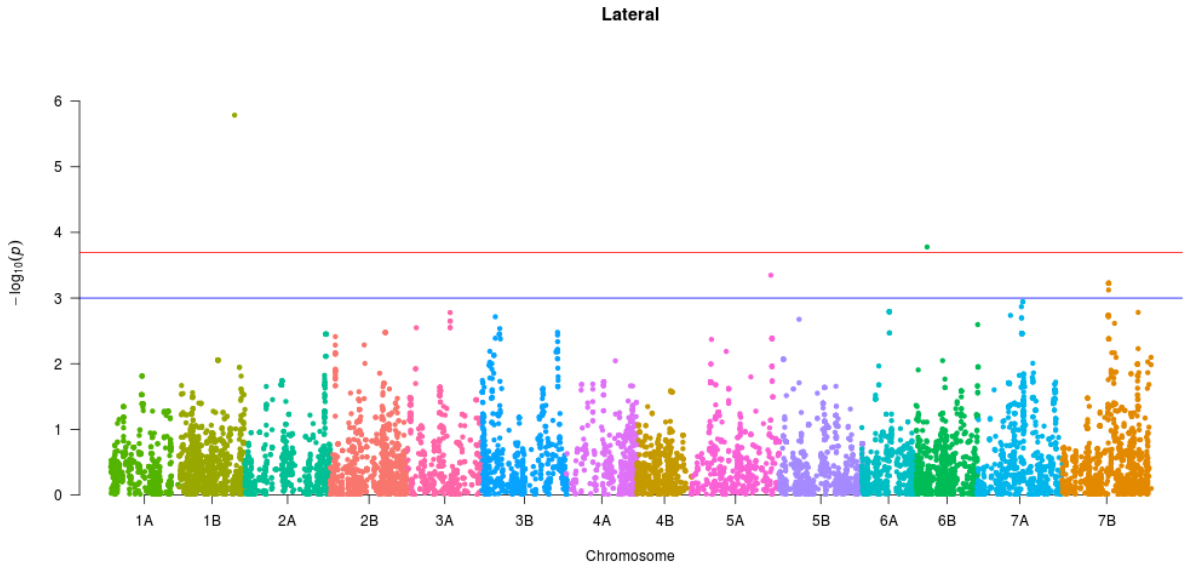
Lateral
−log10(p)
6
5
4
3
2
1
0
1A
1B
2A
2B
3A
3B
4A
4B
5A
5B
6A
6B
7A
7B
Chromosome

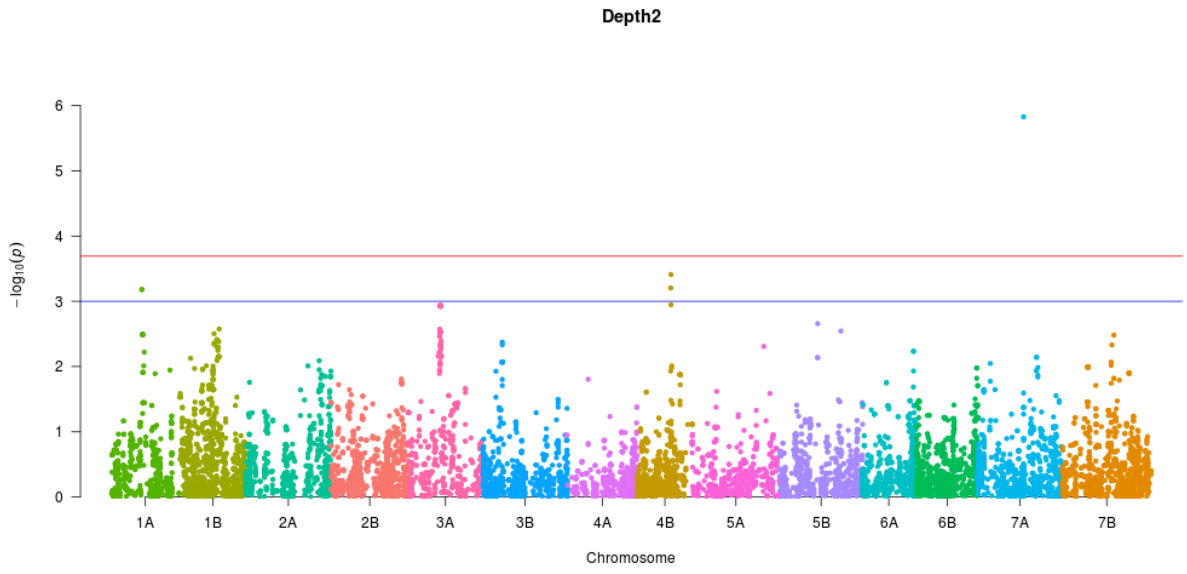
Depth2
−log10(p)
0
1
2
3
4
5
6
1A
1B
2A
2B
3A
3B
4A
4B
5A
5B
6A
6B
7A
7B
Chromosome

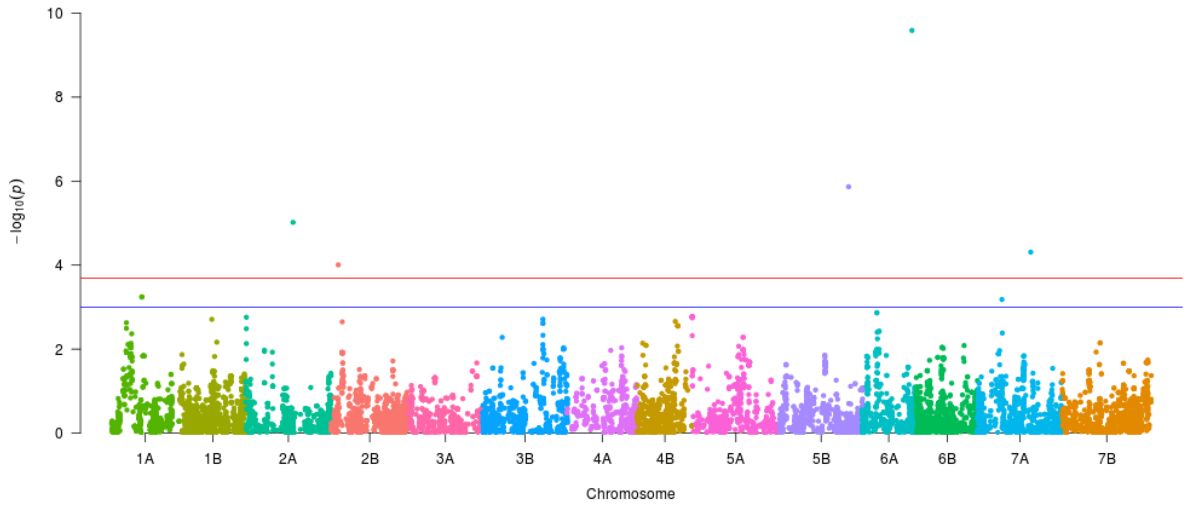
Width
−log10(p)
0
2
4
6
8
10
1A
1B
2A
2B
3A
3B
4A
4B
5A
5B
6A
6B
7A
7B
Chromosome

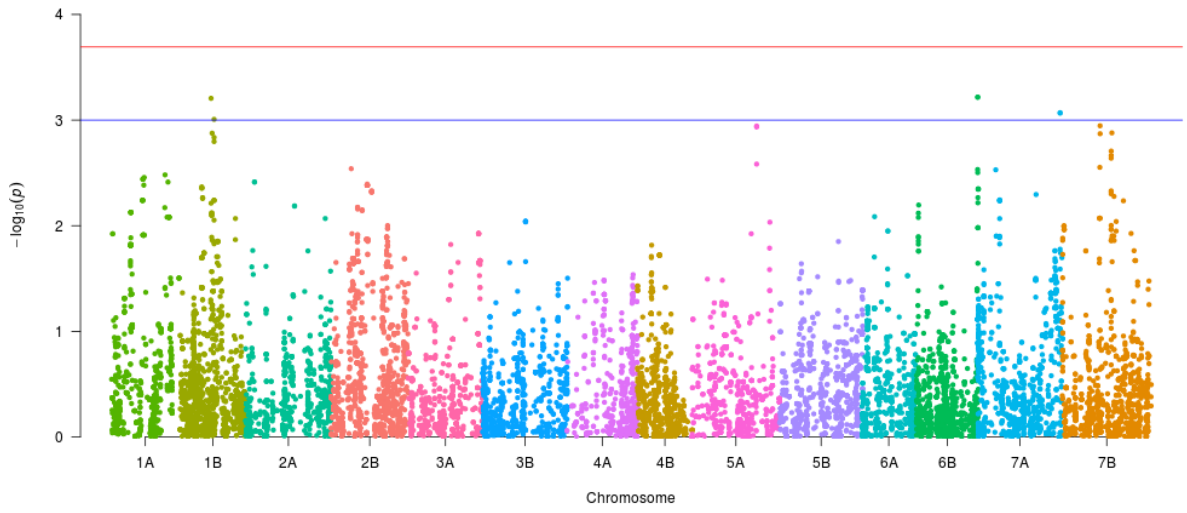
Root_Dry
−log10(p)
0
1
2
3
4
1A
1B
2A
2B
3A
3B
4A
4B
5A
5B
6A
6B
7A
7B
Chromosome

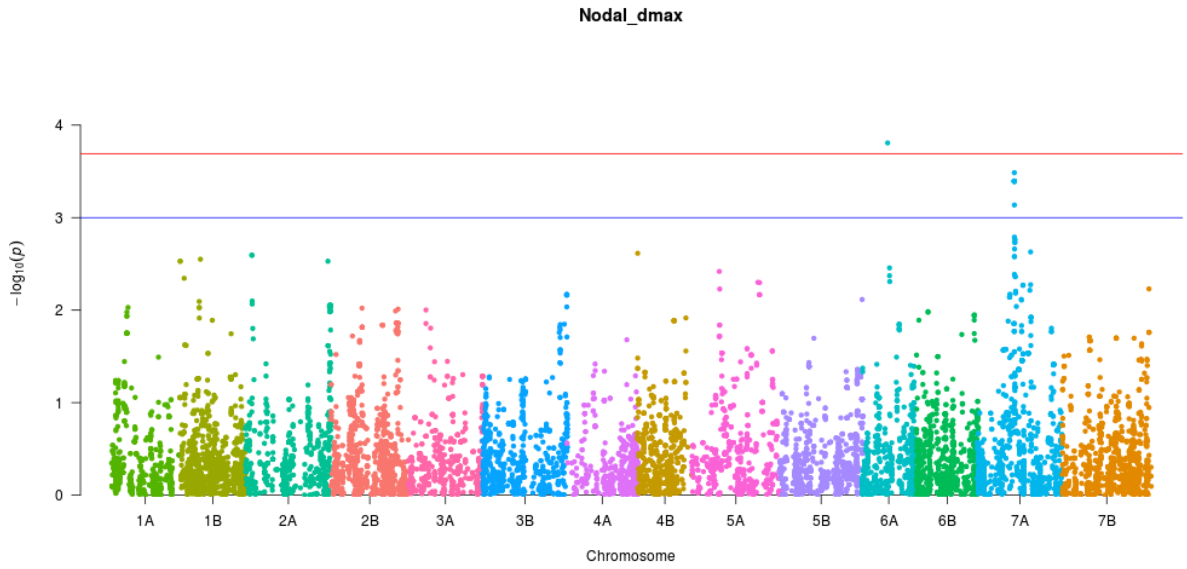
Nodal_dmax
−log10(p)
0
1
2
3
4
1A
1B
2A
2B
3A
3B
4A
4B
5A
5B
6A
6B
7A
7B
Chromosome

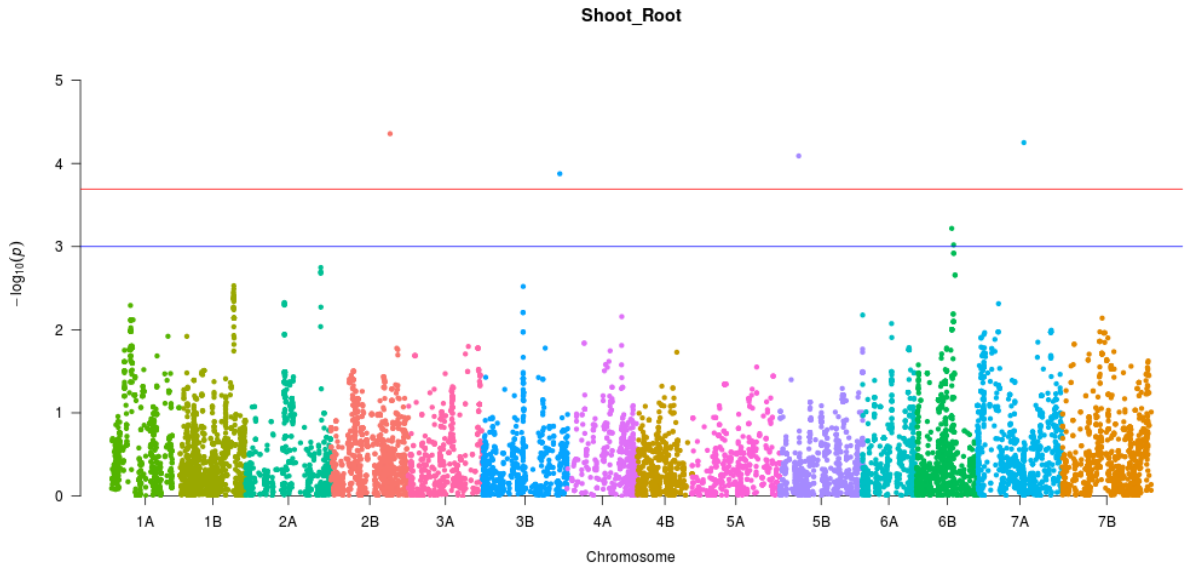
Shoot_Root
−log10(p)
0
1
2
3
4
5
1A
1B
2A
2B
3A
3B
4A
4B
5A
5B
6A
6B
7A
7B
Chromosome

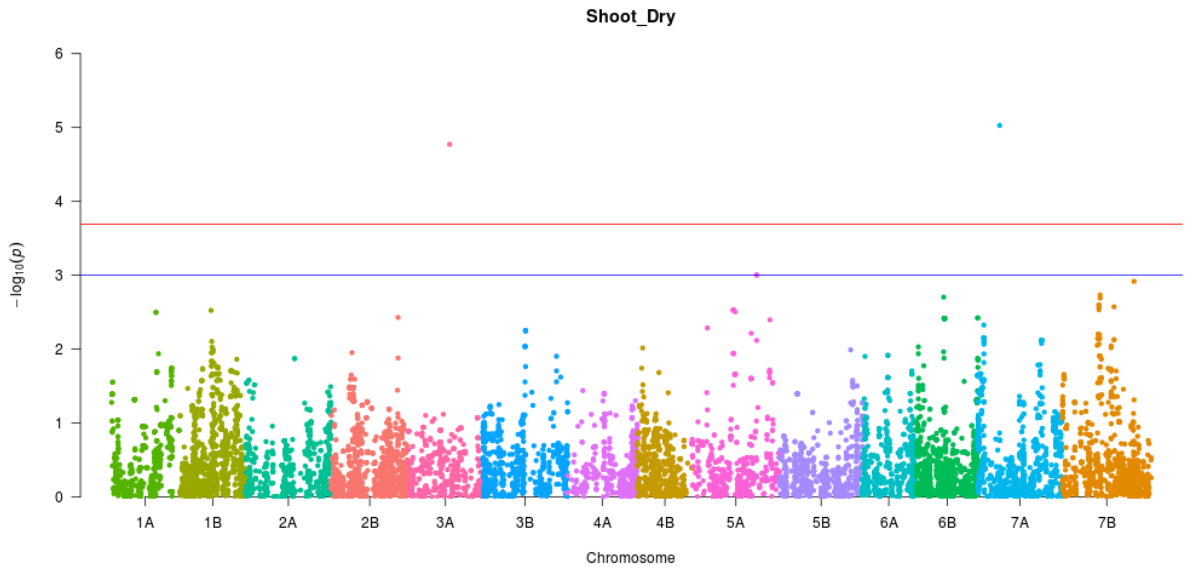
Shoot_Dry
−log10(p)
0
1
2
3
4
5
6
1A
1B
2A
2B
3A
3B
4A
4B
5A
5B
6A
6B
7A
7B
Chromosome

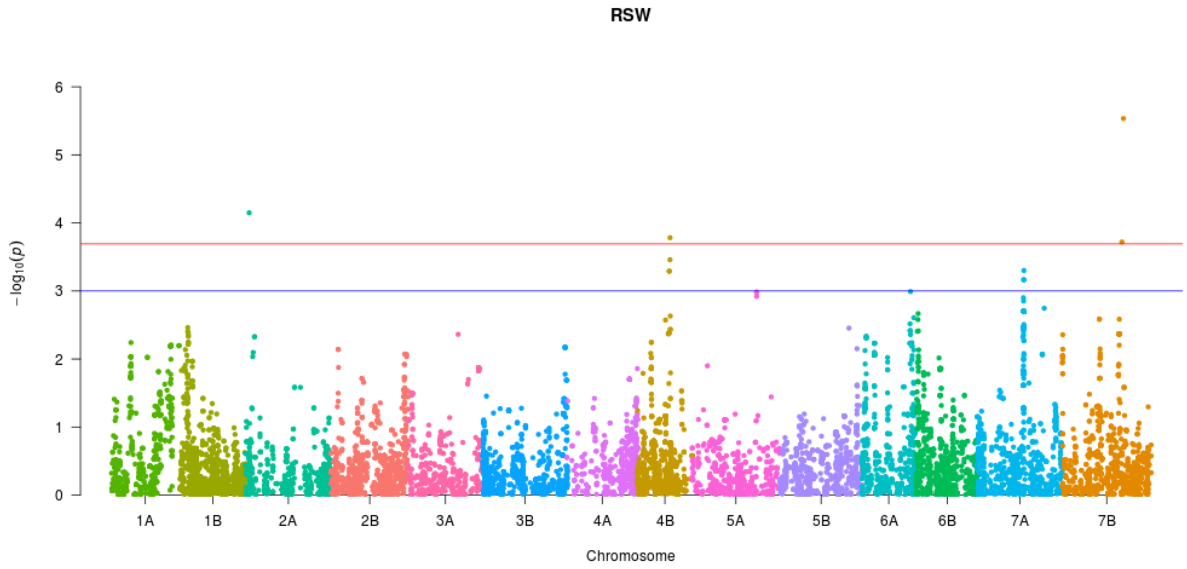
RSW
−log10(p)
0
1
2
3
4
5
6
1A
1B
2A
2B
3A
3B
4A
4B
5A
5B
6A
6B
7A
7B
Chromosome

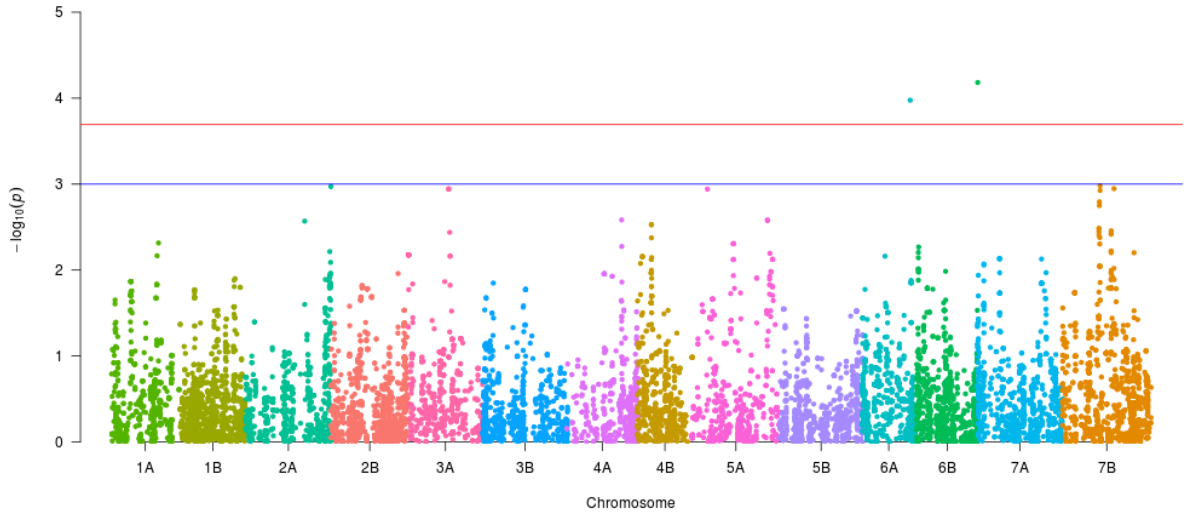
LA
−log10(p)
0
1
2
3
4
5
1A
1B
2A
2B
3A
3B
4A
4B
5A
5B
6A
6B
7A
7B
Chromosome

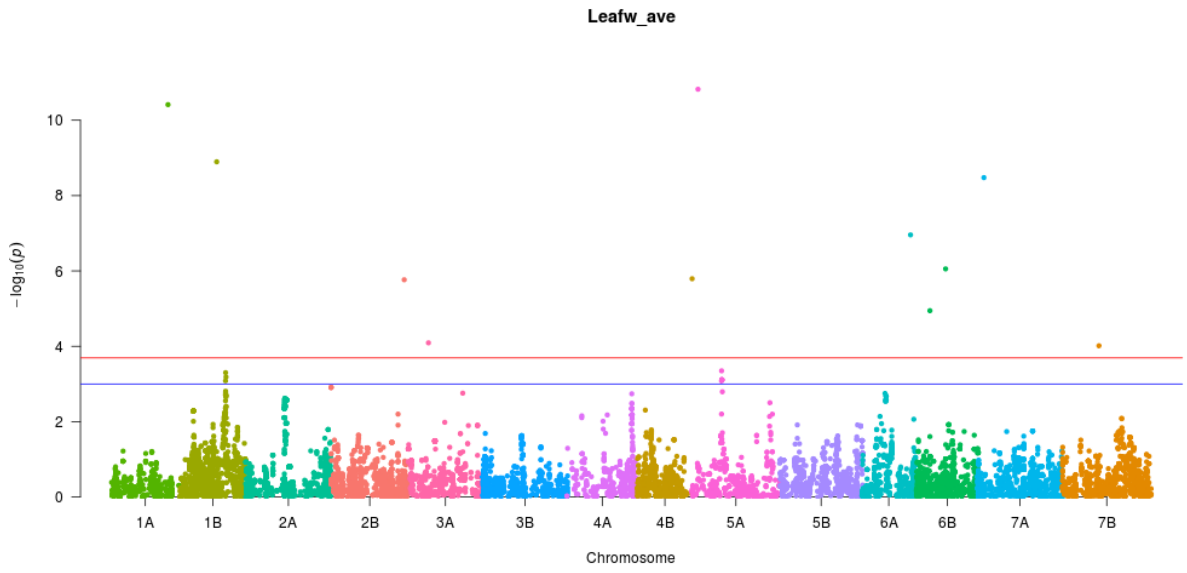
Leafw_ave
−log10(p)
0
2
4
6
8
10
1A
1B
2A
2B
3A
3B
4A
4B
5A
5B
6A
6B
7A
7B
Chromosome

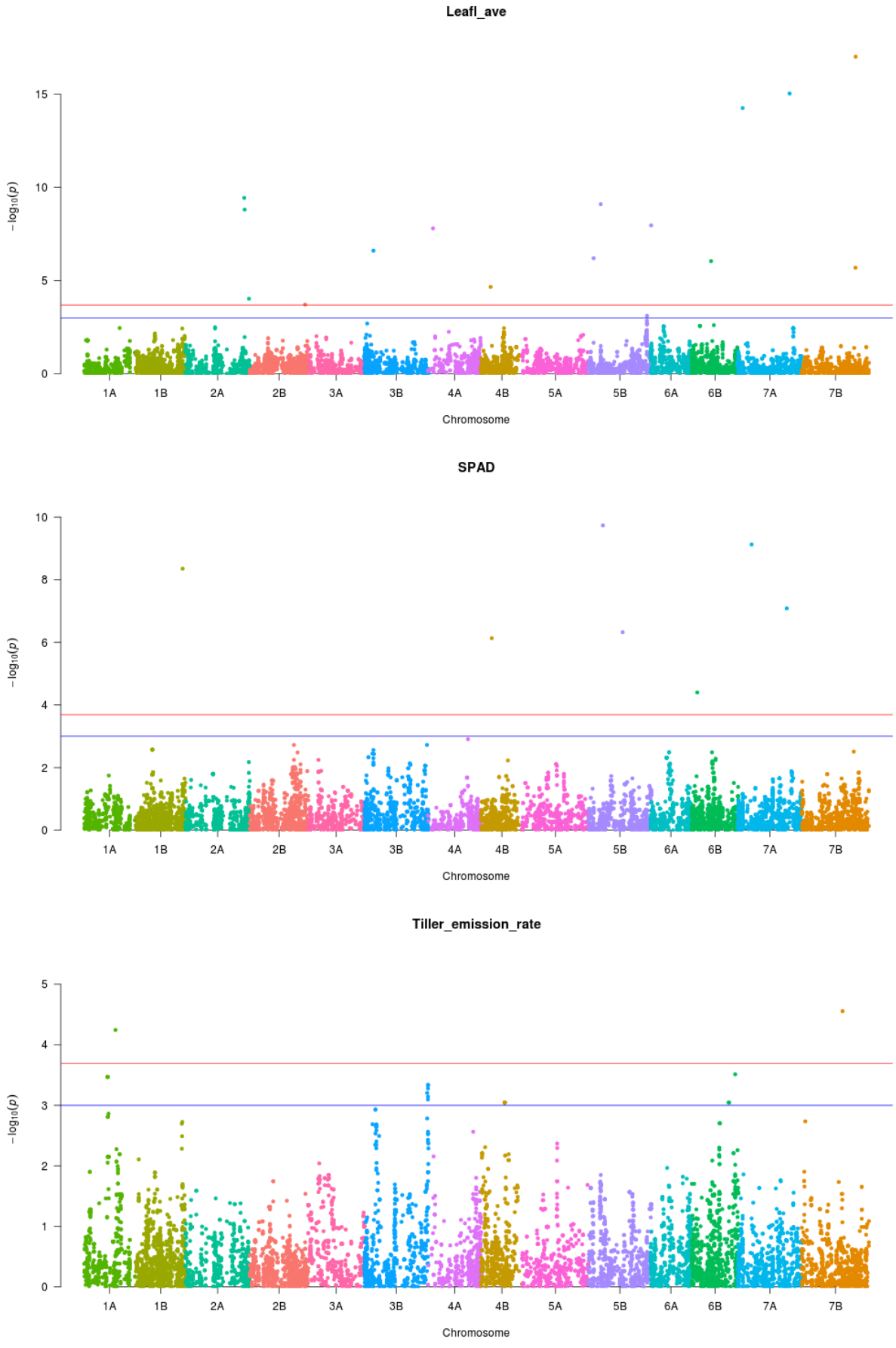

Figure 7-22 Manhattan plots of some key traits. The red horizontal line indicates the major QTL threshold, the blue one the putative QTL threshold

Table 8 QTL clusters. QTL were grouped into clusters when they were less than far twice the LD decay each other. Tag markers are those which had a higher mean R2 with all the other markers of the cluster. Confidence inerval reports the position of the left and right most markers of the QTL cluster. Direction of the effects is referred to the minor allele and is corrected depending on the sign of the correlation coefficients of each of the markers with the tag marker. QTL clusters showing overlapping confidence interval were considered as distinct in case of discordant direction of the effects

Cluster	Tag marker	Chr	Pos (cM)	QTL nb	Phenotypes	Confidence interval	Max - log10(p.val)
Q1	IWB35039	1A	75.1	6	-Depth2; -Width; -Tiller_emission_rate; -Seminal_deep; -Total_deep; -Total_Length	75.1 - 80.9	4.1
Q2	IWB12327	1B	81.2	10	+Lateral_d; +Lateral_deep; +Root_Dry; +T0_dep; +Total_Length; +Seminal; +Ave_LA; +Root_Dry; +Seminal_deep; +Total_deep	74.1 - 87.1	7.2
Q3	IWB35875	1B	93.4	2	-First_tiller_day; -Leafw_ave	93.4 - 93.5	8.9
Q4	IWB72561	1B	140.1	3	+Lateral; +Lateral_dmax; +Lateral_top	140.1 - 140.1	8.6
Q5	IWB66474	1B	152	2	+First_tiller_day; +SPAD	152 - 156.3	8.4
Q6	wPt-7175	2A	8.6	2	-Lateral_dmax; -RSW	7.8 - 8.6	4.1
Q7	IWB70278	2A	101.6	2	+Lateral_deep; -Water_content	101.6 - 102	5.3
Q8	IWB12196	2A	193.4	2	+Leafl_ave; +LSW	193.4 - 197.6	9.4
Q9	IWB9316	2A	208.7	3	-Leaves; -Leafl_ave; -Nod_Sem_ratio	204.3 - 208.7	6.1
Q10	IWB28973	2B	12.2	3	-Lateral_deep; -Lateral_dmax; +Width	12.2 - 17.7	6.4
Q11	IWB55339	2B	51.8	2	-Lateral_d; -Total_Length	51.8 - 55.3	4.9
Q12	IWB66226	2B	103.5	3	-Seminal_dmax; -Seminal_top; +LSW	103.5 - 108.2	5.9
Q13	IWB22762	2B	144.8	4	-Mu_rlen; -Seminal; -Total_deep; +Shoot_Root	140.3 - 146.5	4.4
Q14	IWB39104	2B	166.3	5	+Nodal_d; +Total_deep; -Lateral_top; -Total_Length; -Total_top	165.7 - 166.3	7.6
Q15	IWB28826	2B	181.6	3	+Ave_LA; +Leafl_ave; +Leafw_ave	181.6 - 181.6	5.8
Q16	IWB44601	3A	43.7	3	+First_Nodal_day; -Nodal; -Nod_Sem_ratio	43.7 - 43.7	3.9

Cluster	Tag marker	Chr	Pos (cM)	QTL nb	Phenotypes	Confidence interval	Max - log10(p.val)
Q17	IWB48828	3A	49.9	2	-Leafw_ave; -Mu_LA	49.9 - 54.5	4.1
Q18	IWB67653	3A	102.7	5	-Shoot_Dry; -Total_biomass; -Lateral_d; -Lateral_deep; -LSW	102.7 - 105.3	7.4
Q19	wPt-3133	3A	123.5	2	+Leaves; +Tillers	123.5 - 123.5	4.4
Q20	wPt-1349	3B	36.64	3	-Leafl_ave; -Lateral_d; +Tillers	30.2 - 36.64	8.8
Q21	IWB26362	4A	68.4	2	-Lateral_top; +LSW	64.1 - 68.4	6.6
Q22	IWB11925	4B	34.4	4	+Lateral_deep; +Leafl_ave; -Mu_LA; -SPAD	26.4 - 34.4	6.1
Q23	IWB1109	4B	83.1	4	-Tiller_emission_rate; -RSW; +Total_deep; +Depth2	77 - 83.1	3.8
Q24	IWB25728	5A	14.3	2	+Leafw_ave; -Leaves	14.3 - 14.3	10.8
Q25	IWB71919	5A	67.3	2	-Nodal_top; -Leafw_ave	67.3 - 73	3.3
Q26	IWB35863	5A	160	2	+Shoot_Dry; +Total_biomass	160 - 160	3.2
Q27	IWA3335	5A	199.6	2	+Lateral; -Ave_LA	196.2 - 199.6	8.0
Q28	IWB28778	5B	47.4	2	+Shoot_Root; -SPAD	47.4 - 47.4	9.7
Q29	wPt-3329	5B	146.1	3	-Seminal_dmax; -Lateral_d; -Lateral_deep	144.98 - 146.1	8.2
Q30	IWB30925	6A	62.1	4	+Nodal; +Nodal_dmax; +Nodal_top; +LSW	62.1 - 62.6	7.0
Q31	IWB57413	6A	122.1	4	+LA; +Leafw_ave; +Total_dmaxdep; +Width	118.2 - 122.4	9.6
Q32	IWA2975	6B	65.9	2	-Leafl_ave; +Lateral_top	65.9 - 67.8	6.0
Q33	IWB29294	6B	74.9	2	-Leafw_ave; +Water_content	74.9 - 77.6	6.1
Q34	IWB13090	6B	90.1	2	-Shoot_Root; +Leaves	90.1 - 92.9	4.5
Q35	IWB2096	6B	152.2	4	-Seminal_dmax; -Seminal_top; +LA; +Root_Dry	152.2 - 154.6	5.0
Q36	IWB13845	7A	14.1	3	-Leafl_ave; -Leafw_ave; -Ave_LA	14.1 - 14.2	14.3
Q37	IWB27639	7A	53.1	5	+Lateral_d; -Shoot_Dry; -Total_biomass; -Width; -Nod_Sem_ratio	50.4 - 62.1	5.0
Q38	IWB46670	7A	82.2	2	-First_Nodal_day; +Nodal	82.2 - 82.6	3.2
Q39	IWB53919	7A	89.6	2	-Nodal_dmax; +Lateral_d	89.6 - 89.8	9.6

Cluster	Tag marker	Chr	Pos (cM)	QTL nb	Phenotypes	Confidence interval	Max - log10(p.val)
Q40	IWB51612	7A	112.6	11	-Depth2; -Lateral_deep; -Mu_rlen; -Seminal; -Seminal_deep; -Total_deep; -Total_Length; -Seminal_top; +RSW; +Shoot_Root; +Mu_LA	112.6 - 114	7.1
Q41	IWB11768	7A	136.2	2	+Width; -Tillers	130.5 - 136.2	4.3
Q42	IWB57762	7A	157.3	3	-First_tiller_day; +Lateral_d; +SPAD	157.3 - 159.2	7.1
Q43	IWB28062	7A	181.8	2	-Lateral_d; +Total_dmaxdep	181.8 - 181.8	6.2
Q44	IWB61376	7A	203.4	4	-Root_Dry; -Seminal_dmax; -Seminal_top; -Total_top	203.4 - 203.4	4.9
Q45	IWB8973	7B	0	2	+Ave_LA; -First_Nodal_day	0 - 0	4.2
Q46	IWB47779	7B	90	4	+Ave_LA; +Leafw_ave; -T0_dep; +Seminal_top	90 - 96.1	6.2
Q47	IWB41721	7B	114.2	2	+Lateral; +Lateral_dmax	114.2 - 114.2	5.9
Q48	IWB73754	7B	120.4	2	+Water_content; +Lateral_deep	120.4 - 122.1	4.7
Q49	IWB68493	7B	165	4	+Seminal_top; +Total_top; +Total_dmax; +Lateral_top	161.7 - 169.8	7.4

4. General considerations and perspectives

Drought tolerance is an extremely complex trait, determined by complex mechanisms involving each organ of the plant all along its life cycle. High-throughput phenotyping platforms permit us to dissect part of this complexity allowing the detailed screening of populations suitable for genetic study. This notwithstanding, a simpler trait does not necessarily imply a simple genetic basis. Is therefore crucial not only to identify those key traits involved in drought response but also dissect the genetic basis of them to understand how heritable they are and therefore how easily they could be introgressed in a certain genetic background. Another critical point is to identify an optimal phenotyping technique which permits the screening of large populations in the cheapest and quickest way. From what we observed in these studies, root phenotyping, even when performed with less sophisticated techniques, might be very informative on the behaviour of plants and their relationships with water at least during the entire vegetative stage. Anyway, modern approaches cannot avoid investigating plants in their integrity, thus considering roots and shoots cross-relationships holistically. From the studies above exposed, emerged the crucial role of shoot and roots carbon partitioning. In the maize experiment we demonstrated that plants showing a more shoot-oriented carbon partitioning are also more water use efficient. How this might affect the behaviour of these plants in field conditions has to be verified since this strategy might be detrimental for root development and therefore on water uptake in harsher scenarios. On the other hand, the wheat experiment permitted us to identify, among others, a chromosomal region inducing a more root-oriented carbon partitioning. This region was found to be differentially selected from breeders with the deep rooting allelic form preferentially selected in drought tolerance-oriented breeding programs (ICARDA) and the shoot oriented allelic form predominant in CIMMYT germplasm selected to maximize productivity in optimal conditions. Understand the physiological mechanisms underlying shoot/root carbon partitioning is therefore crucial to properly select for a specific environment. What emerged from these studies is that a key role is played by root architecture. A low seminal root number was found to trigger a more shoot oriented carbon partitioning resulting in higher shoot water use efficiency. Lateral roots on the contrary, seem to be involved in a more root system favourable resource allocation. Unfortunately, to validate these hypothesis, it is compulsory to work on comparable genetic background. GWAS, by permitting the identification of the key chromosomal region underling a certain trait, will permit us to relatively easily introgress certain target QTL in homogeneous genetic background and, finally, to validate the most important QTL and move to the gene cloning procedure.

Bibliografy

Abdel-Ghani, A. H., Hu, S., Chen, Y., Brenner, E. A., Kumar, B., Blanco, M., et al. (2016). Genetic architecture of plant height in maize phenotype-selected introgression families. *Plant Breed.* 135, 429–438. doi:10.1111/pbr.12387.

Akaike, H. (1974). A new look at the statistical model identification. *IEEE Trans. Automat. Contr.* 19, 716–723. doi:10.1109/TAC.1974.1100705.

Alderman, H., Hoddinott, J., and Kinsey, B. (2006). Long term consequences of early childhood malnutrition. *Oxf. Econ. Pap.* 58, 450–474. doi:10.1093/oep/gpl008.

Araus, J. L., and Cairns, J. E. (2014). Field high-throughput phenotyping: the new crop breeding frontier. *Trends Plant Sci.* 19, 52–61. doi:10.1016/J.TPLANTS.2013.09.008.

Araus, J. L., Slafer, G. A., Reynolds, M. P., and Royo, C. (2002). Plant Breeding and Drought in C3 Cereals: What Should We Breed For? *Ann. Bot.* 89, 925–940. doi:10.1093/aob/mcf049.

Asseng, S., Ewert, F., Martre, P., Rötter, R. P., Lobell, D. B., Cammarano, D., et al. (2015). Rising temperatures reduce global wheat production. *Nat. Clim. Chang.* 5, 143–147. doi:10.1038/nclimate2470.

Avni, R., Nave, M., Barad, O., Baruch, K., Twardziok, S. O., Gundlach, H., et al. (2017). Wild emmer genome architecture and diversity elucidate wheat evolution and domestication. *Science* 357, 93–97. doi:10.1126/science.aan0032.

Barabaschi, D., Tondelli, A., Desiderio, F., Volante, A., Vaccino, P., Valè, G., et al. (2016). Next generation breeding. *Plant Sci.* 242, 3–13. doi:10.1016/J.PLANTSCI.2015.07.010.

Barrangou, R., Fremaux, C., Deveau, H., Richards, M., Boyaval, P., Moineau, S., et al. (2007). CRISPR Provides Acquired Resistance Against Viruses in Prokaryotes. *Science (80-.).* 315, 1709–1712. doi:10.1126/science.1138140.

Barrett, J. C., Fry, B., Maller, J., and Daly, M. J. (2005). Haploview: analysis and visualization of LD and haplotype maps. *Bioinformatics* 21, 263–265. doi:10.1093/bioinformatics/bth457.

Bates, D., Mächler, M., Bolker, B., and Walker, S. (2015). Fitting Linear Mixed-Effects Models Using lme4. *J. Stat. Softw.* 67, 1–48. doi:10.18637/jss.v067.i01.

Becker, S. R., Byrne, P. F., Reid, S. D., Bauerle, W. L., McKay, J. K., and Haley, S. D. (2016). Root traits contributing to drought tolerance of synthetic hexaploid wheat in a greenhouse study. *Euphytica* 207, 213–224. doi:10.1007/s10681-015-1574-1.

Belford, R. K., Klepper, B., and Rickman, R. W. (1987). Studies of Intact Shoot-Root Systems of Field-Grown Winter Wheat. II. Root and Shoot Developmental Patterns as Related to Nitrogen Fertilizer1. *Agron. J.* 79, 310. doi:10.2134/agronj1987.00021962007900020027x.

Bengough, A. G., Gordon, D. C., Al-Menaie, H., Ellis, R. P., Allan, D., Keith, R., et al. (2004). Gel observation chamber for rapid screening of root traits in cereal seedlings. *Plant Soil* 262, 63–70. doi:10.1023/B:PLSO.0000037029.82618.27.

Bevan, M. W., Flavell, R. B., and Chilton, M.-D. (1983). A chimaeric antibiotic resistance gene as a selectable marker for plant cell transformation. *Nature* 304, 184–187. doi:10.1038/304184a0.

Bishopp, A., and Lynch, J. P. (2015). The hidden half of crop yields. *Nat. Plants* 1, 15117. doi:10.1038/nplants.2015.117.

Blum, A. (2009). Effective use of water (EUW) and not water-use efficiency (WUE) is the target of crop yield improvement under drought stress. *F. Crop. Res.* 112, 119–123. doi:10.1016/j.fcr.2009.03.009.

Bonferroni, C. E. (1936). Teoria statistica delle classi e calcolo delle probabilità. *Pubbl. del R Ist. Super. di Sci. Econ. e Commer. di Firenze* 8, 3–62.

Borisjuk, L., Rolletschek, H., and Neuberger, T. (2012). Surveying the plant's world by magnetic resonance imaging. *Plant J.* 70, 129–146. doi:10.1111/j.1365-313X.2012.04927.x.

Borojevic, K., and Borojevic, K. (2005a). Historic Role of the Wheat Variety Akakomugi in Southern and Central European Wheat Breeding Programs. *Breed. Sci.* 55, 253–256. doi:10.1270/jsbbs.55.253.

Borojevic, K., and Borojevic, K. (2005b). The Transfer and History of "Reduced Height Genes" (Rht) in Wheat from Japan to Europe. *J. Hered.* 96, 455–459. doi:10.1093/jhered/esi060.

Bouchet, S., Servin, B., Bertin, P., Madur, D., Combes, V., Dumas, F., et al. (2013). Adaptation of Maize to Temperate Climates: Mid-Density Genome-Wide Association Genetics and Diversity Patterns Reveal Key Genomic Regions, with a Major Contribution of the Vgt2 (ZCN8) Locus.

PLoS One 8, e71377. doi:10.1371/journal.pone.0071377.

Bradbury, P. J., Zhang, Z., Kroon, D. E., Casstevens, T. M., Ramdoss, Y., and Buckler, E. S. (2007). TASSEL: software for association mapping of complex traits in diverse samples. *Bioinformatics* 23, 2633–2635. doi:10.1093/bioinformatics/btm308.

Burton, A. L., Johnson, J. M., Foerster, J. M., Hirsch, C. N., Buell, C. R., Hanlon, M. T., et al. (2014). QTL mapping and phenotypic variation for root architectural traits in maize (Zea mays L.). *Theor. Appl. Genet.* 127, 2293–2311. doi:10.1007/s00122-014-2353-4.

Cabrera-Bosquet, L., Crossa, J., von Zitzewitz, J., Serret, M. D., and Luis Araus, J. (2012). High-throughput Phenotyping and Genomic Selection: The Frontiers of Crop Breeding ConvergeF. *J. Integr. Plant Biol.* 54, 312–320. doi:10.1111/j.1744-7909.2012.01116.x.

Cabrera-Bosquet, L., Fournier, C., Brichet, N., Welcker, C., Suard, B., and Tardieu, F. (2016). High-throughput estimation of incident light, light interception and radiation-use efficiency of thousands of plants in a phenotyping platform. *New Phytol.* 212, 269–281. doi:10.1111/nph.14027.

Cai, Y., Chen, L., Liu, X., Guo, C., Sun, S., Wu, C., et al. (2018). CRISPR/Cas9-mediated targeted mutagenesis of *GmFT2a* delays flowering time in soya bean. *Plant Biotechnol. J.* 16, 176–185. doi:10.1111/pbi.12758.

Canè, M. A., Maccaferri, M., Nazemi, G., Salvi, S., Francia, R., Colalongo, C., et al. (2014). Association mapping for root architectural traits in durum wheat seedlings as related to agronomic performance. *Mol. Breed.* 34, 1629–1645. doi:10.1007/s11032-014-0177-1.

Casal, J. J. (1988). Light quality effects on the appearance of tillers of different order in wheat (Triticum aestivum). *Ann. Appl. Biol.* 112, 167–173. doi:10.1111/j.1744-7348.1988.tb02052.x.

Chardon, F., Hourcade, D., Combes, V., and Charcosset, A. (2005). Mapping of a spontaneous mutation for early flowering time in maize highlights contrasting allelic series at two-linked QTL on chromosome 8. *Theor. Appl. Genet.* 112, 1–11. doi:10.1007/s00122-005-0050-z.

Chen, Y., Ghanem, M. E., and Siddique, K. H. (2017). Characterising root trait variability in chickpea (Cicer arietinum L.) germplasm. *J. Exp. Bot.* 68, 1987–1999. doi:10.1093/jxb/erw368.

Chimungu, J. G., Maliro, M. F. A., Nalivata, P. C., Kanyama-Phiri, G., Brown, K. M., and Lynch, J.

P. (2015). Utility of root cortical aerenchyma under water limited conditions in tropical maize (Zea mays L.). *F. Crop. Res.* 171, 86–98. doi:10.1016/J.FCR.2014.10.009.

Clark, R. T., MacCurdy, R. B., Jung, J. K., Shaff, J. E., McCouch, S. R., Aneshansley, D. J., et al. (2011). Three-dimensional root phenotyping with a novel imaging and software platform. *Plant Physiol.* 156, 455–65. doi:10.1104/pp.110.169102.

Coe, E., Cone, K., McMullen, M., Chen, S.-S., Davis, G., Gardiner, J., et al. (2002). Access to the maize genome: an integrated physical and genetic map. *Plant Physiol.* 128, 9–12. doi:10.1104/PP.010953.

Collins, N. C., Tardieu, F., and Tuberosa, R. (2008). Quantitative trait loci and crop performance under abiotic stress: where do we stand? *Plant Physiol.* 147, 469–486. doi:10.1104/pp.108.118117.

Comas, L. H., Becker, S. R., Cruz, V. M. V., Byrne, P. F., and Dierig, D. A. (2013). Root traits contributing to plant productivity under drought. *Front. Plant Sci.* doi:10.3389/fpls.2013.00442.

Coupel-Ledru, A., Lebon, É., Christophe, A., Doligez, A., Cabrera-Bosquet, L., Péchier, P., et al. (2014). Genetic variation in a grapevine progeny (Vitis vinifera L. cvs Grenache×Syrah) reveals inconsistencies between maintenance of daytime leaf water potential and response of transpiration rate under drought. *J. Exp. Bot.* 65, 6205–18. doi:10.1093/jxb/eru228.

D'Amato, F., Scarascia, G. T., Monti, L. M., and Bozzini, A. (1962). Types and frequencies of chlorophyll mutations in Durum wheat induced by radiations and chemicals. *Radiat. Bot.* 2, 217–239. doi:10.1016/S0033-7560(62)80104-5.

D'Halluin, K., Vanderstraeten, C., Van Hulle, J., Rosolowska, J., Van Den Brande, I., Pennewaert, A., et al. (2013). Targeted molecular trait stacking in cotton through targeted double-strand break induction. *Plant Biotechnol. J.* 11, 933–941. doi:10.1111/pbi.12085.

Dalton, F. N. (1995). In-situ root extent measurements by electrical capacitance methods. *Plant Soil* 173, 157–165. doi:10.1007/BF00155527.

Daryanto, S., Wang, L., and Jacinthe, P.-A. (2016). Global Synthesis of Drought Effects on Maize and Wheat Production. *PLoS One* 11, e0156362. doi:10.1371/journal.pone.0156362.

Dunnett, C. W. (1955). A Multiple Comparison Procedure for Comparing Several Treatments with

a Control. *J. Am. Stat. Assoc.* 50, 1096. doi:10.2307/2281208.

Fiorani, F., and Schurr, U. (2013). Future Scenarios for Plant Phenotyping. *Annu. Rev. Plant Biol.* 64, 267–291. doi:10.1146/annurev-arplant-050312-120137.

Fisher, R. A. (1922). On the Interpretation of χ2 from Contingency Tables, and the Calculation of P. *J. R. Stat. Soc.* 85, 87–94. doi:10.2307/2340521.

Fleury, D., Jefferies, S., Kuchel, H., and Langridge, P. (2010). Genetic and genomic tools to improve drought tolerance in wheat. *J. Exp. Bot.* 61, 3211–22. doi:10.1093/jxb/erq152.

Furbank, R. T., and Tester, M. (2011). Phenomics – technologies to relieve the phenotyping bottleneck. *Trends Plant Sci.* 16, 635–644. doi:10.1016/J.TPLANTS.2011.09.005.

Ganal, M. W., Durstewitz, G., Polley, A., Bérard, A., Buckler, E. S., Charcosset, A., et al. (2011). A large maize (Zea mays L.) SNP genotyping array: development and germplasm genotyping, and genetic mapping to compare with the B73 reference genome. *PLoS One* 6, e28334. doi:10.1371/journal.pone.0028334.

Ghanem, M. E., Hichri, I., Smigocki, A. C., Albacete, A., Fauconnier, M.-L., Diatloff, E., et al. (2011). Root-targeted biotechnology to mediate hormonal signalling and improve crop stress tolerance. *Plant Cell Rep.* 30, 807–823. doi:10.1007/s00299-011-1005-2.

Gioia, T., Galinski, A., Lenz, H., M[illegible]ller, C., Lentz, J., Heinz, K., et al. (2017). GrowScreen-PaGe, a non-invasive, high-throughput phenotyping system based on germination paper to quantify crop phenotypic diversity and plasticity of root traits under varying nutrient supply. *Funct. Plant Biol.* 44, 76. doi:10.1071/FP16128.

Gioia, T., Nagel, K. A., Beleggia, R., Fragasso, M., Ficco, D. B. M., Pieruschka, R., et al. (2015). Impact of domestication on the phenotypic architecture of durum wheat under contrasting nitrogen fertilization. *J. Exp. Bot.* 66, 5519–30. doi:10.1093/jxb/erv289.

Gregory, P. J., Bengough, A. G., Grinev, D., Schmidt, S., Thomas, W. (Bill) T. B., Wojciechowski, T., et al. (2009). Root phenomics of crops: opportunities and challenges. *Funct. Plant Biol.* 36, 922. doi:10.1071/FP09150.

Gupta, P., Balyan, H., and Gahlaut, V. (2017). QTL Analysis for Drought Tolerance in Wheat: Present Status and Future Possibilities. *Agronomy* 7, 5. doi:10.3390/agronomy7010005.

Gupta, P. K., Langridge, P., and Mir, R. R. (2010). Marker-assisted wheat breeding: present status and future possibilities. *Mol. Breed.* 26, 145–161. doi:10.1007/s11032-009-9359-7.

Hartung, F., and Schiemann, J. (2014). Precise plant breeding using new genome editing techniques: opportunities, safety and regulation in the EU. *Plant J.* 78, 742–752. doi:10.1111/tpj.12413.

Herrera-Estrella, L., Depicker, A., Van Montagu, M., and Schell, J. (1983). Expression of chimaeric genes transferred into plant cells using a Ti-plasmid-derived vector. *Nature* 303, 209–213. doi:10.1038/303209a0.

Hicks, S. C., Okrah, K., Paulson, J. N., Quackenbush, J., Irizarry, R. A., and Bravo, H. C. (2017). Smooth quantile normalization. *Biostatistics*. doi:10.1093/biostatistics/kxx028.

Hochberg, Y., and Benjamini, Y. (1990). More powerful procedures for multiple significance testing. *Stat. Med.* 9, 811–818. doi:10.1002/sim.4780090710.

Hochholdinger, F., and Tuberosa, R. (2009). Genetic and genomic dissection of maize root development and architecture. *Curr. Opin. Plant Biol.* 12, 172–177. doi:10.1016/j.pbi.2008.12.002.

Hochman, Z., Gobbett, D. L., and Horan, H. (2017). Climate trends account for stalled wheat yields in Australia since 1990. *Glob. Chang. Biol.* 23, 2071–2081. doi:10.1111/gcb.13604.

Hodge, A. (2004). The plastic plant: root responses to heterogeneous supplies of nutrients. *New Phytol.* 162, 9–24. doi:10.1111/j.1469-8137.2004.01015.x.

Hothorn, T., Bretz, F., and Westfall, P. (2008). Simultaneous Inference in General Parametric Models. *Biometrical J.* 50, 346–363.

Hund, A., Fracheboud, Y., Soldati, A., Frascaroli, E., Salvi, S., and Stamp, P. (2004). QTL controlling root and shoot traits of maize seedlings under cold stress. *Theor. Appl. Genet.* 109, 618–629. doi:10.1007/s00122-004-1665-1.

Hund, A., Trachsel, S., and Stamp, P. (2009). Growth of axile and lateral roots of maize: I development of a phenotying platform. *Plant Soil* 325, 335–349. doi:10.1007/s11104-009-9984-2.

International Wheat Genome Sequencing Consortium (IWGSC), T. I. W. G. S. C. (2014). A chromosome-based draft sequence of the hexaploid bread wheat (Triticum aestivum) genome.

Science 345, 1251788. doi:10.1126/science.1251788.

Iyer-Pascuzzi, A. S., Symonova, O., Mileyko, Y., Hao, Y., Belcher, H., Harer, J., et al. (2010). Imaging and analysis platform for automatic phenotyping and trait ranking of plant root systems. *Plant Physiol.* 152, 1148–57. doi:10.1104/pp.109.150748.

Jeudy, C., Adrian, M., Baussard, C., Bernard, C., Bernaud, E., Bourion, V., et al. (2016). RhizoTubes as a new tool for high throughput imaging of plant root development and architecture: test, comparison with pot grown plants and validation. *Plant Methods* 12, 31. doi:10.1186/s13007-016-0131-9.

Jinek, M., Chylinski, K., Fonfara, I., Hauer, M., Doudna, J. A., and Charpentier, E. (2012). A programmable dual-RNA-guided DNA endonuclease in adaptive bacterial immunity. *Science* 337, 816–21. doi:10.1126/science.1225829.

Jompuk, C., Fracheboud, Y., Stamp, P., and Leipner, J. (2005). Mapping of quantitative trait loci associated with chilling tolerance in maize (Zea mays L.) seedlings grown under field conditions. *J. Exp. Bot.* 56, 1153–1163. doi:10.1093/jxb/eri108.

Jones, J. B. (1982). Hydroponics: Its history and use in plant nutrition studies. *J. Plant Nutr.* 5, 1003–1030. doi:10.1080/01904168209363035.

Kadam, N. N., Yin, X., Bindraban, P. S., Struik, P. C., and Jagadish, K. S. V (2015). Does morphological and anatomical plasticity during the vegetative stage make wheat more tolerant of water deficit stress than rice? *Plant Physiol.* 167, 1389–401. doi:10.1104/pp.114.253328.

Kahm, M., Hasenbrink, G., Lichtenberg-Fraté, H., Ludwig, J., and Kschischo, M. (2010). grofit : Fitting Biological Growth Curves with *R*. *J. Stat. Softw.* 33, 1–21. doi:10.18637/jss.v033.i07.

Kemp, C. D. (1960). Methods of Estimating the Leaf Area of Grasses from Linear Measurements. *Ann. Bot.* 24, 491–499. doi:10.1093/oxfordjournals.aob.a083723.

Klepper, B., Belford, R. K., and Rickman, R. W. (1984). Root and Shoot Development in Winter Wheat1. *Agron. J.* 76, 117. doi:10.2134/agronj1984.00021962007600010029x.

Kolmer, J. A., Singh, R. P., Garvin, D. F., Viccars, L., William, H. M., Huerta-Espino, J., et al. (2008). Analysis of the Rust Resistance Region in Wheat Germplasm. *Crop Sci.* 48, 1841. doi:10.2135/cropsci2007.08.0474.

Kuijken, R. C. P., van Eeuwijk, F. A., Marcelis, L. F. M., and Bouwmeester, H. J. (2015). Root phenotyping: from component trait in the lab to breeding. *J. Exp. Bot.* 66, 5389–5401. doi:10.1093/jxb/erv239.

Lagudah, E. S., Krattinger, S. G., Herrera-Foessel, S., Singh, R. P., Huerta-Espino, J., Spielmeyer, W., et al. (2009). Gene-specific markers for the wheat gene Lr34/Yr18/Pm38 which confers resistance to multiple fungal pathogens. *Theor. Appl. Genet.* 119, 889–898. doi:10.1007/s00122-009-1097-z.

Langridge, P., and Reynolds, M. P. (2015). Genomic tools to assist breeding for drought tolerance. *Curr. Opin. Biotechnol.* 32, 130–5. doi:10.1016/j.copbio.2014.11.027.

Liao, M., Fillery, I. R. P., and Palta, J. A. (2004). Early vigorous growth is a major factor influencing nitrogen uptake in wheat. *Funct. Plant Biol.* 31, 121. doi:10.1071/FP03060.

Lopez, G., Pallas, B., Martinez, S., Lauri, P.-É., Regnard, J.-L., Durel, C.-É., et al. (2015). Genetic Variation of Morphological Traits and Transpiration in an Apple Core Collection under Well-Watered Conditions: Towards the Identification of Morphotypes with High Water Use Efficiency. *PLoS One* 10, e0145540. doi:10.1371/journal.pone.0145540.

Lynch, J. P. (2013). Steep, cheap and deep: an ideotype to optimize water and N acquisition by maize root systems. *Ann. Bot.* 112, 347–57. doi:10.1093/aob/mcs293.

Maccaferri, M., Cane', M., Sanguineti, M. C., Salvi, S., Colalongo, M. C., Massi, A., et al. (2014). A consensus framework map of durum wheat (Triticum durum Desf.) suitable for linkage disequilibrium analysis and genome-wide association mapping. *BMC Genomics* 15, 873. doi:10.1186/1471-2164-15-873.

Maccaferri, M., El-Feki, W., Nazemi, G., Salvi, S., Canè, M. A., Colalongo, M. C., et al. (2016). Prioritizing quantitative trait loci for root system architecture in tetraploid wheat. *J. Exp. Bot.* 67, 1161–78. doi:10.1093/jxb/erw039.

Maccaferri, M., Ricci, A., Salvi, S., Milner, S. G., Noli, E., Martelli, P. L., et al. (2015). A high-density, SNP-based consensus map of tetraploid wheat as a bridge to integrate durum and bread wheat genomics and breeding. *Plant Biotechnol. J.* 13, 648–663. doi:10.1111/pbi.12288.

Maccaferri, M., Sanguineti, M. C., Demontis, A., El-Ahmed, A., Garcia Del Moral, L., Maalouf, F., et al. (2011). Association mapping in durum wheat grown across a broad range of water regimes.

J. Exp. Bot. 62, 409–438. Available at: http://www.ncbi.nlm.nih.gov/pubmed/21041372.

Mahner, M., and Kary, M. (1997). What Exactly Are Genomes, Genotypes and Phenotypes? And What About Phenomes? *J. Theor. Biol.* 186, 55–63. doi:10.1006/JTBI.1996.0335.

Mairhofer, S., Zappala, S., Tracy, S., Sturrock, C., Bennett, M. J., Mooney, S. J., et al. (2013). Recovering complete plant root system architectures from soil via X-ray μ-Computed Tomography. *Plant Methods* 9, 8. doi:10.1186/1746-4811-9-8.

Malamy, J. E. (2005). Intrinsic and environmental response pathways that regulate root system architecture. *Plant, Cell Environ.* 28, 67–77. doi:10.1111/j.1365-3040.2005.01306.x.

Manolio, T. A., Collins, F. S., Cox, N. J., Goldstein, D. B., Hindorff, L. A., Hunter, D. J., et al. (2009). Finding the missing heritability of complex diseases. *Nature* 461, 747–753. doi:10.1038/nature08494.

Marcussen, T., Sandve, S. R., Heier, L., Spannagl, M., Pfeifer, M., International Wheat Genome Sequencing Consortium, et al. (2014). Ancient hybridizations among the ancestral genomes of bread wheat. *Sci. {(New} York, {N.Y.)}* 345. doi:10.1126/science.1250092.

Marone, D., Laidò, G., Gadaleta, A., Colasuonno, P., Ficco, D. B. M., Giancaspro, A., et al. (2012). A high-density consensus map of A and B wheat genomes. *Theor. Appl. Genet.* 125, 1619–38. doi:10.1007/s00122-012-1939-y.

Masle, J., and Passiowa, J. (1987). The Effect of Soil Strength on the Growth of Young Wheat Plants. *Aust. J. Plant Physiol.* 14, 643. doi:10.1071/PP9870643.

Mayer, J. E., Pfeiffer, W. H., and Beyer, P. (2008). Biofortified crops to alleviate micronutrient malnutrition. *Curr. Opin. Plant Biol.* 11, 166–170. doi:10.1016/J.PBI.2008.01.007.

Meister, R., Rajani, M. S., Ruzicka, D., and Schachtman, D. P. (2014). Challenges of modifying root traits in crops for agriculture. *Trends Plant Sci.* 19, 779–788. doi:10.1016/j.tplants.2014.08.005.

Melino, V. J., Fiene, G., Enju, A., Cai, J., Buchner, P., and Heuer, S. (2015). Genetic diversity for root plasticity and nitrogen uptake in wheat seedlings. *Funct. Plant Biol.* 42, 942. doi:10.1071/FP15041.

Mickelbart, M. V., Hasegawa, P. M., and Bailey-Serres, J. (2015). Genetic mechanisms of abiotic stress tolerance that translate to crop yield stability. *Nat. Rev. Genet.* 16, 237–251. doi:10.1038/nrg3901.

Millet, E. J., Welcker, C., Kruijer, W., Negro, S., Coupel-Ledru, A., Nicolas, S. D., et al. (2016). Genome-Wide Analysis of Yield in Europe: Allelic Effects Vary with Drought and Heat Scenarios. *Plant Physiol.* 172, 749–764. doi:10.1104/pp.16.00621.

Moose, S. P., and Mumm, R. H. (2008). Molecular Plant Breeding as the Foundation for 21st Century Crop Improvement. *Plant Physiol.* 147, 969–977. doi:10.1104/pp.108.118232.

Müller, O., and Krawinkel, M. (2005). Malnutrition and health in developing countries. *CMAJ* 173, 279–86. doi:10.1503/cmaj.050342.

Nagel, K. A., Putz, A., Gilmer, F., Heinz, K., Fischbach, A., Pfeifer, J., et al. (2012). GROWSCREEN-Rhizo is a novel phenotyping robot enabling simultaneous measurements of root and shoot growth for plants grown in soil-filled rhizotrons. *Funct. Plant Biol.* 39, 891. doi:10.1071/FP12023.

Nakhforoosh, A., Grausgruber, H., Kaul, H.-P., and Bodner, G. (2014). Wheat root diversity and root functional characterization. *Plant Soil* 380, 211–229. doi:10.1007/s11104-014-2082-0.

Neuffer, M. G., and Ficsor, G. (1963). Mutagenic Action of Ethyl Methanesulfonate in Maize. *Science* 139, 1296–7. doi:10.1126/science.139.3561.1296.

Oladosu, Y., Rafii, M. Y., Abdullah, N., Hussin, G., Ramli, A., Rahim, H. A., et al. (2016). Principle and application of plant mutagenesis in crop improvement: a review. *Biotechnol. Biotechnol. Equip.* 30, 1–16. doi:10.1080/13102818.2015.1087333.

Osakabe, K., Osakabe, Y., and Toki, S. (2010). Site-directed mutagenesis in Arabidopsis using custom-designed zinc finger nucleases. *Proc. Natl. Acad. Sci. U. S. A.* 107, 12034–9. doi:10.1073/pnas.1000234107.

Parmar, N., Singh, K. H., Sharma, D., Singh, L., Kumar, P., Nanjundan, J., et al. (2017). Genetic engineering strategies for biotic and abiotic stress tolerance and quality enhancement in horticultural crops: a comprehensive review. *3 Biotech* 7, 239. doi:10.1007/s13205-017-0870-y.

Peng, J., Sun, D., Peng, Y., and Nevo, E. (2013). Gene discovery in *Triticum dicoccoides* , the direct progenitor of cultivated wheats. *Cereal Res. Commun.* 41, 1–22. doi:10.1556/CRC.2012.0030.

Pestsova, E., Lichtblau, D., Wever, C., Presterl, T., Bolduan, T., Ouzunova, M., et al. (2016). QTL mapping of seedling root traits associated with nitrogen and water use efficiency in maize.

Euphytica 209, 585–602. doi:10.1007/s10681-015-1625-7.

Petolino, J. F., Worden, A., Curlee, K., Connell, J., Strange Moynahan, T. L., Larsen, C., et al. (2010). Zinc finger nuclease-mediated transgene deletion. *Plant Mol. Biol.* 73, 617–628. doi:10.1007/s11103-010-9641-4.

Poehlman, J. M. (1987). "Plant Breeders and Their Work," in *Breeding Field Crops* (Dordrecht: Springer Netherlands), 1–15. doi:10.1007/978-94-015-7271-2_1.

Poethig, R. S. (1990). Phase Change and the Regulation of Shoot Morphogenesis in Plants. *Science (80-.).* 250, 923–930. doi:10.1126/science.250.4983.923.

Postic, F., and Doussan, C. (2016). Benchmarking electrical methods for rapid estimation of root biomass. *Plant Methods* 12, 33. doi:10.1186/s13007-016-0133-7.

Presterl, T., Ouzunova, M., Schmidt, W., Möller, E. M., Röber, F. K., Knaak, C., et al. (2007). Quantitative trait loci for early plant vigour of maize grown in chilly environments. *Theor. Appl. Genet.* 114, 1059–1070. doi:10.1007/s00122-006-0499-4.

Ray, D. K., Ramankutty, N., Mueller, N. D., West, P. C., and Foley, J. A. (2012). Recent patterns of crop yield growth and stagnation. *Nat. Commun.* 3, 1293. doi:10.1038/ncomms2296.

Revelle, W. (2017). psych: Procedures for Psychological, Psychometric, and Personality Research. Available at: https://cran.r-project.org/package=psych.

Rexroad, C. E., and Vallejo, R. L. (2009). Estimates of linkage disequilibrium and effective population size in rainbow trout. *BMC Genet.* 10, 83. doi:10.1186/1471-2156-10-83.

Reynolds, M., Manes, Y., Izanloo, A., and Langridge, P. (2009). Phenotyping approaches for physiological breeding and gene discovery in wheat. *Ann. Appl. Biol.* 155, 309–320. doi:10.1111/J.1744-7348.2009.00351.X.

Reynolds, M. P., and Langridge, P. (2016). Physiological breeding. *Curr. Opin. Plant Biol.* 31, 162–171. doi:10.1016/J.PBI.2016.04.005.

Reynolds, M., and Tuberosa, R. (2008). Translational research impacting on crop productivity in drought-prone environments. *Curr. Opin. Plant Biol.* 11, 171–179. doi:10.1016/j.pbi.2008.02.005.

Richards, R., and Passioura, J. (1989). A breeding program to reduce the diameter of the major xylem

vessel in the seminal roots of wheat and its effect on grain yield in rain-fed environments. *Aust. J. Agric. Res.* 40, 943. doi:10.1071/AR9890943.

Roy, S. J., Tucker, E. J., and Tester, M. (2011). Genetic analysis of abiotic stress tolerance in crops. *Curr. Opin. Plant Biol.* 14, 232–239. doi:10.1016/J.PBI.2011.03.002.

Ruta, N., Stamp, P., Liedgens, M., Fracheboud, Y., and Hund, A. (2010). Collocations of QTLs for Seedling Traits and Yield Components of Tropical Maize under Water Stress Conditions. *Crop Sci.* 50, 1385. doi:10.2135/cropsci2009.01.0036.

Saengwilai, P., Nord, E. A., Chimungu, J. G., Brown, K. M., and Lynch, J. P. (2014). Root Cortical Aerenchyma Enhances Nitrogen Acquisition from Low-Nitrogen Soils in Maize. *Plant Physiol.* doi:10.1104/pp.114.241711.

Salvi, S., Corneti, S., Bellotti, M., Carraro, N., Sanguineti, M. C., Castelletti, S., et al. (2011). Genetic dissection of maize phenology using an intraspecific introgression library. {*BMC*} *plant Biol.* 11, 4. doi:10.1186/1471-2229-11-4.

Salvi, S., Giuliani, S., Ricciolini, C., Carraro, N., Maccaferri, M., Presterl, T., et al. (2016). Two major quantitative trait loci controlling the number of seminal roots in maize co-map with the root developmental genes rtcs and rum1. *J. Exp. Bot.* 67, 1149–59. doi:10.1093/jxb/erw011.

Salvi, S., Porfiri, O., and Ceccarelli, S. (2013). Nazareno Strampelli, the "Prophet" of the green revolution. *J. Agric. Sci.* 151, 1–5. doi:10.1017/S0021859612000214.

Salvi, S., and Tuberosa, R. (2005). To clone or not to clone plant QTLs: present and future challenges. *Trends Plant Sci.* 10, 297–304. Available at: http://www.ncbi.nlm.nih.gov/pubmed/15949764.

Salvi, S., Tuberosa, R., Chiapparino, E., Maccaferri, M., Veillet, S., van Beuningen, L., et al. (2002). Toward positional cloning of Vgt1, a {QTL} controlling the transition from the vegetative to the reproductive phase in maize. *Plant Mol. Biol.* 48, 601–613.

Sanahuja, G., Banakar, R., Twyman, R. M., Capell, T., and Christou, P. (2011). Bacillus thuringiensis: a century of research, development and commercial applications. *Plant Biotechnol. J.* 9, 283–300. doi:10.1111/j.1467-7652.2011.00595.x.

Sandhu, N., Raman, K. A., Torres, R. O., Audebert, A., Dardou, A., Kumar, A., et al. (2016). Rice Root Architectural Plasticity Traits and Genetic Regions for Adaptability to Variable Cultivation

and Stress Conditions. *Plant Physiol.* 171, 2562–76. doi:10.1104/pp.16.00705.

Scarascia Mugnozza, G. T. (2005). The contribution of Italian wheat geneticists : From Nazareno Strampelli to Francesco D ' Amato. 53–75.

Schnable, P. S., Ware, D., Fulton, R. S., Stein, J. C., Wei, F., Pasternak, S., et al. (2009). The B73 maize genome: complexity, diversity, and dynamics. *Science (80-.).* 326, 1112–1115. Available at: http://www.ncbi.nlm.nih.gov/pubmed/19965430.

Segura, V., Vilhjálmsson, B. J., Platt, A., Korte, A., Seren, Ü., Long, Q., et al. (2012). An efficient multi-locus mixed-model approach for genome-wide association studies in structured populations. *Nat. Genet.* 44, 825–30. doi:10.1038/ng.2314.

Shama Rao, H. K., and Sears, E. R. (1964). Chemical mutagenesis in Triticum aestivum. *Mutat. Res. Mol. Mech. Mutagen.* 1, 387–399. doi:10.1016/0027-5107(64)90032-6.

Shewry, P. R. (2009). The HEALTHGRAIN programme opens new opportunities for improving wheat for nutrition and health. *Nutr. Bull.* 34, 225–231. doi:10.1111/j.1467-3010.2009.01747.x.

Shukla, V. K., Doyon, Y., Miller, J. C., DeKelver, R. C., Moehle, E. A., Worden, S. E., et al. (2009). Precise genome modification in the crop species Zea mays using zinc-finger nucleases. *Nature* 459, 437–441. doi:10.1038/nature07992.

Somers, D. J., Isaac, P., and Edwards, K. (2004). A high-density microsatellite consensus map for bread wheat (Triticum aestivum L.). *Theor. Appl. Genet.* 109, 1105–14. doi:10.1007/s00122-004-1740-7.

Steinemann, S., Schön, C.-C., and Hochholdinger, F. (2016). Development and validation of a DNA-based root phenotyping method in maize (Zea mays L.) List of contents. Available at: https://mediatum.ub.tum.de/doc/1286877/1286877.pdf [Accessed March 12, 2018].

Szalma, S. J., Hostert, B. M., LeDeaux, J. R., Stuber, C. W., and Holland, J. B. (2007). QTL mapping with near-isogenic lines in maize. *Theor. Appl. Genet.* 114, 1211–1228. doi:10.1007/s00122-007-0512-6.

Taramino, G., Sauer, M., Stauffer, J. L., Multani, D., Niu, X., Sakai, H., et al. (2007). The maize (Zea mays L.) RTCS gene encodes a LOB domain protein that is a key regulator of embryonic seminal and post-embryonic shoot-borne root initiation. *Plant J.* 50, 649–659. doi:10.1111/j.1365-

313X.2007.03075.x.

Tardieu, F., Draye, X., and Javaux, M. (2017). Root Water Uptake and Ideotypes of the Root System: Whole-Plant Controls Matter. *Vadose Zo. J.* doi:10.2136/vzj2017.05.0107.

Tester, M., and Langridge, P. (2010b). Breeding technologies to increase crop production in a changing world. *Science* 327, 818–22. doi:10.1126/science.1183700.

Tester, M., and Langridge, P. (2010a). Breeding technologies to increase crop production in a changing world. *Science* 327, 818–22. doi:10.1126/science.1183700.

The R Core Team (2016). R: A Language and Environment for Statistical Computing.

Tomar, R. S. S., Tiwari, S., Vinod, Naik, B. K., Chand, S., Deshmukh, R., et al. (2016). Molecular and Morpho-Agronomical Characterization of Root Architecture at Seedling and Reproductive Stages for Drought Tolerance in Wheat. *PLoS One* 11, e0156528. doi:10.1371/journal.pone.0156528.

Topp, C. N. (2016). Hope in Change: The Role of Root Plasticity in Crop Yield Stability. *Plant Physiol.* 172, 5–6. doi:10.1104/pp.16.01257.

Townsend, J. A., Wright, D. A., Winfrey, R. J., Fu, F., Maeder, M. L., Joung, J. K., et al. (2009). High-frequency modification of plant genes using engineered zinc-finger nucleases. *Nature* 459, 442–445. doi:10.1038/nature07845.

Trachsel, S., Kaeppler, S. M., Brown, K. M., and Lynch, J. P. (2011). Shovelomics: high throughput phenotyping of maize (Zea mays L.) root architecture in the field. *Plant Soil* 341, 75–87. doi:10.1007/s11104-010-0623-8.

Trachsel, S., Messmer, R., Stamp, P., Ruta, N., and Hund, A. (2010). QTLs for early vigor of tropical maize. *Mol. Breed.* 25, 91–103. doi:10.1007/s11032-009-9310-y.

Trachsel, S., Sun, D., SanVicente, F. M., Zheng, H., Atlin, G. N., Suarez, E. A., et al. (2016). Identification of QTL for Early Vigor and Stay-Green Conferring Tolerance to Drought in Two Connected Advanced Backcross Populations in Tropical Maize (Zea mays L.). *PLoS One* 11, e0149636. doi:10.1371/journal.pone.0149636.

Tuberosa, R. (2012). Phenotyping for drought tolerance of crops in the genomics era. *Front. Physiol.* 3, 347. doi:10.3389/fphys.2012.00347.

Tuberosa, R., Sanguineti, M. C., Landi, P., Giuliani, M. M., Salvi, S., and Conti, S. (2002). Identification of {QTLs} for root characteristics in maize grown in hydroponics and analysis of their overlap with {QTLs} for grain yield in the field at two water regimes. *Plant Mol. Biol.* 48, 697–712.

Vadez, V., Kholova, J., Zaman-Allah, M., and Belko, N. (2013). Water: the most important "molecular" component of water stress tolerance research. *Funct. Plant Biol.* 40, 1310. doi:10.1071/FP13149.

Vega, S. H., Sauer, M., Orkwiszewski, J. A. J., and Poethig, R. S. (2002). The early phase change gene in maize. *Plant Cell* 14, 133–47. doi:10.1105/TPC.010406.

Vigouroux, Y., Glaubitz, J. C., Matsuoka, Y., Goodman, M. M., Sanchez G., J., and Doebley, J. (2008). Population structure and genetic diversity of New World maize races assessed by DNA microsatellites. *Am. J. Bot.* 95, 1240–1253. doi:10.3732/ajb.0800097.

Wang, Y., Geng, L., Yuan, M., Wei, J., Jin, C., Li, M., et al. (2017). Deletion of a target gene in Indica rice via CRISPR/Cas9. *Plant Cell Rep.* 36, 1333–1343. doi:10.1007/s00299-017-2158-4.

Wasson, A. P., Rebetzke, G. J., Kirkegaard, J. A., Christopher, J., Richards, R. A., and Watt, M. (2014). Soil coring at multiple field environments can directly quantify variation in deep root traits to select wheat genotypes for breeding. *J. Exp. Bot.* 65, 6231–6249. doi:10.1093/jxb/eru250.

Wasson, A. P., Richards, R. A., Chatrath, R., Misra, S. C., Prasad, S. V. S., Rebetzke, G. J., et al. (2012). Traits and selection strategies to improve root systems and water uptake in water-limited wheat crops. *J. Exp. Bot.* 63, 3485–3498. doi:10.1093/jxb/ers111.

Watt, M., Moosavi, S., Cunningham, S. C., Kirkegaard, J. A., Rebetzke, G. J., and Richards, R. A. (2013). A rapid, controlled-environment seedling root screen for wheat correlates well with rooting depths at vegetative, but not reproductive, stages at two field sites. *Ann. Bot.* 112, 447–455. doi:10.1093/aob/mct122.

Wei, X., Wang, B., Peng, Q., Wei, F., Mao, K., Zhang, X., et al. (2015). Heterotic loci for various morphological traits of maize detected using a single segment substitution lines test-cross population. *Mol. Breed.* 35, 94. doi:10.1007/s11032-015-0287-4.

Wen, W., He, Z., Gao, F., Liu, J., Jin, H., Zhai, S., et al. (2017). A High-Density Consensus Map of Common Wheat Integrating Four Mapping Populations Scanned by the 90K SNP Array. *Front.*

Plant Sci. 8, 1389. doi:10.3389/fpls.2017.01389.

Wickham, H. (2009). *ggplot2: Elegant Graphics for Data Analysis*. Springer-Verlag New York Available at: http://ggplot2.org.

Wissuwa, M., Kretzschmar, T., and Rose, T. J. (2016). From promise to application: root traits for enhanced nutrient capture in rice breeding. *J. Exp. Bot.* 67, 3605–3615. doi:10.1093/jxb/erw061.

Wolak, M. E., Fairbairn, D. J., and Paulsen, Y. R. (2012). Guidelines for Estimating Repeatability. *Methods Ecol. Evol. 3(1)129-137*.

Wu, Q.-H., Chen, Y.-X., Zhou, S.-H., Fu, L., Chen, J.-J., Xiao, Y., et al. (2015). High-Density Genetic Linkage Map Construction and QTL Mapping of Grain Shape and Size in the Wheat Population Yanda1817 × Beinong6. *PLoS One* 10, e0118144. doi:10.1371/journal.pone.0118144.

Young, L. M., Evans, M. L., Hertel, R., Jarret, H., Fantin, D., and Gilroy, S. (1990). Correlations between Gravitropic Curvature and Auxin Movement across Gravistimulated Roots of Zea mays. *PLANT Physiol.* 92, 792–796. doi:10.1104/pp.92.3.792.

Yu, P., Gutjahr, C., Li, C., and Hochholdinger, F. (2016). Genetic Control of Lateral Root Formation in Cereals. *Trends Plant Sci.* 21, 951–961. doi:10.1016/j.tplants.2016.07.011.

Zamir, D. (2001). Improving plant breeding with exotic genetic libraries. *Nat. Rev. Genet.* 2, 983–989. doi:10.1038/35103590.

Zhou, H., He, M., Li, J., Chen, L., Huang, Z., Zheng, S., et al. (2016). Development of Commercial Thermo-sensitive Genic Male Sterile Rice Accelerates Hybrid Rice Breeding Using the CRISPR/Cas9- mediated TMS5 Editing System. doi:10.1038/srep37395.

Zhu, J., Ingram, P. A., Benfey, P. N., and Elich, T. (2011). From lab to field, new approaches to phenotyping root system architecture. *Curr. Opin. Plant Biol.* 14, 310–317. doi:10.1016/J.PBI.2011.03.020.

Zhu, J., Kaeppler, S. M., and Lynch, J. P. (2005). Mapping of QTL controlling root hair length in maize (Zea mays L.) under phosphorus deficiency. *Plant Soil* 270, 299–310. doi:10.1007/s11104-004-1697-y.

Zimin, A. V, Puiu, D., Hall, R., Kingan, S., Clavijo, B. J., and Salzberg, S. L. (2017). The first near-complete assembly of the hexaploid bread wheat genome, Triticum aestivum. *Gigascience* 6, 1–7.

doi:10.1093/gigascience/gix097.

Zurek, P. R., Topp, C. N., and Benfey, P. N. (2015). Quantitative trait locus mapping reveals regions of the maize genome controlling root system architecture. *Plant Physiol.* 167, 1487–96. doi:10.1104/pp.114.251751.

Zwietering, M. H., Jongenburger, I., Rombouts, F. M., and van 't Riet, K. (1990). Modeling of the bacterial growth curve. *Appl. Environ. Microbiol.* 56, 1875–81. Available at: http://www.ncbi.nlm.nih.gov/pubmed/16348228 [Accessed July 12, 2016].

Ringraziamenti

Vorrei ringraziare tutti coloro che hanno partecipato al lavoro da cui è nata questa tesi. Grazie per la professionalità con cui avete svolto il vostro compito. In particolare, vorrei ringraziare i miei supervisori, il prof. Silvio Salvi, il prof. Roberto Tuberosa e il dott. Marco Maccaferri. Vi ringrazio per la fiducia che avete riposto in me, per la passione che mi avete trasmesso, per il sapere che avete condiviso. Grazie per avermi aiutato quando più ne ho avuto bisogno.

Ringrazio chi mi ha accolto quando sono stato all'estero, per la diponibilità, l'amicizia, per non avermi fatto sentire estraneo.

Un ringraziamento particolare va a tutti i membri del mio gruppo. Grazie per avermi aiutato ma soprattutto per essere stati tra gli amici più cari che ho avuto. Grazie ad Eder, Danara, Fabio, Francesco, Giuseppe, Linda, Martina, Priyanka, Riccardo, Sandra e Simona. Sono stato bene con voi. Vi porterò sempre nel mio cuore.

Grazie alla mia famiglia, a mio padre, mia madre, mio fratello e Loredana. Siete insostituibili. Ovunque sono stato, per quanto lontano, vi ho sentiti sempre accanto a me. Il vostro affetto travalica tutte le frontiere, supera tutte le asperità. Grazie per il vostro amore incondizionato.

Ed infine grazie alla gioia mia, Rosalinda, la donna della mia vita. Con te accanto non ho mai temuto di non farcela, di non riuscire a rialzarmi. Il tuo amore riempie la mia vita e la rende degna di essere vissuta. Tutto ciò di buono che ho fatto in questi anni l'ho fatto per te, per vedere i tuoi occhi risplendere di felicità.